

**AWARD NUMBER:** W81XWH-16-1-0284

**TITLE:** Development of New Therapeutics Targeting Biofilm Formation by the Opportunistic Pulmonary Pathogens *Pseudomonas aeruginosa* and *Aspergillus Fumigatus*

**PRINCIPAL INVESTIGATOR:** Lynne Howell

**RECIPIENT:** Hospital for Sick Children, Toronto (ON), Canada

**REPORT DATE:** JANUARY 2021

**TYPE OF REPORT:** Final Technical Report

**PREPARED FOR:** U.S. Army Medical Research and Materiel Command  
Fort Detrick, Maryland 21702-5012

**DISTRIBUTION STATEMENT:** Approved for Public Release; Distribution Unlimited

The views, opinions and/or findings contained in this report are those of the author(s) and should not be construed as an official Department of the Army position, policy or decision unless so designated by other documentation.

# REPORT DOCUMENTATION PAGE

*Form Approved*  
OMB No. 0704-0188

Public reporting burden for this collection of information is estimated to average 1 hour per response, including the time for reviewing instructions, searching existing data sources, gathering and maintaining the data needed, and completing and reviewing this collection of information. Send comments regarding this burden estimate or any other aspect of this collection of information, including suggestions for reducing this burden to Department of Defense, Washington Headquarters Services, Directorate for Information Operations and Reports (0704-0188), 1215 Jefferson Davis Highway, Suite 1204, Arlington, VA 22202-4302. Respondents should be aware that notwithstanding any other provision of law, no person shall be subject to any penalty for failing to comply with a collection of information if it does not display a currently valid OMB control number. **PLEASE DO NOT RETURN YOUR FORM TO THE ABOVE ADDRESS.**

<b>1. REPORT DATE</b> Jan 2021		<b>2. REPORT TYPE</b> Final Technical Report		<b>3. DATES COVERED</b> 15 Sep 2016 - 14 Sep 2020	
<b>4. TITLE AND SUBTITLE</b>  Development of New Therapeutics Targeting Biofilm Formation by the Opportunistic Pulmonary Pathogens <i>Pseudomonas aeruginosa</i> and <i>Aspergillus fumigatus</i>				<b>5a. CONTRACT NUMBER</b> W81XWH-16-1-0284	
				<b>5b. GRANT NUMBER</b> PR150786-P1	
				<b>5c. PROGRAM ELEMENT NUMBER</b>	
<b>6. AUTHOR(S)</b>  Lynne Howell  E-Mail: howell@sickkids.ca				<b>5d. PROJECT NUMBER</b>	
				<b>5e. TASK NUMBER</b>	
				<b>5f. WORK UNIT NUMBER</b>	
<b>7. PERFORMING ORGANIZATION NAME(S) AND ADDRESS(ES)</b>  Hospital for Sick Children                      55 University Avenue Toronto ON M5G 1X8 Canada				<b>8. PERFORMING ORGANIZATION REPORT NUMBER</b>	
<b>9. SPONSORING / MONITORING AGENCY NAME(S) AND ADDRESS(ES)</b>  U.S. Army Medical Research and Materiel Command Fort Detrick, Maryland 21702-5012				<b>10. SPONSOR/MONITOR'S ACRONYM(S)</b>	
				<b>11. SPONSOR/MONITOR'S REPORT NUMBER(S)</b>	
<b>12. DISTRIBUTION / AVAILABILITY STATEMENT</b> Approved for Public Release; Distribution Unlimited					
<b>13. SUPPLEMENTARY NOTES</b>					
<b>14. ABSTRACT</b>  The bacterium <i>Pseudomonas aeruginosa</i> and fungus <i>Aspergillus fumigatus</i> are common causes of pulmonary disease in immunocompromised patients. During infection, both organisms form biofilms making them resistant to both antimicrobials and the immune system. This biofilm formation is dependent on exopolysaccharide synthesis. We have previously shown that the glycoside hydrolases (GH) PelA, PslG, Sph3 and Ega3 disrupt <i>P. aeruginosa</i> and <i>A. fumigatus</i> biofilms <i>in vitro</i> .  In this project we have (i) optimized the production endotoxin free GHs to increase yields significantly; (ii) identified antimicrobials that are potentiated by the GHs <i>in vitro</i> ; (iii) demonstrated that intratracheal administration of the 4 GHs in mice is well tolerated; (iv) determined the half-life of each GH alone or in combination <i>in vivo</i> ; (v) demonstrated that GHs can mitigate infection both alone and in combination with antifungals in an acute model of invasive aspergillosis; and (vi) demonstrated potentiation of the antibiotic ciprofloxacin when a combination of PslG/PelA was co administered in a <i>P. aeruginosa</i> model of mouse infection.  In summary, the results generated demonstrate that treatment with GHs alone or in combination with antimicrobials could significantly improve outcomes of pulmonary infections.					
<b>15. SUBJECT TERMS</b> <i>Pseudomonas aeruginosa</i> ; <i>Aspergillus fumigatus</i> ; virulence; biofilm; exopolysaccharide; glycoside hydrolase; antimicrobial potentiation.					
<b>16. SECURITY CLASSIFICATION OF:</b>			<b>17. LIMITATION OF ABSTRACT</b>  Unclassified	<b>18. NUMBER OF PAGES</b>  106	<b>19a. NAME OF RESPONSIBLE PERSON</b> USAMRMC
<b>a. REPORT</b> Unclassified	<b>b. ABSTRACT</b> Unclassified	<b>c. THIS PAGE</b> Unclassified			<b>19b. TELEPHONE NUMBER (include area code)</b>

Standard Form 298 (Rev. 8-98)  
Prescribed by ANSI Std. Z39.18

## **TABLE OF CONTENTS**

**Page No. 106**

- 1. Introduction**
- 2. Keywords**
- 3. Accomplishments**
- 4. Impact**
- 5. Changes/Problems**
- 6. Products**
- 7. Participants & Other Collaborating Organizations**
- 8. Special Reporting Requirements**
- 9. Appendices**

## 1. INTRODUCTION.

The bacteria *Pseudomonas aeruginosa* and fungus *Aspergillus fumigatus* are common causes of pulmonary disease in immunocompromised patients. These infections are associated with high morbidity and mortality, underscoring the urgent need for new effective therapies for these conditions. During pulmonary infection, both pathogens form biofilms, which enhance resistance to antimicrobials and immune defenses. Biofilm formation is dependent on the synthesis of matrix exopolysaccharides – Pel and Psl for *P. aeruginosa*, and galactosaminogalactan (GAG) for *A. fumigatus*. Exopolysaccharide-deficient mutants of *P. aeruginosa* and *A. fumigatus* are less virulent in animal models, suggesting that these glycans are promising therapeutic targets. We have identified and produced recombinant versions of microbial glycoside hydrolase (GH) enzymes, PelA, and PslG from *P. aeruginosa* and Ega3, and Sph3 from *A. fumigatus*, which degrade exopolysaccharides and disrupt biofilms *in vitro*. We hypothesize that treatment with these GHs alone or in combination with antimicrobials will be well tolerated and improve outcomes in experimental pulmonary infection with *P. aeruginosa* and *A. fumigatus*. We therefore propose the following studies: (1) To characterize the ability of recombinant GH enzymes to enhance the activity of antimicrobial agents against *P. aeruginosa* and *A. fumigatus in vitro*, (2) Perform tolerability and pharmacokinetic studies of intratracheal therapy with recombinant GH in mice, and (3) Evaluate the efficacy of GH therapy alone and in combination with antimicrobials for the treatment of acute and chronic *P. aeruginosa* and *A. fumigatus* infection mouse models. In the short term, these studies will provide solid preliminary data for the preclinical evaluation of pulmonary GH therapy against two of the most important opportunistic pulmonary pathogens. In the long-term, these results can also be extended to develop GH therapy pulmonary infections with other exopolysaccharide-producing pathogens such as *Staphylococcus*, *Acinetobacter* and *Mucor* species.

## KEYWORDS.

*Pseudomonas aeruginosa*; *Aspergillus fumigatus*; virulence; biofilm; exopolysaccharide; glycoside hydrolase; antimicrobial potentiation.

## 2. ACCOMPLISHMENTS:

What were the major goals of the project?

Please note this is partnered award with research being performed at McGill University (PI: Sheppard) and The Hospital for Sick Children (PI: Howell). The material presented herein pertains to both awards. Award numbers: W81XWH-16-1-0283 and W81XWH-16-1-0284

SPECIFIC AIM 1: to characterize the ability of the hydrolases to enhance the activity of antimicrobial agents *in vitro*.

**Major Task 1: Identify antimicrobials that are potentiated in the presence of candidate hydrolases.**

Subtask 1: Express and purify Sph3, Ega3, PelA and PslG for subtasks 1-3.

Subtask 2: Test Sph3, PelA and Ega3 in checkerboard combinations with antifungals against *A. fumigatus* biofilms.

Subtask 3: Test PslG/PelA and PslG/Ega3 in checkerboard combinations with antibiotics against *P. aeruginosa* biofilms.

Subtask 4: Test candidate hydrolase-antimicrobial combinations in an in vitro fluid biofilm culture model system.

*Milestone: Identification of hydrolase-antimicrobial combinations that synergize against A. fumigatus and P. aeruginosa. These antimicrobials will be prioritized and used in Aim3.*

SPECIFIC AIM 2: to perform preliminary tolerability and pharmacokinetic studies of candidate hydrolases *in vivo*.

**Major Task 2: Test candidate hydrolases for toxicity in vivo.**

Subtask 1: Submit documents for Animal use approvals.

*Milestone: Obtain animal use approvals.*

Subtask 2: Express and purify recombinant PelA and PslG for subtasks 3 – 4.

Subtask 3: Test toxicity of pulmonary administration of hydrolase combinations (PslG/PelA and PslG/Ega3 combinations) in immunocompetent mice.

Subtask 4: Test toxicity of pulmonary administration of hydrolases (PslG/PelA and PslG/Ega3 combinations) in immunocompromised mice.

*Milestone: Evaluation of pulmonary toxicity of candidate hydrolase regimens.*

### **Major Task 3: Pharmacokinetic studies of candidate hydrolases**

Subtask 1: Express and purify Sph3, Ega3, PelA and PslG for subtasks 2 – 5.

Subtask 2: Test pharmacokinetics of hydrolases (Sph3, Ega3, PelA and PslG/PelA and PslG / Ega3 combinations) in immunocompetent mice.

Subtask 3: Test pharmacokinetics of hydrolases (Sph3, Ega3, PelA and PslG/PelA and PslG/ Ega3 combinations) in immunocompromised mice.

Subtask 4: Determine concentrations of candidate hydrolases and their combinations using animal tissue samples.

*Milestone: Evaluation of pharmacokinetics of candidate hydrolase regimens.*

### **Major Task 4 (as required): Development of candidate hydrolase variants**

Subtask 1: Express and purify Sph3, Ega3, PelA and PslG for subtasks 2 – 5.

Subtask 2: Test protease resistance of candidate hydrolases against *A. fumigatus* isolates in the epithelial cell damage assay using Western-blot analysis, and mass spectrometry.

Subtask 3: Test protease resistance of candidate hydrolases against *P. aeruginosa* isolates in the epithelial cell damage assay using Western-blot analysis, and mass spectrometry.

Subtask 4: Test chemical modification as a means to increase the stability of candidate hydrolases.

Subtask 5: Test site-specific modification as a means to increase the stability of candidate hydrolases.

*Milestone: Development of stable candidate hydrolases.*

SPECIFIC AIM 3: to evaluate candidate hydrolases alone and in combination with antimicrobial agents in the treatment of experimental *A. fumigatus* and *P. aeruginosa* pulmonary infections *in vivo*.

### **Major Task 5: Test hydrolases for activity in animal models of acute disease**

Subtask 1: Express and purify Sph3, Ega3, PelA and PslG for subtasks 2 – 5.

Subtask 2: Determine the effects of hydrolases (Sph3, Ega3, PelA) on survival of immunosuppressed mice infected with *A. fumigatus*.

Subtask 3: Determine the effects of hydrolases (Sph3, Ega3, PelA) on fungal burden of mice infected with *A. fumigatus*.

Subtask 4: Determine the effects of hydrolases (PslG/PelA and PslG/Ega3 combinations) on bacterial burden of mice infected with three strains of *P. aeruginosa*.

*Milestone: Determine efficacy of candidate hydrolase regimens in the treatment of acute infection with *A. fumigatus* and *P. aeruginosa*.*

### **Major Task 6: Test hydrolases for activity in animal models of chronic disease**

Subtask 1: Express and purify Ega3, PelA and PslG for subtasks 2 – 3.

Subtask 2: Determine the effects of candidate hydrolases (Ega3) on fungal burden of immunocompetent mice chronically infected with *A. fumigatus*.

Subtask 3: Determine the effects of candidate hydrolases (PslG/PelA and PslG/Ega3 combinations) on bacterial burden of immunocompetent mice chronically infected with *P. aeruginosa*.

*Milestone: Determine efficacy of candidate hydrolase regimens in the treatment of chronic infection with A. fumigatus and P. aeruginosa.*

### **Major Task 7: Test hydrolases for synergy with antimicrobials**

Subtask 1: Express and purify Sph3, Ega3, PelA and PslG for subtasks 2 – 3.

Subtask 2: Determine the effects of hydrolase (Sph3, Ega3, PelA)-antifungal combinations on fungal burden of mice infected with *A. fumigatus*.

Subtask 3: Determine the effects of hydrolase (PslG/PelA and PslG/Ega3)-antibiotic combinations on burden of mice infected with *P. aeruginosa*.

*Milestone: Show a proof-of-concept for candidate hydrolases for use in treatment of A. fumigatus and P. aeruginosa. Get ready to initiate trials of delivery systems and detailed pharmacodynamics experiments as a prelude to Phase I clinical trials.*

## What was accomplished under these goals?

SPECIFIC AIM 1: TO CHARACTERIZE THE ABILITY OF THE HYDROLASES TO ENHANCE THE ACTIVITY OF ANTIMICROBIAL AGENTS *IN VITRO*.

### MAJOR TASK 1: IDENTIFY ANTIMICROBIALS THAT ARE POTENTIATED IN THE PRESENCE OF CANDIDATE GLYCOSIDE HYDROLASES (GH).

**Subtask 1: Express and purify Sph3, Ega3, PelA and PslG for subtasks 1-3.** Dr Howell's lab. SOW Time Period: Months 1-9. Completion level = 100%.

#### Background:

Before the initiation of the grant, our labs were able to produce the GHs Sph3, PelA and PslG in an *E. coli* expression system. This method reliably provide sufficient amounts of GH for *in vitro* experiments. However, *in vivo* experiments, as planned per SOW, required the production of substantial quantities of pure endotoxin-free protein. Therefore, we switched production from our standard *E. coli* system to either the endotoxin free *E. coli* bacterial system ClearColi® or to the *Pichia pastoris* yeast system PichiaPink® and ultimately mammalian cells (see Major Task 4 Subtask 5, p.44-49).

#### Developments:

1- GH production in a bacterial system.

##### *Methodology:*

In our original protocol the GH coding sequence was cloned into a vector that allows the proteins to be produced with a histidine tag. After cell growth, the culture supernatant was harvested and buffered at pH 8. Finally, the GHs were purified using nickel affinity and size exclusion chromatography. At the start of this grant we switched the production of Sph3, PelA and PslG has been transferred and optimized in the bacterial system ClearColi®.

##### *Results:*

Successful optimization efforts involved: growth in both richer, and autoinduction media; growth in Fernbach flasks and with higher shaking speeds to improve aeration of rich media.

These changes in protocol allowed an increase in the production of GHs up to 8 times, as compared to the original production protocol. Final yields were 125 mg of Sph3 / liter of culture medium, and more than 80 mg of PelA, and PslG (Table 1), which were more than adequate for our needs for the planned *in vivo* assays.

Protein	Media & Volume (L)	Protein Yield (mg)	Protein Yield (mg) / Media Volume (L)	Protein Yield (mg) / Cell weight (g)
<b>Sph3</b>	Luria Broth (LB), 3L	84mg	28	8
	LB, 2L	36mg	18	6.8
	Terrific Broth (TB), 1L, fernbach	125mg	125	19.3
<b>PelA</b>	LB, 4L	94.57mg	24	9.8
	LB, 2L	35.52mg	17.8	7.4
	TB , 1L, fernbach	84.15mg	84.2	17.4
<b>PslG</b>	LB, 4L	32.3mg	8	3.8
	TB, 2L	28.9mg	14.4	6.6
	Autoinduction, 0.5L, fernbach	41.48mg	83	10.5

Table 1. Optimization of GH production in *E. coli*. For each GH, the first line represents the original protocol; the following lines represent optimization progress.

While the optimization proved effective for Sph3, PelA and PslG, we were unable to produce soluble Ega3 in *E. coli* and therefore optimization of this GH was performed in the PichiaPink<sup>®</sup> yeast system.

## 2- GH production in a yeast system.

### *Methodology:*

To move from the bacterial system to yeast system, the GH gene coding sequence was modified by codon optimization. The yeast codon optimized *pslG* and *pelA* genes were purchased from Bio Basics Inc and cloned in vectors pD912 and pD915. This allowed the genes to be incorporated into the yeast *Pichia pastoris* genome under the control of an *AOX1* promoter, for induction in the presence of methanol, and with an N-terminal alpha-factor secretion signal (Figure 1). Once translated, the protein is packaged, the alpha-factor is removed and the protein secreted into the yeast growth media using native secretion machinery. Culture supernatant is harvested, filtered and buffered at pH 8 and the protein purified using ammonium sulfate precipitation, followed by size exclusion chromatography.

These vectors are IP-free and will allow for downstream scale-up which, once optimized, will allow for higher protein expression in a fermenter. This methodology is industry standard for the production of therapeutic proteins and our adoption will facilitate high yield, endotoxin-free expression that can take us through pre-clinical development and can be further scaled and utilized in a GLP facility for clinical trials.

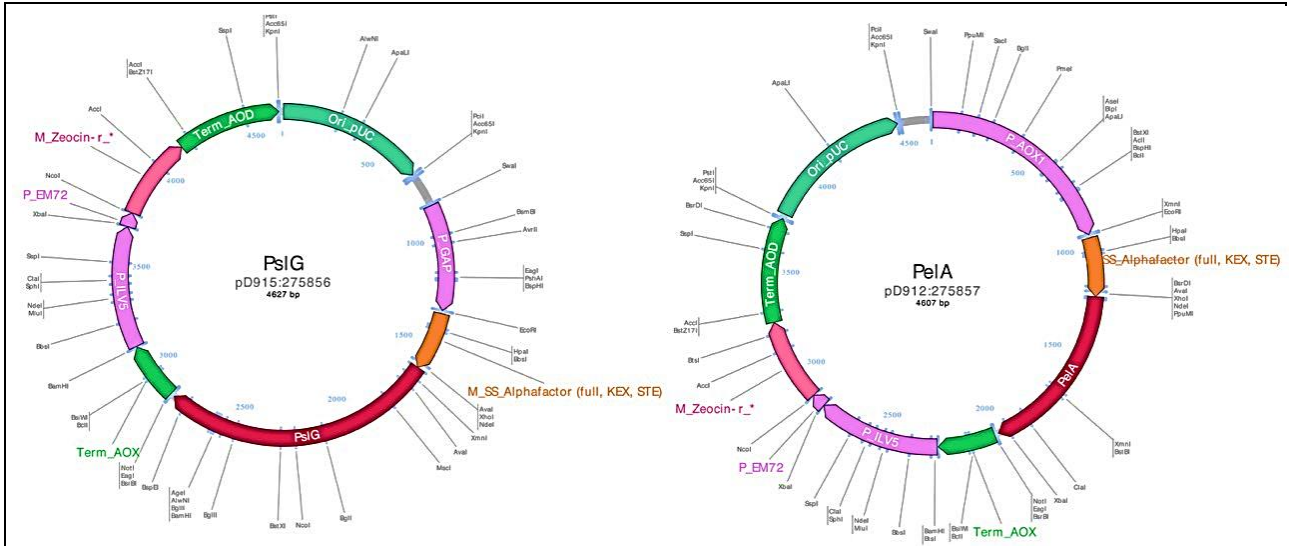


Figure 1. Genetic map of the vectors (pD915 and pD912) used for expression of GHs in *P. pastoris*. The coding sequence of the desired GH (red) was cloned after the N-terminal alpha-factor secretion signal ( $\alpha$ -factor) and is therefore under the control of the *AOX1* promoter and terminator ( $P_{AOX1}$  and  $T_{AOX1}$ ). A zeocin cassette serves as a marker for the selection of successful transformants.

Unlike *psIG* and *pelA*, *ega3* was cloned in the pPink $\alpha$ -HC plasmid (Invitrogen) (Figure 2). Again, the gene is under the control of the *AOX1* promoter, for induction in the presence of methanol, and a N-terminal alpha-factor secretion signal is also added to the protein, for its packaging and secretion in the medium.

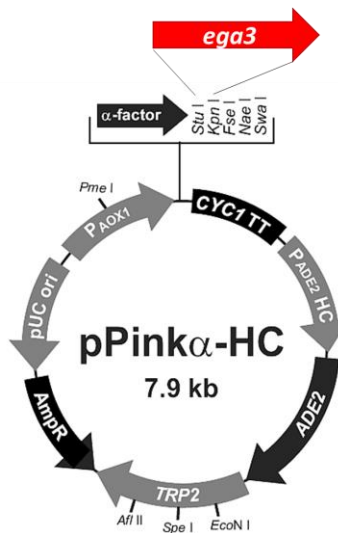


Figure 2. Genetic map of the vector used for expression of *ega3* in *P. pastoris*. The coding sequence of *ega3* (red) was cloned after the N-terminal alpha-factor secretion signal ( $\alpha$ -factor) and is under control of the *AOX1* promoter ( $P_{AOX1}$ ) and *cyc1* terminator (*cyc1TT*). A *ade2* cassette serves as a marker for the selection of successful transformants.

Results:

Originally, we had proposed to move the production of Sph3, PelA and PslG to *P. pastoris*. The first steps were successfully performed, in pD915 and pD912 (Figure 3). However, given the improvements to the *E. coli* ClearColi® production protocol (described above), we decided to keep Sph3, PelA and PslG production in the bacterial system. Only optimization of Ega3 production has been undertaken in *P. pastoris*.

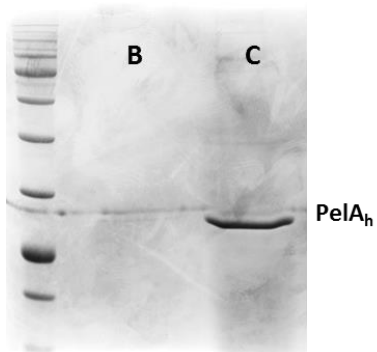


Figure 3: SDS PAGE gel of PelA<sub>h</sub> hydrolase production in *P. pastoris* yeast culture supernatant containing before (B.) and after concentration (C).

Production of Ega3 was inconsistent, leading to the need to re-optimize the expression protocol to ensure sufficient protein supply for Subtasks 2-4. We therefore explored: growth at higher shaking speed to improve aeration; stepwise expression: starvation of the cells; acclimation to methanol by addition of small amounts; addition of more methanol to start protein expression; addition of a second round of expression, transferring cells to new expression media; decreasing the pH of the media to pH6 to reduce degradation of Ega3 (Figure 4).

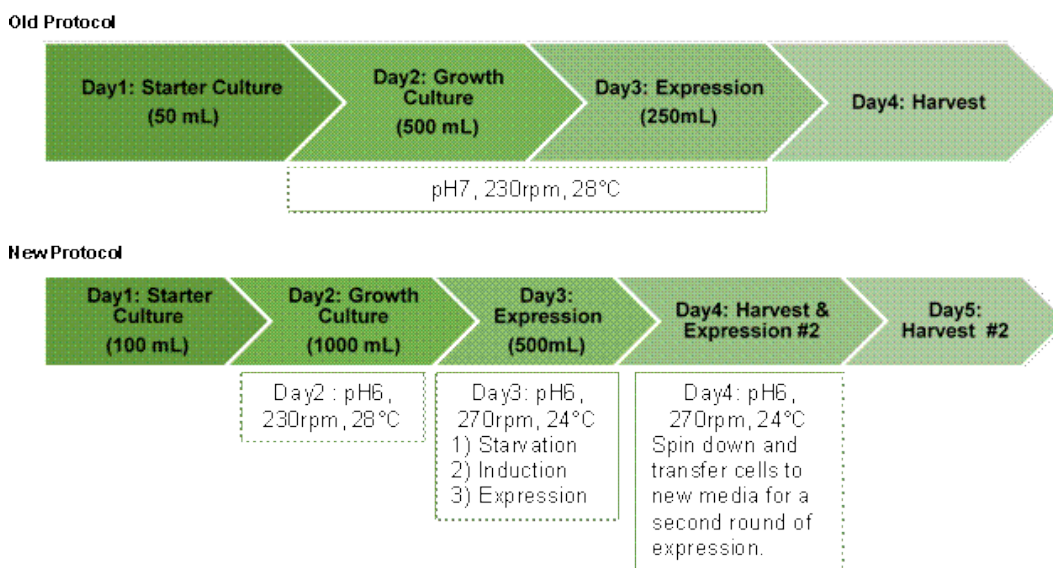


Figure 4. Schematic comparison of the old and new GH production methods in *P. pastoris*.

The improvements in protocol increased the yield of the protein by 7 fold to a final yield of 11.6 mg of protein / liter of culture medium (Table 2).

Protein	Media pH	Growth Volume (L)	Expression Volume (L)	Protein Yield (mg)	Protein Yield (mg) / Growth Volume (L)
Ega3	7	5.8L	2.9L	8.6mg	1.5
	7	6L	3L	10.3mg	1.7
	7	2L	2L	13.0mg	6.5
	6	4L	2L	31.6mg	7.9
	6	4L	4L	46.5 mg	11.6

Table 2. Optimization of GH production in *P. pastoris*. The first line represents our original protocol.

### 3- Control of GH quality:

**Methodology:** The activity of each enzyme was checked and quantified using our standard biofilm assays, to assess whether there were any negative impacts to the enzyme as a consequence of the changes in the expression/purification protocol. Briefly,  $10^5$  conidia/mL of *A. fumigatus* or planktonic cells of *P. aeruginosa* at  $OD_{600\text{ nm}} = 0.005$  were grown at  $37^\circ\text{C}$  for 24 h in order to form a biofilm; biofilm was washed then incubated with studied GH, at varied concentrations, or a buffer control. After 1h incubation and washes with PBS, the remaining biofilm was stained by crystal violet, destained, and the destaining solution was measured at an  $OD_{595\text{ nm}}$ .

**Results:** We observed a similar biofilm disruption activity throughout the protocol modifications (data not shown).

Subsequently, biofilm were routinely performed on all subsequent GH production batches, before their use in other tasks.

**Subtask 2: Test Sph3, PelA and Ega3 in checkerboard combinations with antifungals against *A. fumigatus* biofilms.** Dr Sheppard's lab. SOW Time Period: Months 1-9. Completion level = 100%.

#### 1- Antifungal potentiation with a fixed concentration of GH:

##### **Methodology:**

Antifungal effects on *A. fumigatus* were measured by quantifying metabolic activity using the well-described XTT assay, a widely used method for measuring cell metabolic activity. Briefly, *A. fumigatus* biofilms were pre-grown at  $37^\circ\text{C}$  for 9 h in RPMI media in 24 well plates; after which a gradient of antifungal drug was added to the wells in the presence or absence of  $0.5\ \mu\text{M}$  of the indicated GH. Plates were incubated for an additional 15 h and fungal viability was then measured using the XTT metabolic assay. The  $\text{MIC}_{50}$  was defined as the minimum concentration of antifungal required to inhibit fungal metabolism by 50%.

Preliminary data generated while the DoD proposal was under review suggested that PslG may be effective against fungal biofilms (data not shown) . We therefore decided to include treatment with this hydrolase in our studies.

##### **Results:**

In initial studies, voriconazole, the initial representative of the azole class of antifungals was not potentiated by GHs (data detailed in section "5. CHANGES/PROBLEMS"). We therefore replaced voriconazole with posaconazole in all subsequent assays. Treatment with  $0.5\ \mu\text{M}$  of any of the hydrolases in combination with posaconazole, amphotericin B or caspofungin resulted in a

significant enhancement of the drug efficacy against *A. fumigatus*, as shown by MIC<sub>50</sub> reduction (Figure 5). We therefore moved to assessing GH-antifungal potentiation in checkerboard assays.

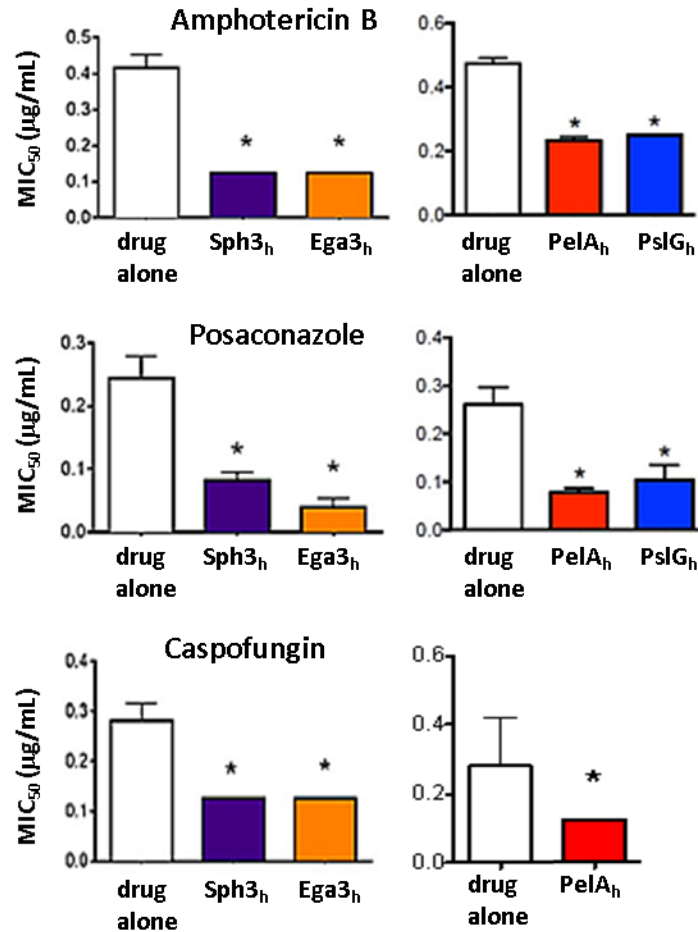


Figure 5: Impact of addition of 0.5 μM of GHs on the MIC<sub>90</sub> of antifungal drugs as determined by XXT assay. The combination of caspofungin/PslG was not included in these initial screening assays but was evaluated in the full checkerboard assays (Figure 7). \* indicates a statistically significant difference compared to drug alone ( $p < 0.05$  by ANNOVA).

## 2- GH-antifungal checkerboard assays

### *Methodology:*

Direct comparisons of the XTT metabolic assay with visual/fungal biomass growth studies, suggested that GH treatment resulted in artificially high metabolic readings at sub-lethal antifungal concentrations. This observation likely reflects enhanced reagent penetration into exopolysaccharide-deficient hyphae following GH treatment (see section “4. IMPACT” and “5. CHANGES/PROBLEMS”). We therefore elected to replace the XTT metabolic assay with visual scoring of the inhibitory effect of drugs, in absence or presence of GH.

For visual scoring, fungal inhibition was scored in accordance with the guidelines stipulated by the Clinical and Laboratory Standards Institute (CLSI) Reference Method for Broth Dilution Antifungal Susceptibility Testing of Filamentous Fungi (Figure 6). In this assay,  $1 \times 10^4$  conidia of strain Af293

were added to 96-well plates containing the GH-antifungal combination of interest and incubated for 24 h at 37°C, 5% CO<sub>2</sub>. Plates were then examined microscopically. For quality control, the minimum inhibitory concentration required for a 90% reduction in fungal growth (MIC<sub>90</sub>) was recorded. For antifungal potentiation, the minimum effective concentration (MEC) was recorded. As per CLSI guidelines, for the echinocandin caspofungin, change in fungal morphology was used rather than growth inhibition. For each combination of antifungal/GH, at least 3 independent experiments were performed.

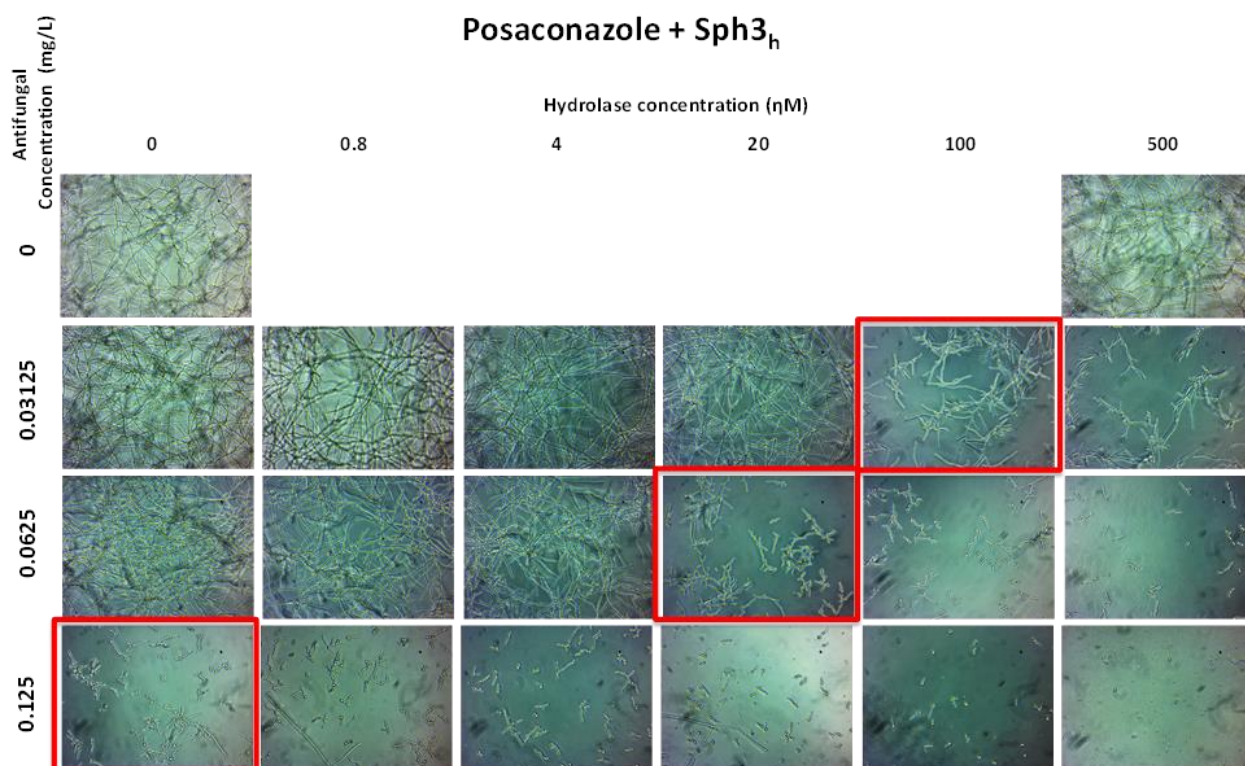


Figure 6. Example of visual scoring. Red boxes indicate the MIC<sub>90</sub>. The changes in MIC<sub>90</sub> highlight the significantly increased antifungal activity of posaconazole in the presence of Sph3.

**Results:**

With the exception of the amphotericin B/PelA combination, all GH/antifungal combinations demonstrated increased activity against *A. fumigatus* than antifungals alone (Figure 7). The GH concentration required to observe a reduction in MEC varied from 0.8 nM (posaconazole/Sph3 and caspofungin/any GH) to 100 nM (posaconazole/PelA). Based on overall MEC value reduction, the most effective GH/antifungal combinations were posaconazole/Sph3 and caspofungin/PelA. These two combinations were therefore prioritized for further studies *in vivo* (Major Task 7 Subtask 2).

Posaconazole-Sph3			Amphotericin B-Sph3			Caspofungin-Sph3		
		MEC			MEC			MEC
Hydrolase conc. (nM)	0	0.500	Hydrolase conc. (nM)	0	0.833	Hydrolase conc. (nM)	0	0.500
	0.8	0.333		0.8	0.833		0.8	0.333
	4	0.333		4	0.667		4	0.333
	20	0.250		20	0.500		20	0.250
	100	0.208		100	0.500		100	0.167
	500	0.167		500	0.417		500	0.125

Posaconazole-Ega3			Amphotericin B-Ega3			Caspofungin-Ega3		
		MEC			MEC			MEC
Hydrolase conc. (nM)	0	0.375	Hydrolase conc. (nM)	0	0.667	Hydrolase conc. (nM)	0	0.583
	0.8	0.375		0.8	0.667		0.8	0.500
	4	0.375		4	0.667		4	0.333
	20	0.3125		20	0.500		20	0.250
	100	0.1875		100	0.500		100	0.208
	500	0.1875		500	0.500		500	0.208

Posaconazole-PelA			Amphotericin B-PelA			Caspofungin-PelA		
		MEC			MEC			MEC
Hydrolase conc. (nM)	0	0.500	Hydrolase conc. (nM)	0	0.667	Hydrolase conc. (nM)	0	0.833
	0.8	0.500		0.8	0.667		0.8	0.417
	4	0.500		4	0.667		4	0.333
	20	0.500		20	0.667		20	0.250
	100	0.417		100	0.667		100	0.208
	500	0.333		500	0.667		500	0.208

Figure 7. Minimal effective concentration (MEC,  $\mu\text{g}/\text{mL}$ ) for posaconazole, amphotericin B and caspofungin in presence of the indicated concentration of GHs as per visual scoring in a fungal inhibition assay.

**Subtask 3: Test PslG/PelA and PslG/Ega3 in checkerboard combinations with antibiotics against *P. aeruginosa* biofilms.** Dr Howell's lab. SOW Time Period: Months 1-9. Completion level = 100%.

Background: Our preliminary studies indicated that GH treatment enhanced the antimicrobial activity of colistin. We sought to expand these studies to examine the effects of GH therapy on the activity of other antibiotics in checkerboard assays.

Accomplishments:

1- Antibacterial potentiation with a fixed concentration of GH:

Methodology:

Device: Although, our original plan was to use the Calgary Biofilm Device (CBD), to complete our assays, for reasons described in section "5. CHANGES/PROBLEMS", the CBD did not function as expected. We therefore developed an alternate protocol, based on our standing biofilm tube assay, described previously in our 2016 *Science Advances* publication (Baker et al, *Sci Adv.* 2016: e1501632). In this assay, bacteria are grown for 24 h and then subjected to hydrolase + antibiotic combinations. Following incubation, the biofilm is mechanically disrupted and the cells are enumerated using serial dilutions.

Again, we experienced some difficulties with the reproducibility of the drug potentiation assay using this standing biofilm tube assay. Therefore, while continuing to develop a reliable assay, we also re-visited with the help of our collaborator Dr Parsek (University of Washington) optimizing the protocol for the Calgary Biofilm Device (CBD). Using a newly published protocol (Habash *et al.*, *Antimicrob. Agents Chemother.* 2017 Oct 24), we successfully addressed these difficulties, and we were able to obtain reproducible results using the CBD.

Bacterial strain: We also faced a problem when growing biofilms of the *P. aeruginosa* PA14 strain at 37°C. While PA14 is able to produce a robust Pel-dependent biofilm at 25°C, as previous published, it is unable to generate adherent biomass at 37°C (as detailed in section "5. CHANGES/PROBLEMS"). We therefore completed the rest of our work using the strain *P. aeruginosa* PA01, for its robust growth at 37°C, although biofilm of PA14 contains predominantly Pel over Psl, which made it our initial choice of a *P. aeruginosa* strain.

Results:

Using a 1 µM fixed concentration of PelA/PslG on biofilms of *P. aeruginosa* PA01, that were grown for 24 h at 37°C, we were able to demonstrate significant potentiation of the antibiotics, tobramycin (an aminoglycoside), ciprofloxacin (a fluoroquinolone) and polymyxin. There was a positive effect for neomycin (another aminoglycoside) but the effect was not statistically significant (Figure 8).

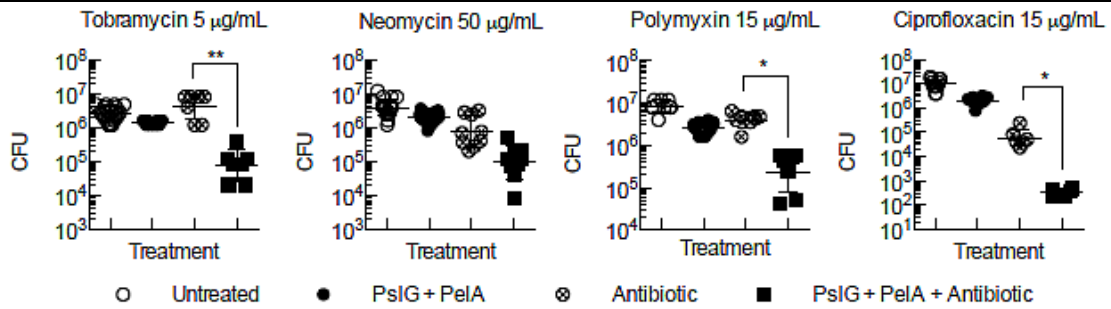


Figure 8. Potentiation of antibiotics efficiency against *P. aeruginosa* by addition of a mix of GHs PelA/PslG at a 1  $\mu$ M concentration each. Several concentrations of antibiotics were used and the herein presented results represent the concentrations would gave the highest potentiation. \* indicates a significant decrease in quantitative culture counting ( $p \leq 0.05$  by ANOVA).

## 2- GH-antibacterial checkerboard assays

### Methodology:

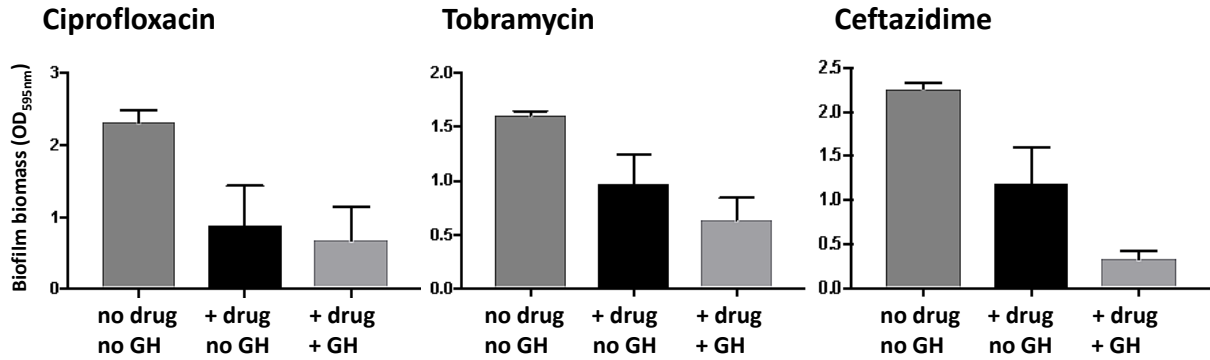
MBEC plates (CBD) were used for the assay at 37°C with the strain *P. aeruginosa* PA01. Biofilm biomass was evaluated using crystal violet staining. All checkerboard assays have been performed in triplicate. One-way ANOVA and multiple comparison test were used for statistical analyses on GraphPad Prism. In addition to tobramycin (aminoglycoside) and ciprofloxacin (fluoroquinolone), which proved to be potentiated by GHs in fixed concentration assays, we elected to also study ceftazidime (an antibiotic of the  $\beta$ -lactam class).

### Results:

As expected, we were able to reproduce the results observed with tobramycin and ciprofloxacin: combining GH with antibiotics resulted in a greater reduction in biofilm biomass than when either the hydrolase or antibiotic were used separately. Ceftazidime was also potentiated by GHs. This potentiation was observed both when adding an increasing concentration of hydrolases to a fixed concentration of antibiotics and when adding a fixed concentration of hydrolases to a gradient of antibiotics. For simplicity, Figure 9 summarizes the optimal potentiation observed, at a single concentration of the antibiotic (15.6  $\mu$ g/ml) and hydrolase combination (1.25  $\mu$ M each).

Of the antibacterial drugs tested, ciprofloxacin and ceftazidime were potentiated the most, when combined with PslG/PelA and PslG/Ega3. Given these results and our experience with dosing ciprofloxacin in mice, ciprofloxacin was selected for use in our first combination studies *in vivo* (Major Task 7 Subtask 3) and ceftazidime used for our second antibiotic combination.

PslG/PelA = 0 or 1.25  $\mu$ M each + antibiotic = 15  $\mu$ g/mL



PslG/Ega3 = 0 or 1.25  $\mu$ M each + antibiotic = 15  $\mu$ g/mL

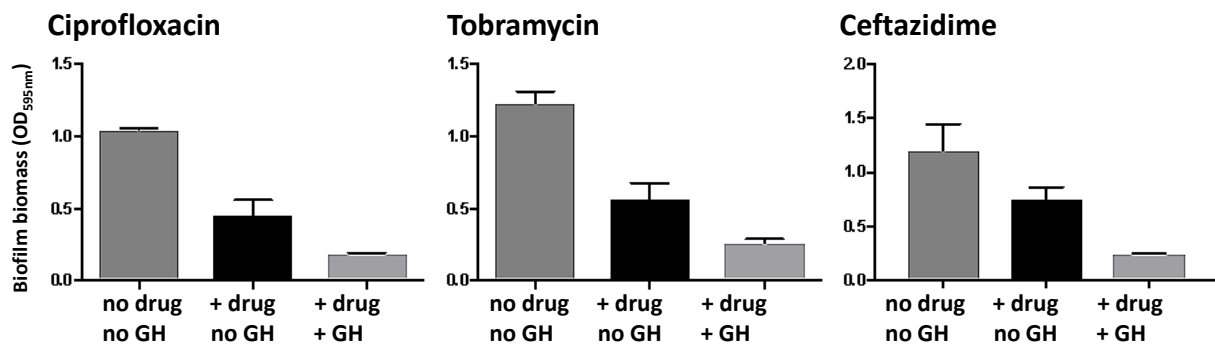


Figure 9. Potentiation of antibiotics efficiency against *P. aeruginosa* by addition of tobramycin, ciprofloxacin or ceftazidime at a concentration of 15  $\mu$ g/mL with GH combinations PslG/PelA or PslG/Ega3 at a concentration of 1.25  $\mu$ M each. The graphs represent the result of triplicated experiments.

**Subtask 4:** Test candidate hydrolase-antimicrobial combinations in an *in vitro* fluid biofilm culture model system. Dr Howell and Sheppard’s labs. SOW Time Period: Months 6-12. Completion level = This task was abandoned as detailed in section “5. CHANGES/PROBLEMS”.

**Methodology:**

We successfully developed a method to grow *A. fumigatus* under flow biofilm conditions. Briefly,  $1.5 \times 10^5$  conidia of RFP-expressing *A. fumigatus* strain Af293 were grown in Brian medium for 9 h. Young hyphae were scraped off, transferred to flow chambers, and incubated at 37°C for 2 h to allow the hyphae to adhere to the chamber surface. Biofilms were then allowed to develop for 24 h at 37°C under constant flow of 1% Brian medium. The resulting biofilms were then stained with FITC-conjugated soy bean agglutinin for GAG detection and imaged by confocal microscopy. Susceptibility of biofilms to GH therapy was evaluated by treating flow-grown biofilms with a 2  $\mu$ M of the GH of interest for 2 h prior to imaging. Mature biofilms were then stained with fluorescent Soybean Agglutinin (SBA-FITC) to visualize galactosaminogalactan (GAG) content

**Results:**

Using an Af293::RFP *A. fumigatus* strain, we were able to optimize the device and to observe, over the course of 24 hours, young hyphae develop into a mature biofilm (Figure 10).

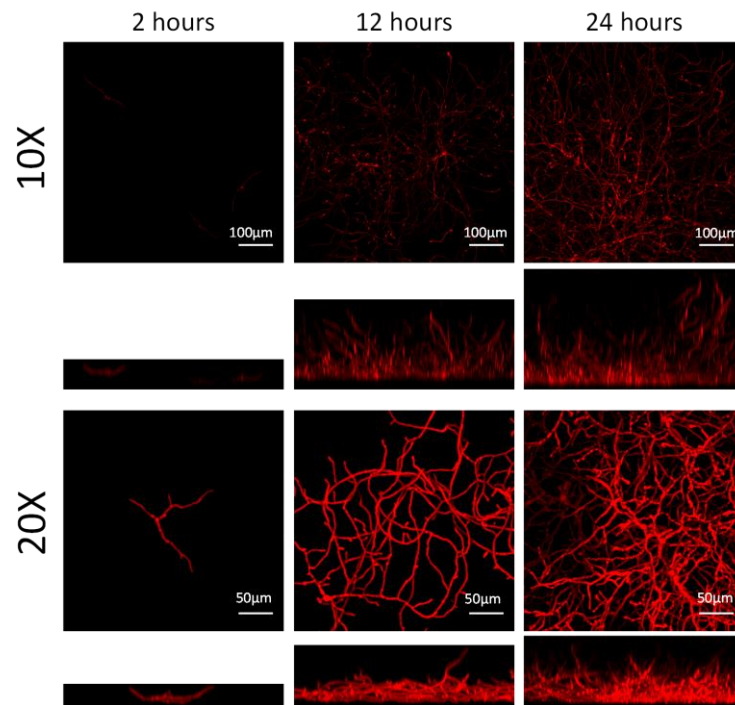


Figure 10. Time-course of Af293::rfp strain grown under dynamic flow cell system. Z-stacks were acquired to generate both top-down and side views.

24h grown hyphae stained strongly with SBA-FITC (green), suggesting that GAG is produced under flow conditions (Figure 11A). Consistent with the anti-GAG activity Sph3, GH-treated biofilms exhibited reduced SBA staining compared to the untreated sample. (Figure 11B)

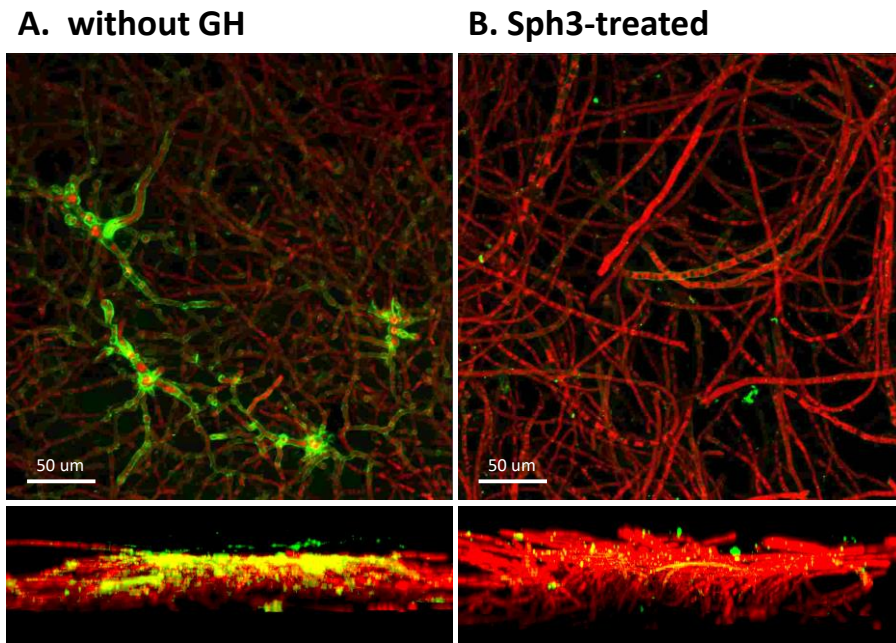


Figure 11. SBA-FITC staining of *A. fumigatus* biofilms grown under flow conditions. A. Untreated *A. fumigatus* biofilms. B. *A. fumigatus* biofilms treated with 2  $\mu$ M of Sph3. Vertical Z-stacks were acquired to generate both top-down (top images) and side views (bottom images) for each sample.

Despite these encouraging preliminary results, we were unable to adapt the XTT assay to quantify fungal viability in a flow system. Given that flow conditions are not expected to be present during airway infection, we chose to not pursue further these studies, as detailed in section “5. CHANGES/PROBLEMS”.

**Milestone Achieved: Identification of hydrolase-antimicrobial combinations that synergize against *A. fumigatus* and *P. aeruginosa*.**

SPECIFIC AIM 2: TO PERFORM PRELIMINARY TOLERABILITY AND PHARMACOKINETIC STUDIES OF CANDIDATE HYDROLASES *IN VIVO*.

**MAJOR TASK 2: TEST CANDIDATE HYDROLASES FOR TOXICITY *IN VIVO*.**

**Subtask 1: Submit documents for Animal use approvals.** Dr Sheppard's lab. SOW Time Period: Months 1-6. Completion level = 100%

IACUC protocol number #2016-7808, was approved by the USAMRMC Animal Care and Use Review Office (ACURO) on 18 Nov 2016. This protocol was previously approved by the McGill University IACUC on 01-JUN-2016.

**Subtask 2: Express and purify recombinant PelA and PslG for subtasks 3 – 4.** Dr Howell's lab. SOW Time Period: Months 6-12. Completion level = 100%.

As presented in Major Task 1 – Subtask 1, sufficient protein, both in quantity and quality (endotoxin-free enzyme, verified activity) was produced to meet all requirements for the other subtasks of Major Task 2.

**Subtask 3: Test toxicity of pulmonary administration of GH combinations (PslG/PelA and PslG/Ega3 combinations) in immunocompetent mice.** Dr Sheppard's lab. SOW Time Period: Months 6-12. Completion level = 100%.

Rationale:

Preliminary studies in our labs indicated that administration of two doses of 0.75 µg Sph3 is well tolerated by immunocompromised mice. Our aim was to expand these studies to test of tolerability to all GHs, at dosage as high as 500 µg, administered as single or multiple doses, and in immunocompetent or immunocompromised mice. These studies are critical to guide dose selection for *in vivo* efficacy studies. Subtask 3 focuses on immunocompetent mice and Subtask 4 uses immunocompromised animals.

Accomplishments:

We have completed a full assessment of monotherapy for each of the GH enzymes, and the required assessment of various GH combination therapies.

Methodology:

Recombinant GH enzymes alone and in combination were administered intratracheally at doses ranging from 1 to 500 µg. Mice were monitored for 7 days, then sacrificed to investigate for signs of pulmonary injury or inflammation. All assays were performed in 2 independent experiments, with groups of 10 mice per condition: 8 mice had their lungs harvested, lavaged for measurement of lactate dehydrogenase (LDH) release and digested with collagenase for pulmonary leukocyte recruitment by flow-cytometry, and their blood drawn for IgE quantification in serum. The lungs of the remaining 2 mice were analyzed by histopathology.

**Results:**

**1- GH monotherapy (PslG, PeIA, Sph3, Ega3):**

Mouse body weight and body temperature: GH treatment had no effect on these parameters (Figure 12, 13)

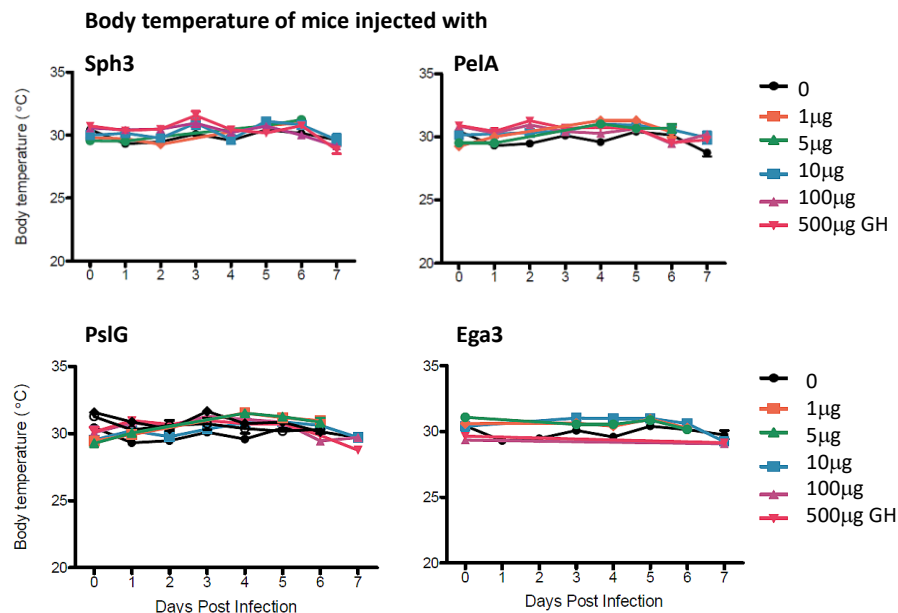


Figure 12. Monitoring of mouse temperature over 7 days after intratracheal injection of the indicated GH in PBS.

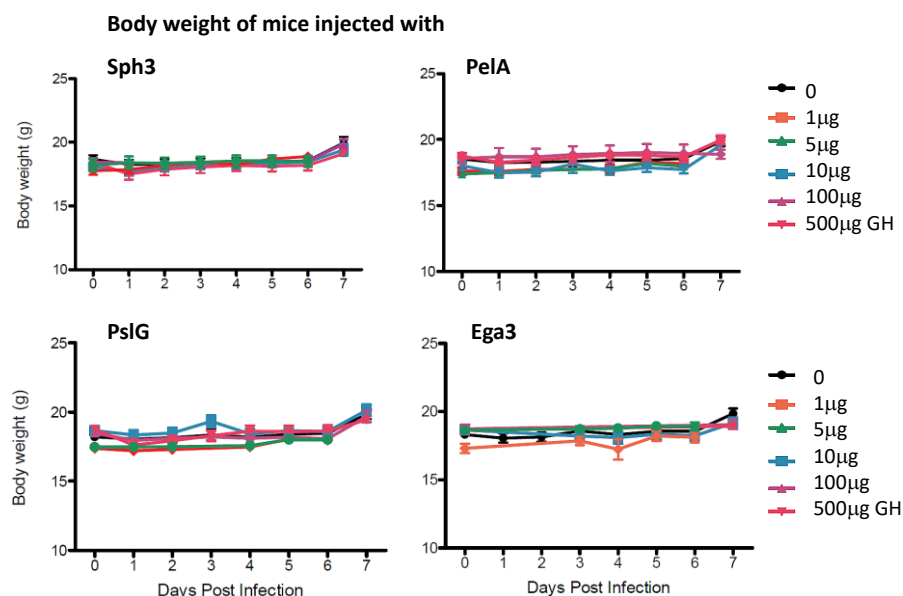


Figure 13. Monitoring of mouse weight over 7 days after intratracheal injection of the indicated GH in PBS.

Pulmonary injury: Except for PeIA at 500 µg and Ega3 at 5 µg, no significant increase in lactate dehydrogenase (LDH) release in the bronchoalveolar lavage (BAL) fluid were observed in GH-treated mice, suggesting that GH therapy does not induce significant pulmonary injury (Figure 14).

No differences between treated and untreated mice were observed with histological examination of pulmonary tissue sections (data not shown).

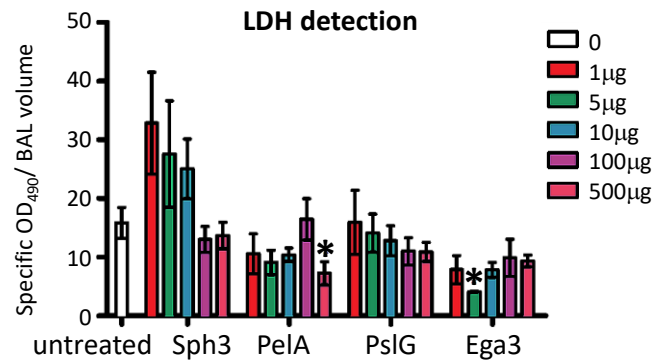


Figure 14. Quantification of lactate dehydrogenase (LDH) activity in the bronchoalveolar lavage (BAL) fluid harvested from mice 7 days following treatment with a single dose of the indicated GH. \* indicates a significant difference with the untreated group, ( $p \leq 0.05$  by ANOVA).

#### Pulmonary leukocyte recruitment:

For all GHs, with the exception of Ega3, significant pulmonary leukocyte recruitment was only observed with the highest intratracheal doses (500 µg) (Figure 15). An increase in pulmonary eosinophil levels was noted with all doses of Ega3, and was statistically significant at doses of 10 µg and higher. Serum IgE levels in GH-exposed mice were measured to determine if this eosinophil recruitment might be reflect a systemic allergic response. Despite observation of increased numbers of pulmonary eosinophils in Ega3-treated mice, IgE levels were not significantly increased following intrapulmonary therapy with doses of up to 500 µg of any of the GH enzymes (Figure 16).

Ega3 is the only GH that is produced in *Pichia pastoris* rather than *E. coli*. Since *P. pastoris* is a eukaryotic yeast, we hypothesized that these findings may result from host reaction to fungal N-glycans. Therefore, we explored the effects of: (i) enzymatically deglycosylating Ega3 post-production; and (ii) expressing the protein in mammalian cells to alter glycosylation (task accomplished and described further, in section “Major Task 4”).

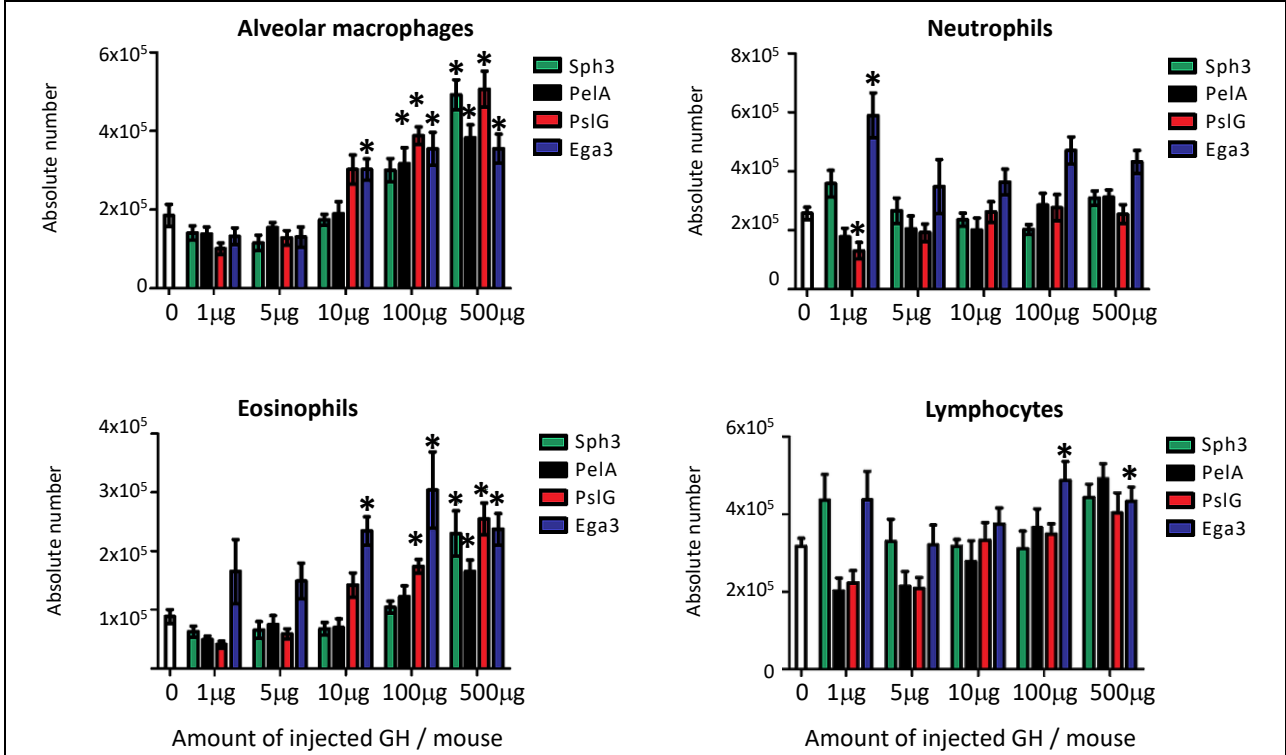


Figure 15. Absolute quantification of leukocyte populations in mouse lungs as measured by flow-cytometry performed on lung digests. Lungs were harvested 7 days following treatment with a single dose of the indicated GH. \* indicates a significant difference with the untreated group, ( $p \leq 0.05$  by ANOVA).

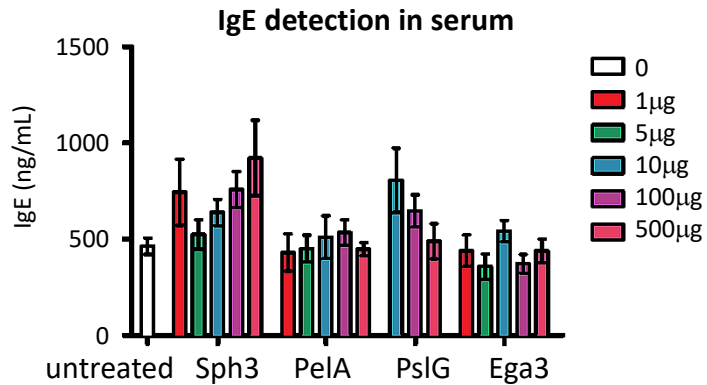


Figure 16. Absolute quantification of IgE in mouse sera as measured by commercial EIA (BD optEIA mouse IgE). Serum was collected 7 days following treatment the indicated GH. No significant difference between the GH-treated and untreated group was observed ( $p \leq 0.05$  by ANOVA).

## 2- GH combination therapies (PslG/PelA and PslG/Ega3):

Mouse body weight and body temperature: GH treatment had no effect on mouse body weight and body temperature. (Figure 17, 18)

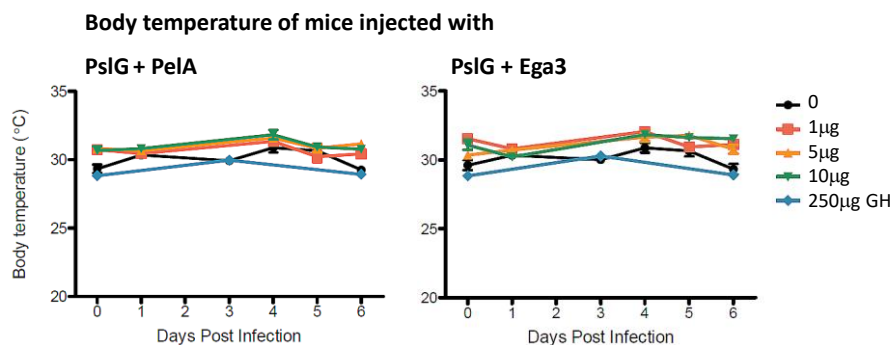


Figure 17. Monitoring of mouse temperature over 7 days after intratracheal injection of the indicated GH combinations in PBS.

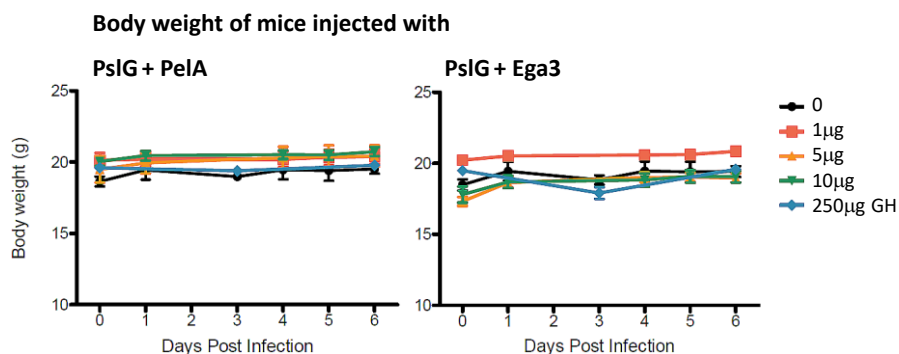


Figure 18. Monitoring of mouse weight over 7 days after intratracheal injection of of the indicated GH combinations in PBS.

Pulmonary injury: Except for the two 10 µg GH doses, no significant increases in lactate dehydrogenase (LDH) release in the bronchoalveolar lavage (BAL) fluid were observed in GH combination-treated mice suggesting that GH combination therapy does not induce significant pulmonary injury (Figure 19). No differences between treated and untreated mice were detected by histological examination of pulmonary tissue sections (data not shown).

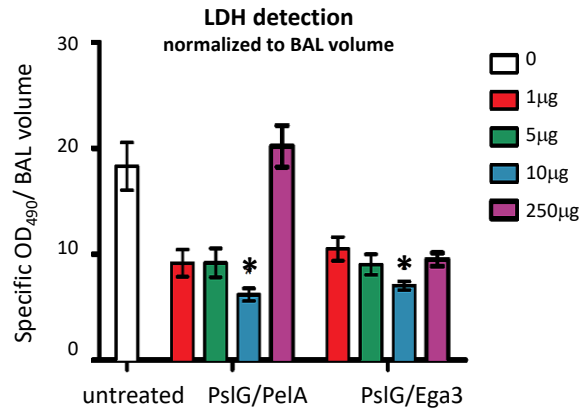


Figure 19. Quantification of lactate dehydrogenase (LDH) activity in bronchoalveolar fluid harvested from mice 7 days following treatment with a single dose of the indicated GH combination. \* indicates a significant difference with the untreated group, ( $p \leq 0.05$  by ANOVA).

Pulmonary leukocyte recruitment: As with GH monotherapy, a significant increase of alveolar macrophages was observed with both GH combinations at the low doses (Figure 20), although interestingly this increase was not observed at the higher combined dose of 250 µg of each GH. In contrast, this higher GH dose was the only one associated with increase in lymphocyte recruitment. As with monotherapy studies, a trend to increased eosinophil recruitment was observed with the high dose of Ega3. Collectively these data suggest that effects of GH therapy on pulmonary leukocyte population is not dose-dependent.

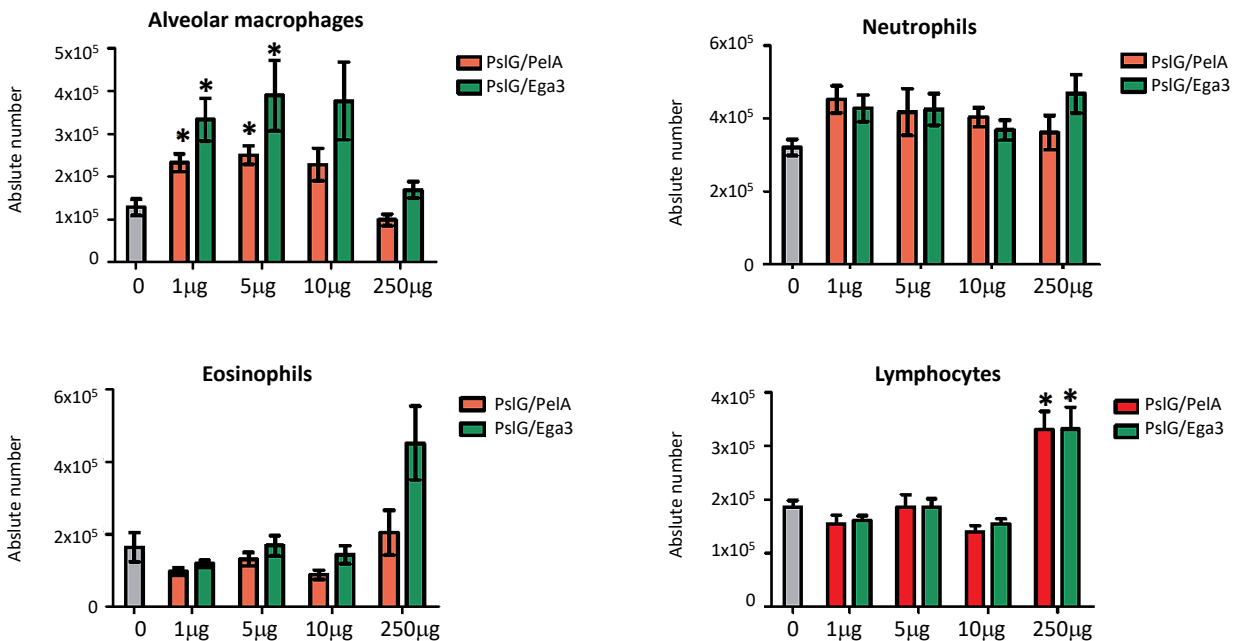


Figure 20. Absolute quantification of leukocyte populations in mouse lungs as measured by flow-cytometry performed on lung homogenates. Lungs were harvested 7 days following treatment with a single dose of the indicated GH combination. \* indicates a significant difference with the untreated group, ( $p \leq 0.05$  by ANOVA).

**Conclusion for Subtask 3:** Intratracheal treatment of immunocompetent mice with GH in monotherapy or in combination therapy at doses of up to 500 µg of single hydrolase (or 250 µg each in combine therapy *i.e.* 500 µg total) was well tolerated.

**Subtask 4: Test tolerability of pulmonary administration of hydrolase combinations (PslG/ PeIA and PslG/Ega3) in immunocompromised mice.** Dr Sheppard's lab. SOW Time Period: Months 6-12. Completion level = 100%.

**Methodology.** Mice were rendered neutropenic by injection of 250 mg/kg cortisone subcutaneously and 250 mg/kg cyclophosphamide intraperitoneally 2 days prior to infection, followed by 250 mg/kg cortisone subcutaneously plus 200 mg/kg cyclophosphamide intraperitoneally 3 days post-infection. At day 0, combinations of recombinant GH enzymes were administered intratracheally at doses ranging from 1 to 250 µg of each GH as a mixture 1:1. Mice were monitored for 7 days, then sacrificed to investigate signs of pulmonary injury or inflammation. Experiments were conducted on groups of 10 mice, on 2 separate occasions. LDH release, pulmonary leukocyte recruitment and histopathology slides were performed as described in Subtask 3.

**Results:**

Data presented hereafter confirmed that, as was observed in immunocompetent mice, no significant pulmonary toxicity was detected in immunosuppressed mice. Injection of GHs up to 500 µg / mouse did not induce lung injury as per lactate dehydrogenase (LDH) release in the BAL fluid (Figure 21) or histological examination (data not shown). No significant leukocyte recruitment was observed in response to combination GH therapy (Figure 22).

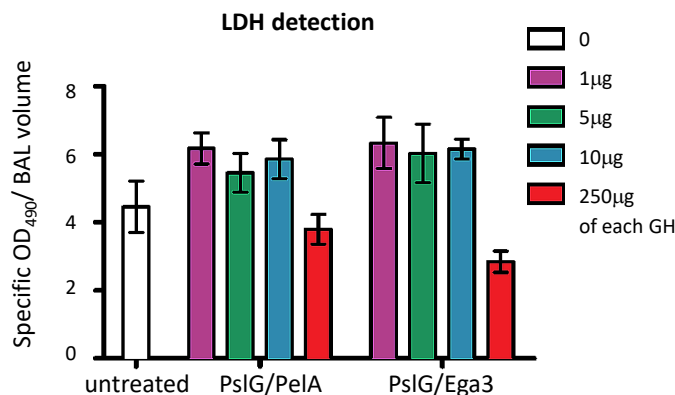


Figure 21. Quantification of lactate dehydrogenase (LDH) activity in the bronchoalveolar fluid harvested from mice 7 days following treatment with a single dose of the indicated GH combination.

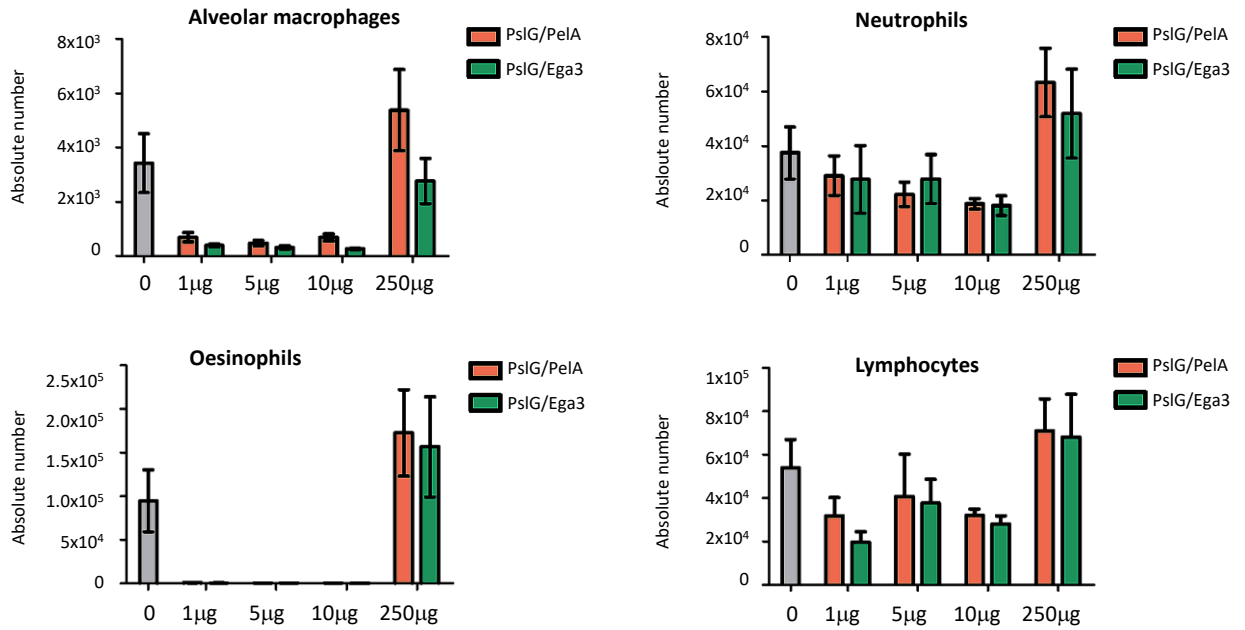


Figure 22. Absolute quantification of leukocyte populations in mouse lungs as measured by flow-cytometry performed on lung digests. Lungs were harvested 7 days following treatment with a single dose of the indicated GH combination.

**Conclusion for Subtask 4:** As anticipated, treatment of immunosuppressed mice with GH combination therapy, demonstrated that intratracheal inoculation at doses of up to 250 µg of each hydrolase (i.e. a maximum of 500 µg of the combine therapy) were well tolerated.

**Major Task 2 Conclusion:**

All GH combinations tested were well tolerated by the host, both in immunocompetent or immunosuppressed mice with the exception of Ega3 produced in *Pichia*. We successfully mitigated this issue by producing Ega3 in mammalian HEK cells. This version of the protein was well tolerated, as detailed in Major Task 4 below. As predicted, immunosuppression reduced the pulmonary recruitment of eosinophils and other leukocytes following GH therapy.

**Milestone Achieved: Evaluation of pulmonary toxicity of candidate hydrolase regimens.**

### **MAJOR TASK 3: PHARMACOKINETIC STUDIES OF CANDIDATE HYDROLASES.**

**Subtask 1: Express and purify recombinant PelA and PslG for subtasks 3 – 4.** Dr Howell's lab. SOW Time Period: Months 6-12. Completion level = 100%.

As presented in Major Task 1 – Subtask 1, sufficient protein, both in quantity and quality (endotoxin-free enzyme, verified activity) was produced to meet all requirements for the other subtasks of Major Task 2.

**Subtask 2: Test pharmacokinetics of GHs** (Sph3, Ega3, PelA and PslG/PelA and PslG/Ega3 combinations) **in immunocompetent mice** [25 mice per group (5 per time point) X 5 GH therapies; 1 group of 25 untreated mice. All performed in duplicate = 300 mice]. Dr Howell and Sheppard's labs. Combined with **Subtask 4: Determine concentrations of candidate hydrolases and their combinations using animal tissue samples.** Dr Howell and Dr Sheppard's lab. SOW Time Period: Months 6-12. Completion level = 100%

#### Background:

Determining the pulmonary GH pharmacokinetics is critical for the design of efficacy studies. Prior to the start of this project polyclonal antibodies that recognize Sph3, PelA or PslG had been produced by our group. As part of this project, we have successfully produced and characterized a polyclonal anti-Ega3 antibody.

#### Accomplishments:

##### 1- Production and validation of an anti-Ega3 antibody.

*Rationale:* The anti-Ega3 antibody was produced using Ega3 produced in *P. pastoris*. The initial validation and pharmacokinetics assays were therefore performed with this protein.

In year 2, as detailed in "MAJOR TASK 4, Subtask 5", we transferred the production of Ega3 in the mammalian cell line HEK293. Comparison between *P. pastoris* produced and HEK293 produced Ega3 showed that our anti-Ega3 antibody recognizes the two GHs with similar efficiency, and that the protein's pharmacokinetics in immunocompetent mice was comparable too. Although we initially begun MAJOR TASK 3 using the *P. pastoris* produced Ega3, the final data presented below were generated with the HEK293 produced Ega3.

*Methodology:* Purified *P. pastoris* produced Ega3 was used to generate antiserum from rabbits. The polyclonal antibodies were produced by CedarLane Laboratories (Burlington, Ontario). The polyclonal anti-Ega3 antibodies produced were evaluated by Western blot analysis using recombinant Ega3 both with and without endoglycosylase (EndoH) treatment. *Results:* Serum from Ega3-vaccinated rabbits recognizes both glycosylated (Ega3) and deglycosylated (Ega3 +EndoH) *in vitro* (Figure 23).

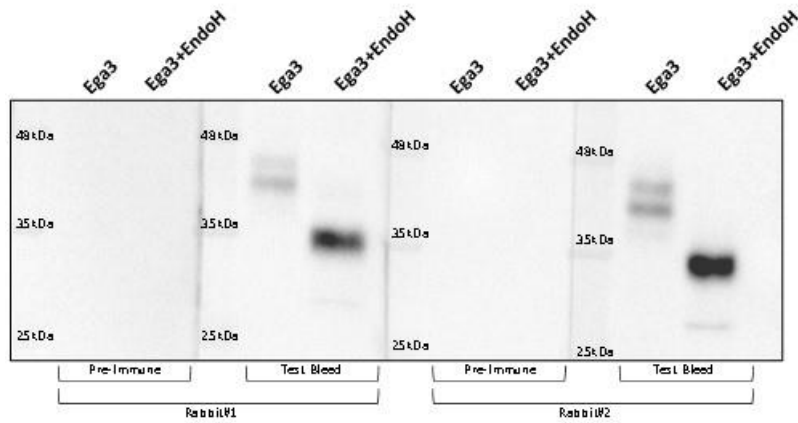


Figure 23. Western-blot of endoglycosylase-H treated or untreated purified Ega3, using rabbit anti-Ega3 antibody from the first bleed as a primary antibody, and goat-anti-rabbit-HRP antibody as a secondary. GH load was 1  $\mu$ g per well and the antibody was diluted 1/1000.

The terminal bleed confirmed the results observed with the first bleed (Figure 24).

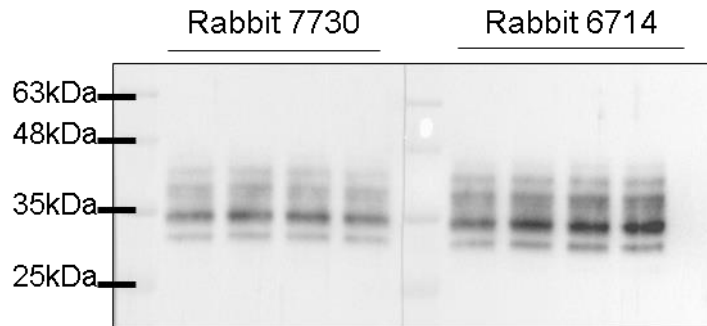


Figure 24. Western-blot of purified Ega3, using rabbit anti-Ega3 antibody from terminal bleed as a primary antibody, and goat-anti-rabbit-HRP antibody as a secondary. GH load was 1  $\mu$ g per well and the antibody was diluted 1/1000.

The anti-Ega3 antibody was thereafter tested against Ega3 as diluted in lung homogenate after tracheal injection in mice (Figure 25).

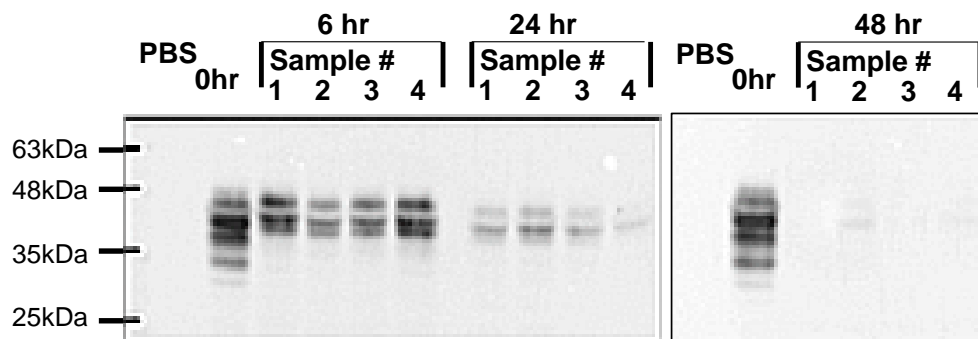
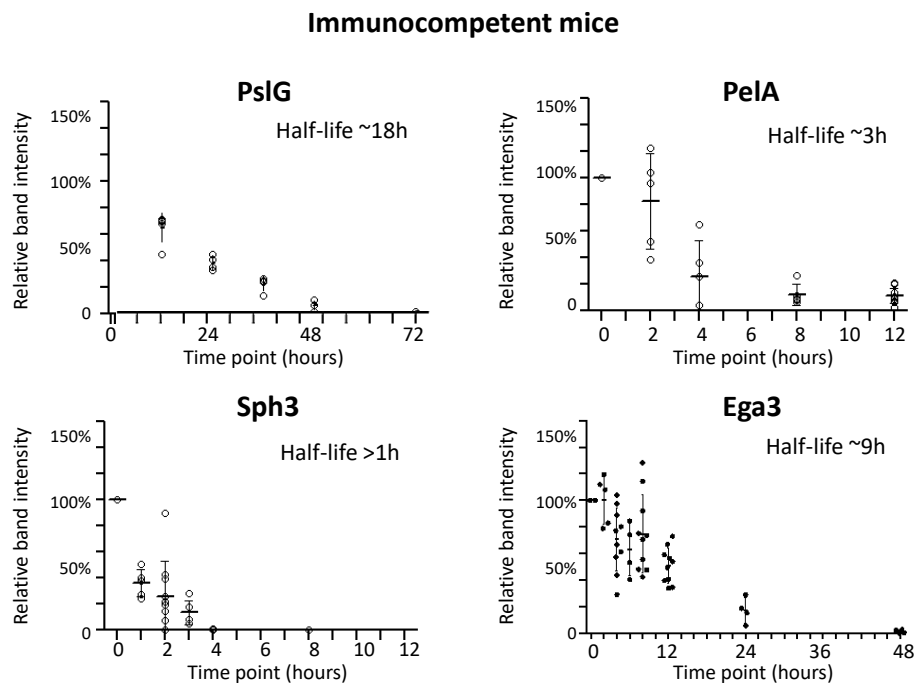


Figure 25. Western-blot of lung homogenates from lung harvested at 0, 6, 24 or 48h after intratracheal injection of 500  $\mu$ g of purified Ega3.

## 2- Pharmacokinetics of recombinant GHs in lungs of immunocompetent mice.

**Methodology:** GHs were administered intratracheally to BALB/C female mice at a dose of 500 µg for single GHs or 250 µg of each GH if they were injected in combination. At time points ranging from 1 to 48 h after GH administration, the mice were sacrificed and their lungs harvested and homogenized in phosphate buffer and a cocktail of protease inhibitors. Lung homogenates were analyzed by Western-blotting using rabbit anti-GH antibodies. A goat-anti-rabbit-HRP antibody was used as the secondary antibody; HRP signal was detected and analyzed by densitometry whereby the percent band intensity was normalized to the total band intensity at the 0h time point for each mouse. A minimum of 4 mice were used for each time point in each experiment. Following the results of the first experiment, earlier or later time-points were added as required to map out the half-life of each GH.

**Results:** All GHs were specifically detected by Western-blot in lung homogenates at early time-points (data not shown), as seen with Ega3 in Figure 25, above. All GHs and GH combinations were assayed a minimum of twice. All pharmacokinetics data were derived from densitometry analysis of Western-blot and are presented graphically in Figure 26. GHs exhibited a wide range of pulmonary half-lives, from less than 1h (Sph3) to 18h (PslG) when administered as monotherapy (Figure 26, Table 3). When administered as combination therapy, we observed that the half-life of PslG was reduced, while PslA and Ega3 half-lives were increased (Figure 26, Table 3).



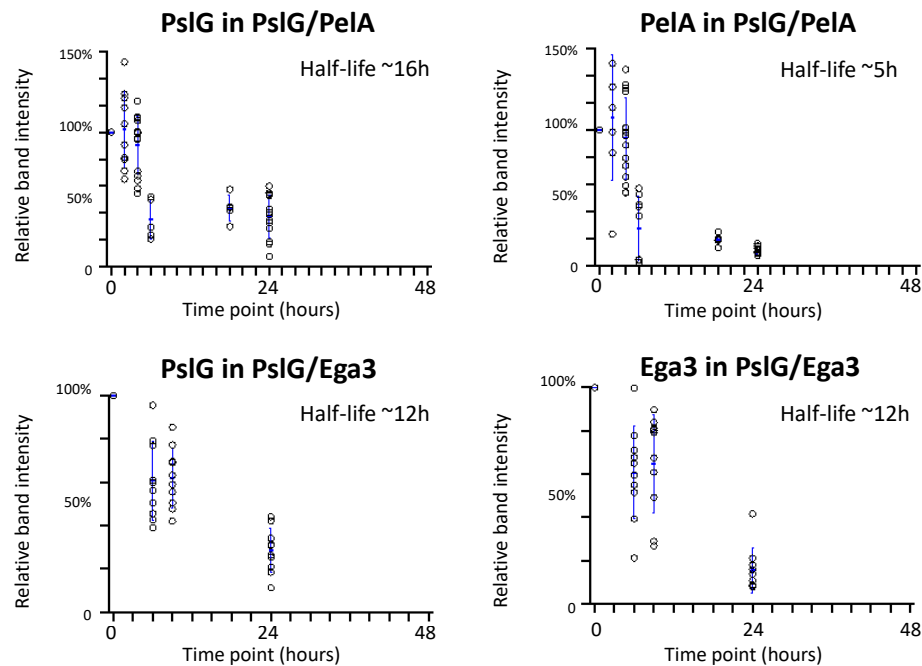


Figure 26. Determination of pulmonary GH pharmacokinetics by Western-blot analysis. GHs were intratracheally administered to immunocompetent mice at a dose of 500  $\mu\text{g}$  of GH if injected alone, or as a mix of 250  $\mu\text{g}$  of each GH if injected as a GH combination. Each square represents the densitometry value from a single mouse. Results are corrected for background signal obtained from untreated mouse lung samples and normalized to the total band intensity at 0h for each GH. Graphs represent the compilation of all experiments performed during the grant period.

**Subtask 3: Test pharmacokinetics of hydrolases (Sph3, Ega3, PeIA and PsIG/PeIA and PsIG/Ega3 combinations) in immunosuppressed mice** [25 mice per group (5 per time point) X 5 hydrolase therapies; 1 group of 25 untreated mice. All performed in duplicate = 300 mice. Howell and Sheppard's labs. Combined with **Subtask 4: Determine concentrations of candidate hydrolases and their combinations using animal tissue samples.** Dr Howell's lab. SOW Time Period: Months 6-12. Completion level = 100%.

Accomplishments:

*Methodology:* Two days prior to treatment, mice were immunosuppressed by injection of 250 mg/kg cortisone subcutaneously and 250 mg/kg cyclophosphamide intraperitoneally. GH injection, lung treatment and pharmacokinetics were performed as described above (Subtask 2).

*Results:* As was observed in immunocompetent mice, GHs exhibited a wide range of pulmonary half-lives, from 3h (Sph3) to 36h (PsIG) (Figure 27, Table 3). The half-life of most GHs (PsIG, PeIA and Sph3, but not Ega3) was increased in leukopenic mice, suggesting that degradation of GHs may at least in part be leukocyte-dependent. Similar to the findings in immunocompetent mice, when GHs were injected in combination, the half-life of PsIG half-life was reduced, while that of Ega3 was increased (Figure 27, Table 3). PeIA half-life was also reduced but to a lesser degree.

### Immunosuppressed mice

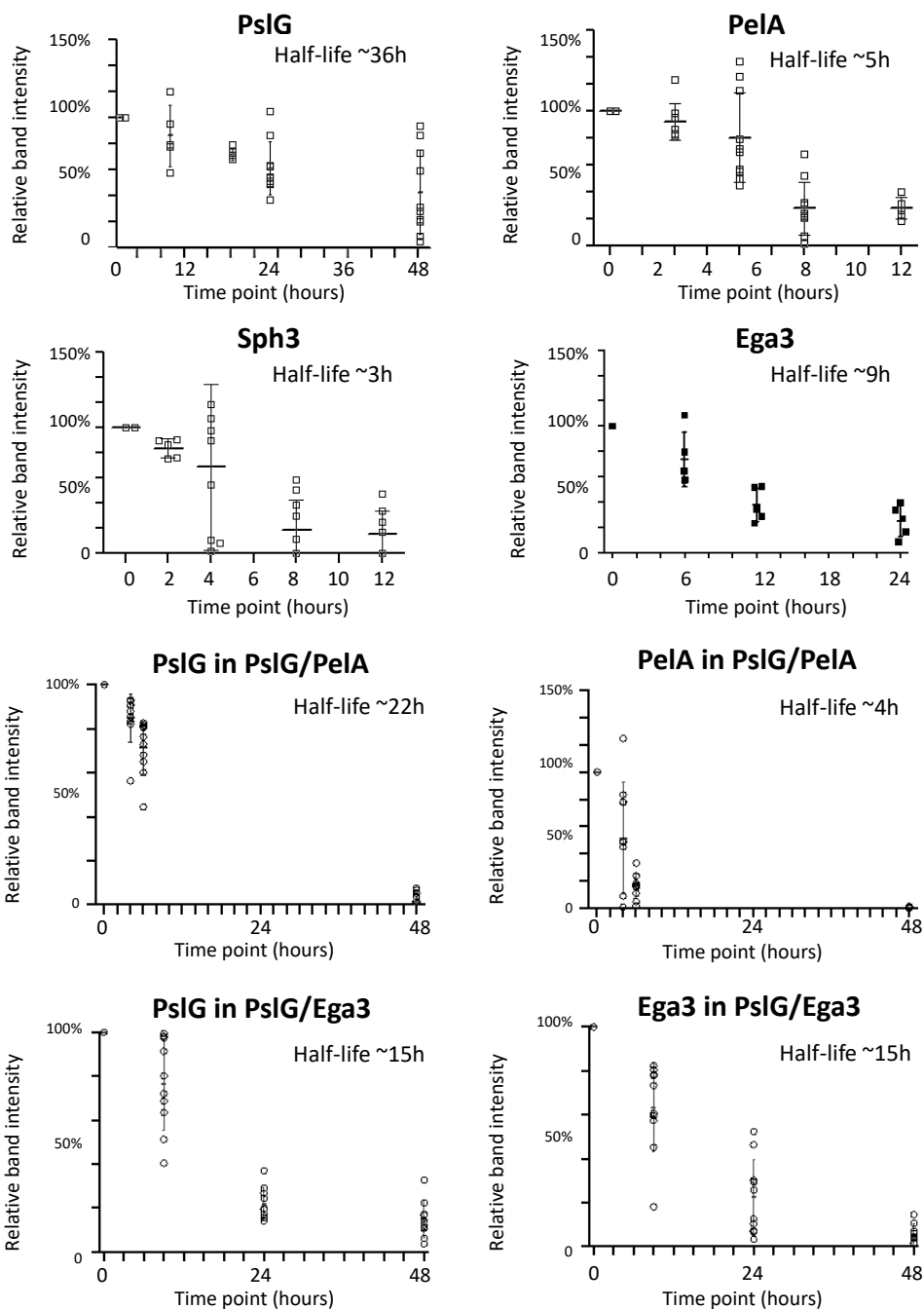


Figure 27. Determination of pulmonary GH pharmacokinetics by Western-blot analysis GHs were intratracheally administered to immunosuppressed mice at a dose of 500  $\mu\text{g}$  of GH if injected alone, or as a mix of 250  $\mu\text{g}$  of each GH if injected as a GH combination. Each square represents the densitometry value from a single mouse. Results are corrected for background signal obtained from untreated mouse lung samples and was normalized to the total band intensity at the 0h time point for each GH. Graphs represent the compilation of all experiments performed during the grant period.

Table 3 summarizes the final pharmacokinetics of GHs as determined by all experiments in **Subtasks 2, 3 and 4.**

Hydrolase	PslG	PelA	Ega3	Sph3	PslG/PelA		PslG/Ega3	
					PslG	PelA	PslG	Ega3
Estimated half-life in immunocompetent mice (Subtask 2)	18h	3h	9h	1h	16h	5h	12h	12h
Estimated half-life in immunocompromised mice (Subtask 3)	36h	5h	9h	3h	22h	4h	15h	15h

Table 3. Estimation of half-life of GHs in mouse lung following intratracheal injection of 500 µg of pure GH in PBS or a combination of 250 µg of each of two GHs administered simultaneously.

**Milestone Achieved: Evaluation of pharmacokinetics of candidate hydrolase regimens.**

#### **MAJOR TASK 4 (as required): DEVELOPMENT OF CANDIDATE HYDROLASE VARIANTS.**

##### *Rationale:*

The results of our pharmacokinetics studies suggest that modification of some of the GHs may be required to increase their half-life. The *in vivo* half-life of PslG was estimated above 18h in immunocompetent mice, and 36h in immunosuppressed mice, thus modification of this GH to increase its pharmacokinetic profile is not required at present. In contrast, the 3 other GHs showed half-lives shorter than 12h, especially Sph3 with a half-life of less than 3h in both mouse models (Table 3). Modification of these GHs may therefore be warranted.

**Subtask 1: Express and purify recombinant PelA and PslG for subtasks 3 – 4.** Dr Howell's lab. SOW Time Period: Months 9-15. Completion level = 100%.

As presented in Major Task 1 – Subtask 1, sufficient protein, both in quantity and quality (endotoxin-free enzyme, verified activity) was produced to meet all requirements for the other subtasks of Major Task 2.

**Subtask 2 and 3: Test protease resistance of candidate hydrolases against *A. fumigatus* and *P. aeruginosa* isolates** in the epithelial cell damage assay using western blot analysis and mass spectrometry (as required). Dr Howell and Sheppard's labs. Months 9-15. Completion level = 100%.

1- Sensitivity to proteases present in BAL fluids, in mouse lung homogenates and Af293 culture supernatant.

*Methodology:* BAL fluid and lung homogenate were collected from uninfected mice. Lungs were harvested and resuspended in phosphate buffer saline (PBS) without protease inhibitors (these lung homogenates were therefore protease inhibitor-free, unlike most other lung homogenates generated and used during this grant period).

To generate *A. fumigatus* Af293 culture supernatants,  $10^6$  conidia were grown for 3 days in 100 mL of Brian synthetic medium, then culture supernatants were harvested and filter sterilized.

For the protease resistance assay, 1  $\mu$ g of-GH was incubated at 37 °C with 60  $\mu$ l of either BAL fluid, lung homogenate, fungal culture supernatant, or PBS with or without commercial protease at 100  $\mu$ g/mL. Samples were collected at the indicated time points. GH degradation was stopped by adding SDS-PAGE buffer and samples were analyzed by SDS-PAGE and Western-blotting.

*Results:* We observed that both Sph3 and PelA were resistant to the proteases present in BAL fluids and lung homogenates obtained from non-infected mice for up to 24 h (Figure 28). Surprisingly, GHs appeared to degrade faster in PBS buffer than in BAL fluids and lung homogenates.

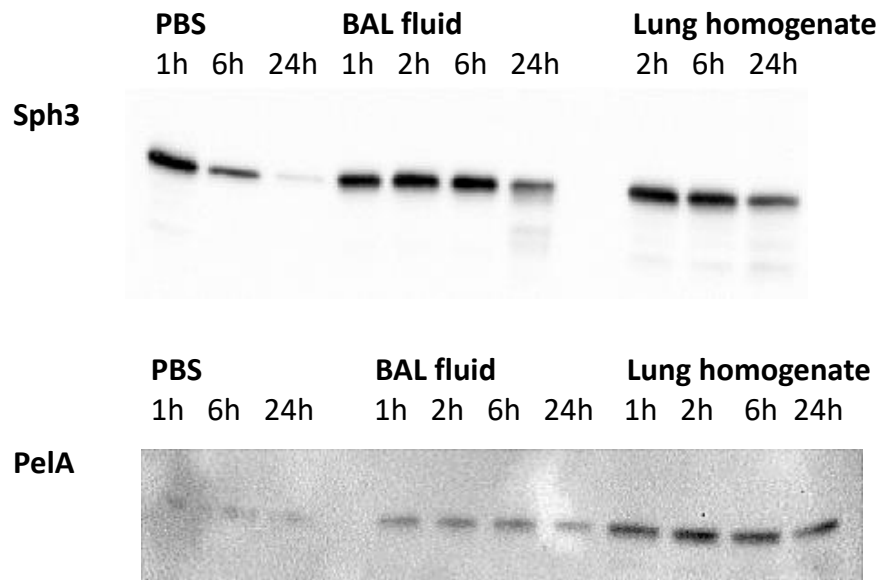


Figure 28: Western-blot monitoring of Sph3 and PelA persistence in PBS, BAL fluids and lung homogenates obtained from non-infected mice.

As these results did not reproduce the short half-lives we determined for these GHs (Table 3), we hypothesized that GH therapy could induce the production of pulmonary proteases. We therefore tested the effects of lung homogenates and BAL fluid from mice pre-exposed to the GH Sph3 on the stability of Sph3 and PelA.

*Methodology:* A single dose of 500  $\mu\text{g}$  of Sph3 was administered intratracheally to immunocompetent mice. The animals were then sacrificed, after 1 day. The lungs were harvested and homogenized as described above. Treated lung homogenate protease activity was assayed against GHs as described above, and in parallel with commercial proteases, BAL fluids and *Aspergillus* culture supernatant.

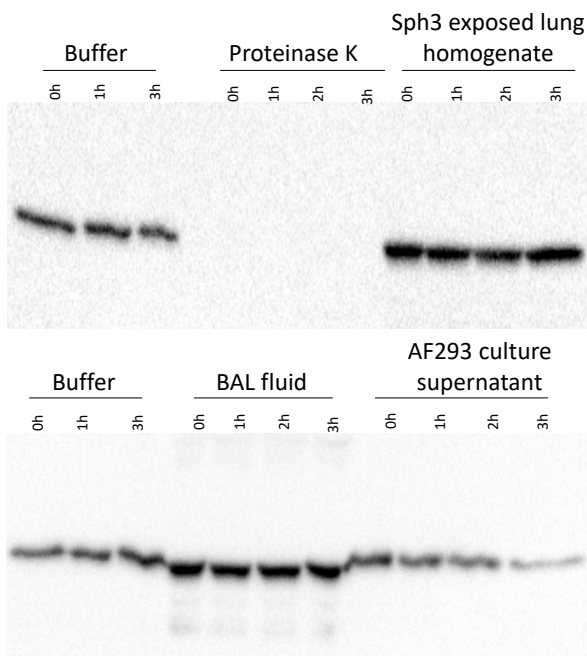
*Results:* Pre-exposing healthy mice to Sph3, one day prior to lung harvesting, did not increase the susceptibility of Sph3 and PelA to proteases present in the lung homogenate (Figure 29): GH degradation was observed only after 24h of incubation, similar to that observed with non-GH exposed lungs (Figure 28).

When incubated with Af293 culture supernatant, GH degradation was visible only at 24h incubation.

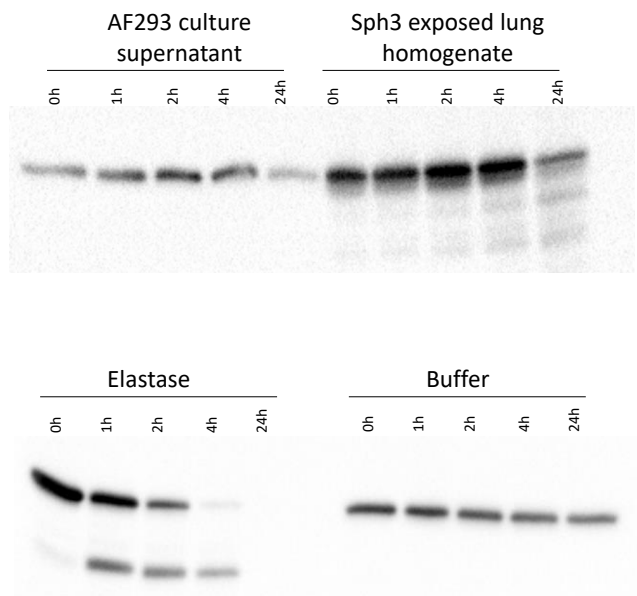
Commercial proteases showed faster proteolysis of GHs: elastase degraded GHs within 1h, proteinase K degraded them in the short time between addition of the protease and sample analysis.

### Sph3

#### First assay

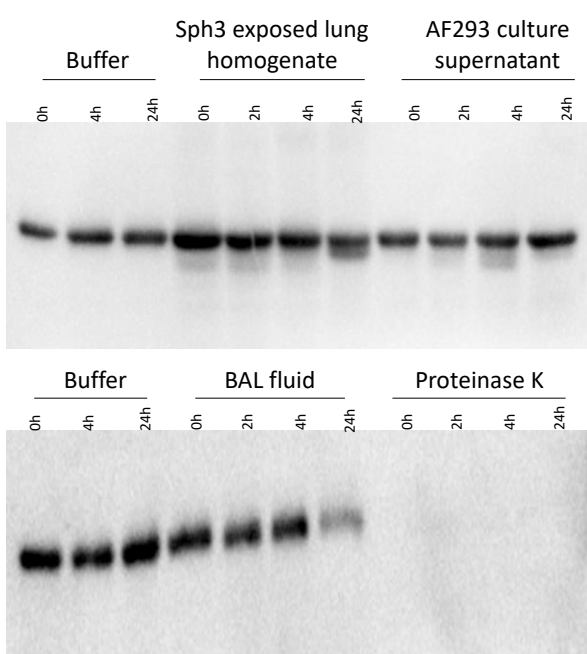


#### Second assay



### PelA

#### First assay



#### Second assay

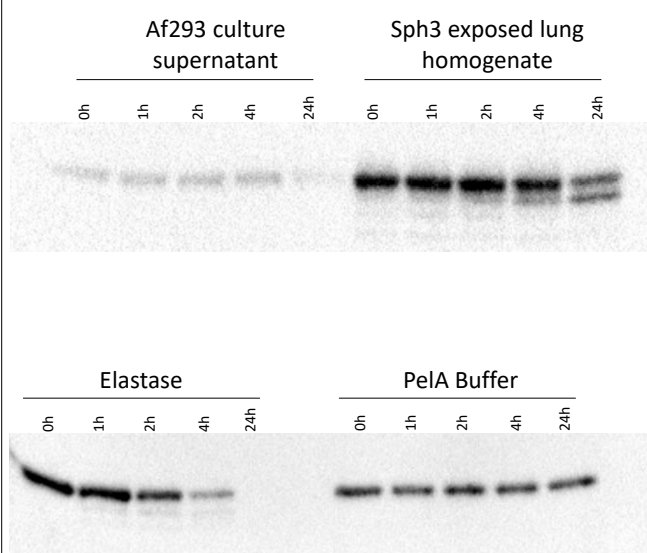


Figure 29: Western-blot monitoring of Sph3 and PelA persistence in BAL fluids and lung homogenates obtained from non-infected mice, in parallel with GHs incubated with commercial proteases (elastase, proteinase K) or *A. fumigatus* culture supernatant.

Degradation by elastase is of interest since this protease is secreted by mammalian neutrophils and we observed an increase in GH half-life in mice rendered neutrophil deficient. As a consequence of this observation, we decided to investigate further GH sensitivity to commercial elastase and to mammalian neutrophil lysate.

## 2- Sensitivity of GHs to commercial elastase.

*Methodology:* 1  $\mu\text{g}$  of-GH was incubated at 37  $^{\circ}\text{C}$  in 60  $\mu\text{l}$  of PBS with or without commercial protease at 100  $\mu\text{g}/\text{mL}$ . At the indicated time points, GH degradation was stopped by adding SDS-PAGE buffer and samples were analyzed by SDS-PAGE and Western-blotting.

*Results:* As previously observed, GHs were sensitive to elastase (Figure 30). Interestingly, the sensitivity was proportional to the measured pharmacokinetics in immunocompetent mice: intact Sph3, PeIA and PslG were detectable up to 4h, 6h and more than 24h, respectively, when exposed to elastase, vs. half-lives of less than 1h, 3h and 18h in mice (Table 3).

For PslG, the main degradation observed was the removal of the 6-Histidine tag as determined by mass spectroscopy (data not shown). Of note, PslG is the GH with the longest half-life in mice.

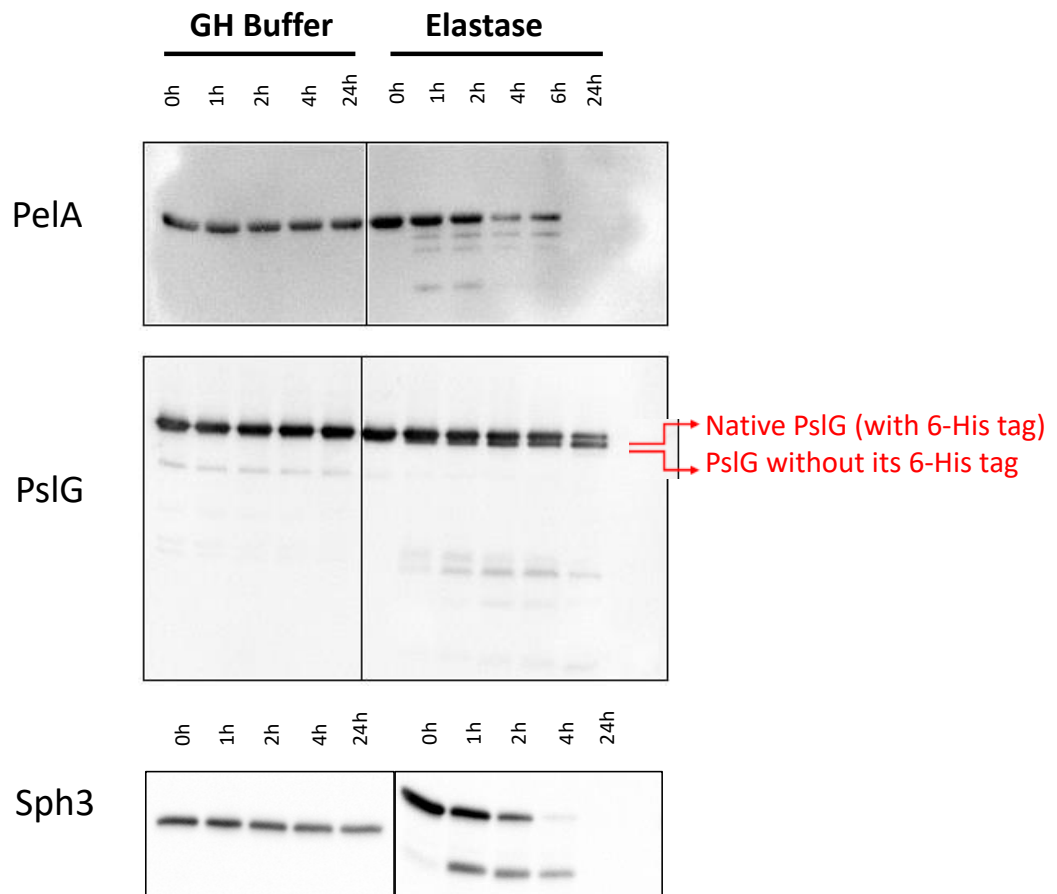


Figure 30: Western-blot monitoring of PeIA, Sph3 and PslG persistence when 1  $\mu\text{g}$  of GH was incubated with 60  $\mu\text{l}$  of elastase at 100  $\mu\text{g}/\text{mL}$ .

## 3- Sensitivity of GHs to neutrophil lysate.

**Methodology:** Cells from the HL60 cell line (derived from peripheral blood leukocytes in a human patient with acute promyelocytic leukemia) were propagated *in vitro*, then differentiated into neutrophils by exposure over 3 days to dimethylsulfoxide (DMSO, 1.3%) and retinoic acid (2.5  $\mu$ M). Differentiated cells were then activated by 1 h exposure to N-formylmethionyl-leucyl-phenylalanine (fMLP, 100 nM), concentrated to  $2 \times 10^7$  cells/ml by gentle centrifugation and stored at  $-80^\circ\text{C}$  until required. On the day of the protease assay, a frozen sample was thawed and vortexed, then either sonicated or treated with RIPA buffer (150 mM NaCl, 5 mM EDTA, 50 mM Tris pH 8, 1% NP40 and 0.1% SDS) to facilitate lysis of the cells. Cell debris were removed by centrifugation. The supernatant was named HL60 lysate and was used in the proteolytic assay. A mix of 1  $\mu$ g of GH and 100  $\mu$ L of HL60 lysate or control buffer was incubated at  $37^\circ\text{C}$ . At the indicated time points, GH degradation was stopped by adding SDS-PAGE buffer and samples were analyzed by SDS-PAGE and Western-blotting with our specific anti-GH antibodies.

**Results:** Little degradation of PelA or Sph3 was observed before 24h when mixed with neutrophil proteases (Figure 31). It is possible that the neutrophil proteases released from  $2 \times 10^7$  cells are not sufficient to degrade the GHs.

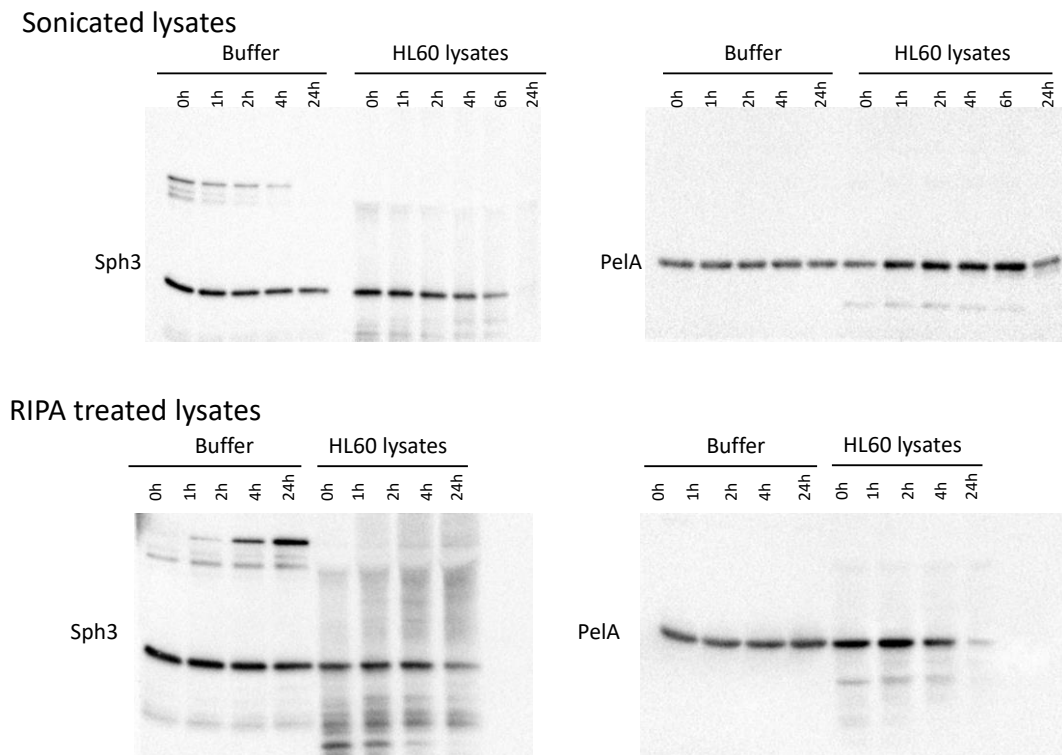


Figure 31: Western-blot monitoring of *in vitro* PelA and Sph3 persistence when 1  $\mu$ g of GH was incubated with 60  $\mu$ L of neutrophil lysates (HL60 lysates).

**Subtask 4: Test chemical modification as a means to increase the stability of candidate hydrolases.** Dr Howell's lab. Months 9-21. Completion level = 100%

*Rationale:* Our pharmacokinetic studies demonstrated that PelA and Sph3 have short half-lives (less than 6h for PelA, and less than 2h for Sph3), in both immunocompetent and immunocompromised mice. In an attempt to improve the stability of these proteins *in vivo*, our first strategy has been to chemically link polyethyleneglycol (PEG) to lysine residues of the GHs. This is one of the most common techniques used to improve stability without affecting the activity of an enzyme.

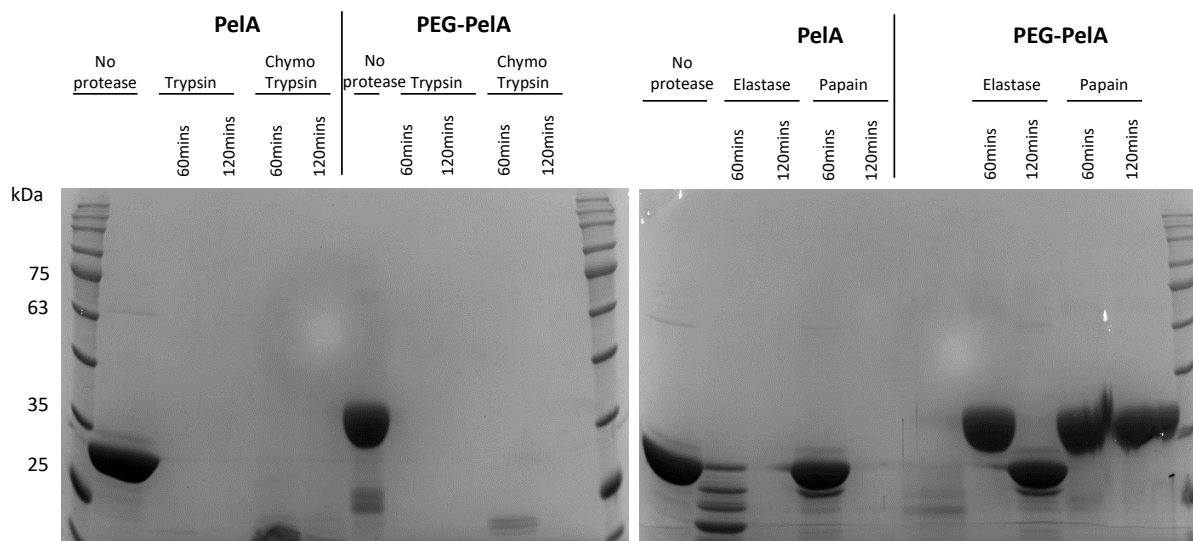
*Methodology:* PEGylation of GHs was performed by using a commercial kit (EZ-Link™ NHS-PEG4 Biotinylation Kit) following manufacturer's instructions. GH modification was visualized on SDS-PAGE as a shift in the migration of the enzyme. GH activity was assayed as previously described (Major task 1 Subtask 1 page 13).

For the protease resistance assay, 1 µg of GH was incubated at 37 °C with 60 µl of either lung homogenate or PBS with or without commercial proteases (trypsin, chymotrypsin, elastase and papain) at 100 µg/mL. At the indicated time points, GH degradation was stopped by adding SDS-PAGE buffer and samples were analyzed by SDS-PAGE and Western-blotting.

*Results:* PEGylation of both PelA and Sph3 was accomplished, as illustrated by the molecular weight shift of the corresponding band in SDS-PAGE (Figure 32). Biofilm disruption assays also showed that PelA retained its enzymatic activity after PEGylation (Figure 33)

Although PEGylation process of PelA and Sph3 was successful and did not affect the enzymatic activity of the GHs, it provided only limited protection against elastase (1h protection), and none against trypsin and chymotrypsin (Figure 33). Only significant protection was against degradation by papain.

In subtask 2, above, we showed that the proteases contained in the lung homogenate failed to degrade Sph3 and PelA. The PEGylated version of these GHs showed the same resistance profile (Figure 34).



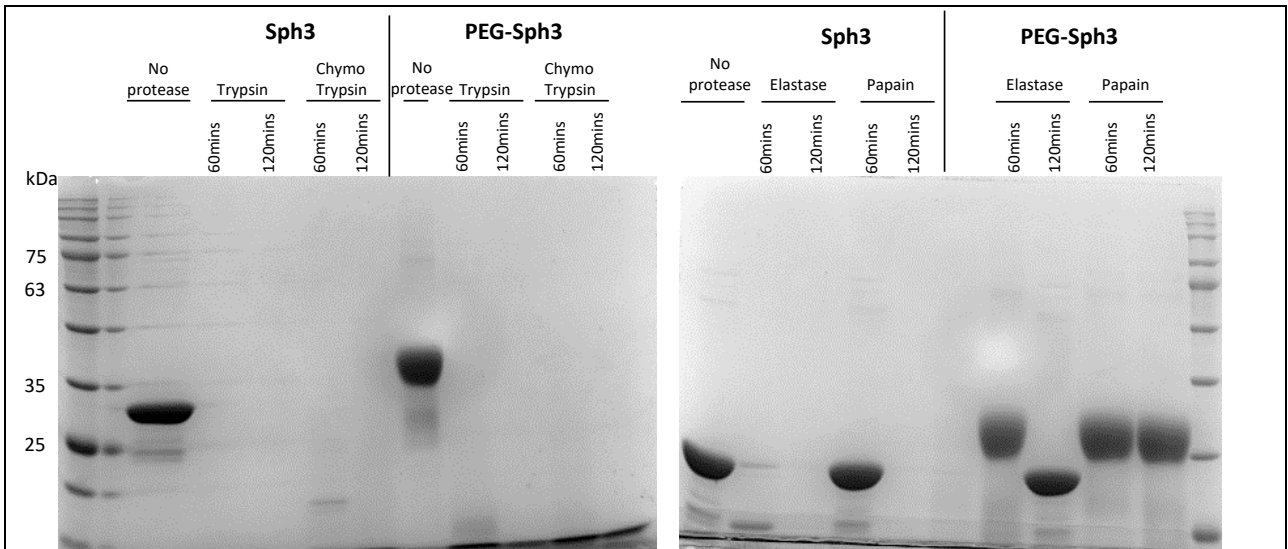


Figure 32. Coomassie stained SDS PAGE gel of native and PEGylated PelA and Sph3. When indicated, an incubation of 60 min or 120 min was performed with the appropriate protease.

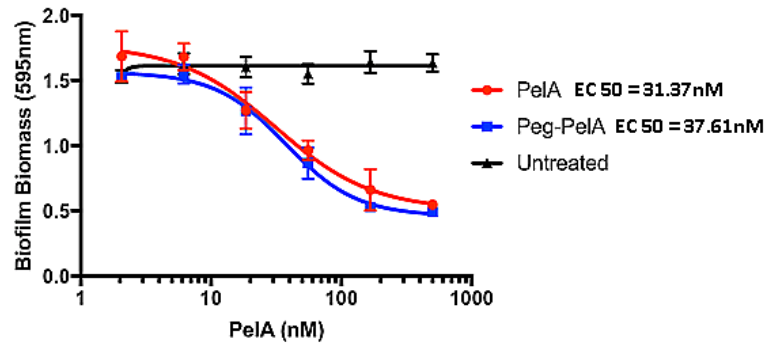


Figure 33: Biofilm disruption assay against *P. aeruginosa* biofilms was performed with native and PEGylated PelA to test the effects of PEGylation on GH activity.

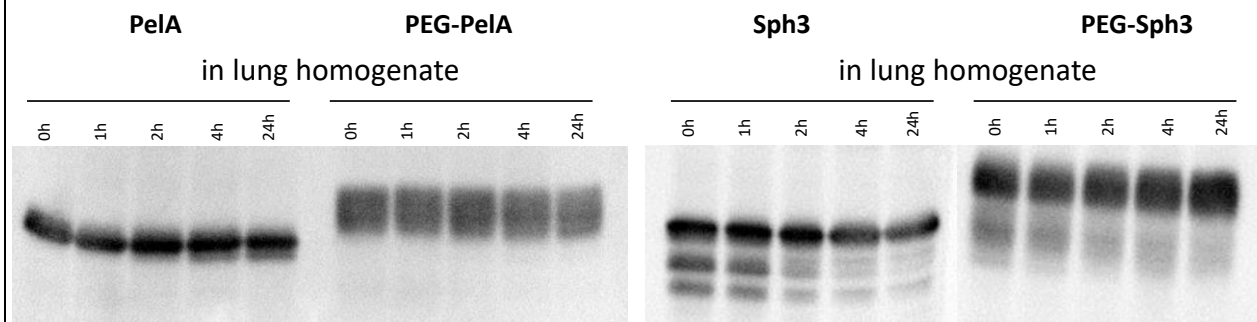


Figure 34. Western-blot monitoring of the persistence of Sph3, PelA and their PEGylated versions, in lung homogenates obtained from non-infected mice.

Given that elastase is important in neutrophils related proteolytic processes, and given that PEGylation provided GHs with a moderate resistance to that protease, we prioritized elastase for further study.

*Methodology* was the same as described above, with an additional step: Western-blots were analyzed by densitometry and graphs were generated to reflect the band intensity changes.

*Results:* in contrast to our previous results, we found that PEGylation decreased the half-life of elastase treated Sph3 and PeIA by approximately 1 hour (Figure 35).

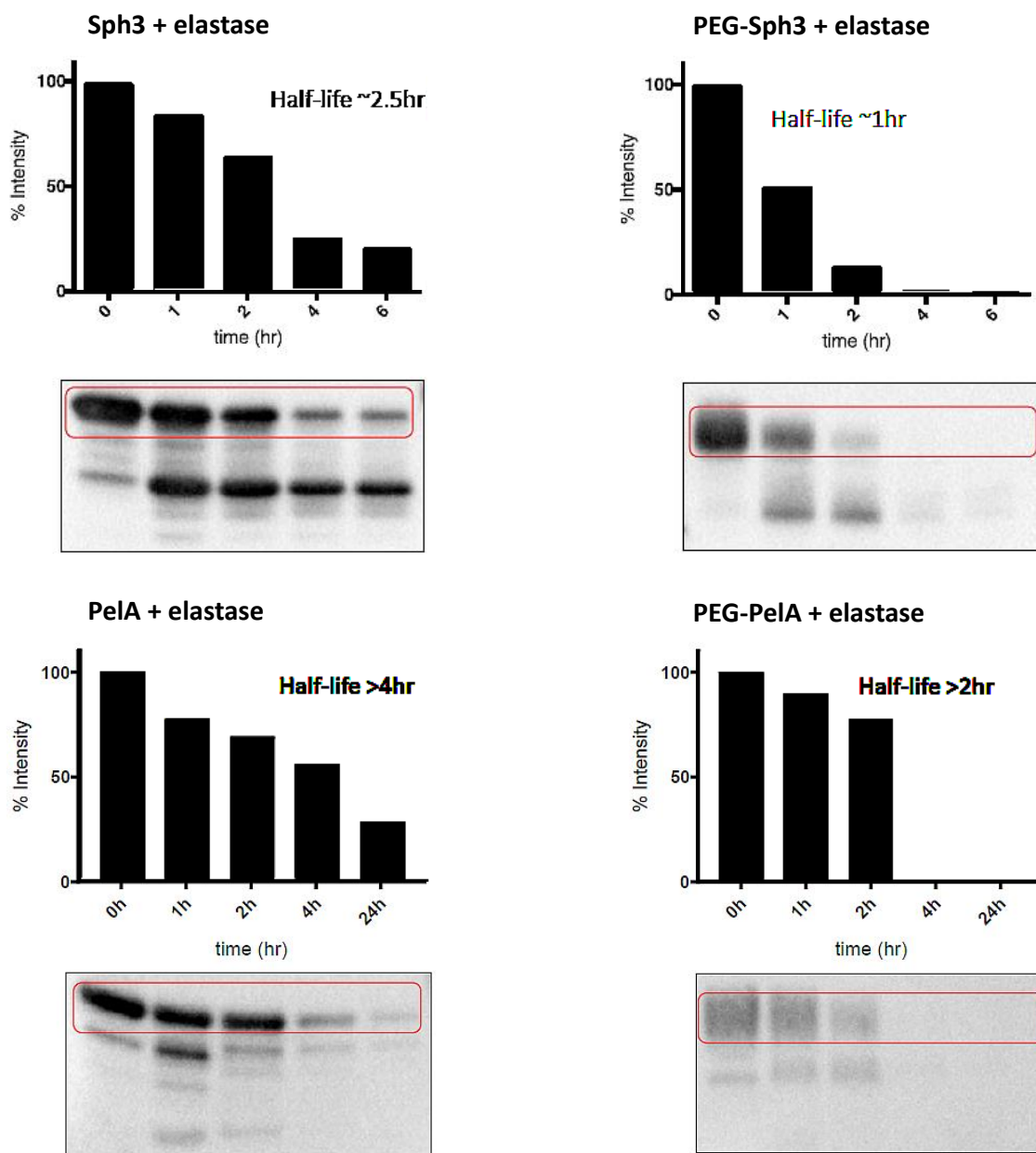


Figure 35. Western-blot monitoring and band density study of Sph3, PeIA and their PEGylated versions persistence when 1 µg of GH was incubated with 60 µl of elastase at 100 µg/mL.

*Subtask 4 conclusion:*

The results of the chemical modifications of hydrolases by PEGylation gave conflicting results and did not show any significant increase in stability of the proteins tested. As other methods (see

Subtask 5, below) of finding more stable variants proved to be more successful, we have abandoned the chemical modification approach.

**Subtask 5: Test site-specific modification as a means to increase the stability of candidate hydrolases.** Dr Howell's lab. Months 9-21. Completion level = 100%

#### **A. Production of Ega3 in a mammalian system.**

Production of Ega3 had to be performed in an organism different from *E. coli* in order to meet our needs in terms of GH amount and purity (endotoxin-free especially) and because, unlike the other GHs, Ega3 was insoluble when produced by *E. coli*. We successfully produced Ega3 in *P. pastoris*, as previously detailed in Major Task 1 Subtask 1 (pages 10-13). The recombinant protein was soluble and endotoxin-free, but as *P. pastoris* is a eukaryotic organism, the resulting protein exhibited fungal-specific glycosylation. We hypothesized this glycosylation pattern was responsible for the higher levels pulmonary eosinophil recruitment seen with this protein, as detailed in Major Task 2 Subtask 3-4 (pages 23-30). Therefore we have explored the possibility of expressing Ega3 in a human embryonic kidney cells line (HEK293) to generate a glycosylated GH which is soluble but which mimics mammalian-like glycosylation patterns.

##### 1- Production of Ega3 in a mammalian cell line and validation.

**Methodology:** The His-tagged *ega3* coding sequence was cloned into a pHL-sec vector under the control of a mammalian promoter. Two different constructs of Ega3 were cloned into the vector: Ega3<sub>46-318</sub> (referred to as Ega3-DSS) and Ega3<sub>68-318</sub> (referred to as Ega3-68) (Figure 36).



Figure 36: Predicted domain boundaries of *ega3* from *A. fumigatus*. Grey arrows indicate that two start sites for the constructs being expressed in Freestyle 293 F and Freestyle 293 S cells. (TM = transmembrane domain).

The plasmids were then transfected into mammalian cell lines (HEK-293 “Freestyle” F and HEK-293 “Freestyle” S) for expression trials using FectoPro transfection reagent. The culture supernatants containing the secreted proteins were harvested at 3 and 6 days to check for protein yield. It was established that incubation of the cells for 6 days post-transfection was essential for optimal protein expression. The cells were spun down and the secreted protein from the supernatant was purified by affinity chromatography, using a His-Trap Column.

Enzymatic activity was evaluated using our standard biofilm assay (Major Task 1 Subtask 1 page 13).

**Results:** In the absence of glycosylation, the expected size is 32 kDa for Ega3 and Ega3–DSS, and 30 kDa for Ega3–68 (loss of the transmembrane domain). Analysis under denaturing conditions (SDS-PAGE) showed a shift in migration for all Ega3 proteins, confirming that Ega3 was glycosylated when produced in a yeast system (*P. pastoris*) as well as in a mammal system (HEK293) (Figure 37).

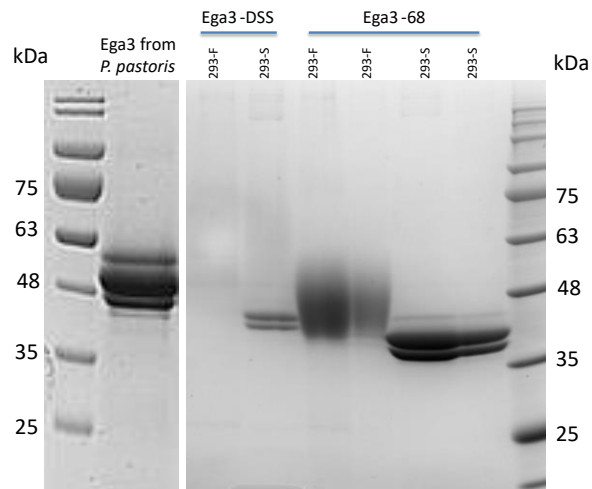


Figure 37. Coomassie stained SDS-PAGE of Ega3 produced in *P. pastoris* or in freestyle HEK expression systems (Ega3-DSS and Ega3-68), following purification.

The expression protocol for these constructs was optimized in the two cell lines to reach yields similar to the *P. pastoris* expression. Ega3-68 showed better expression and yielded 7 mg GH / 200 ml of cell culture (data not shown). When assayed against biofilms of *P. aeruginosa* and of *A. fumigatus*, Ega3-68 showed similar activity, irrespective of the cell line used to produce it (Figure 38). Importantly, that enzymatic activity was comparable to the protein produced in *P. pastoris* (Table 4). This Ega3-68 construct was therefore chosen for further functional studies.

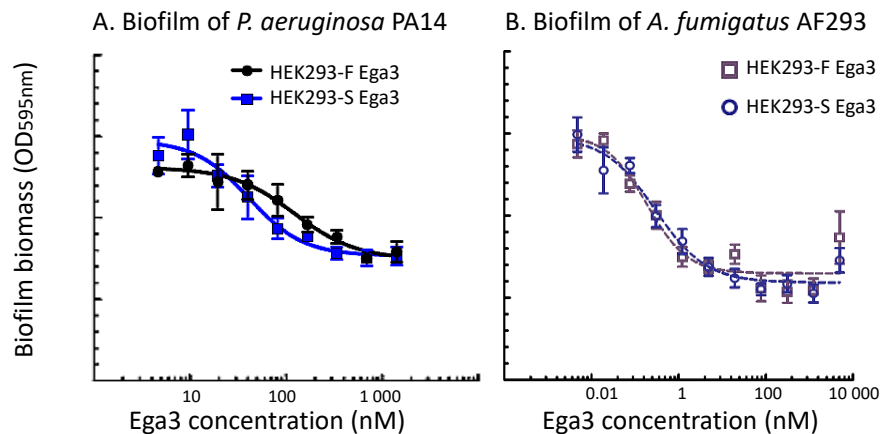


Figure 38: Biofilm disruption assay using Ega3 produced in HEK293-F or in HEK293-S cells against biofilms of (A.) *P. aeruginosa* strain PA14 and (B.) *A. fumigatus* Af293.

Producing organism or cell line	EC <sub>50</sub> on <i>A. fumigatus</i> Af293 biofilm	EC <sub>50</sub> on <i>P. aeruginosa</i> PA14 biofilm
<i>Pichia pastoris</i>	0.70 nM	94.7 nM
HEK293-S	0.19 nM	35.1 nM
HEK293-F	0.29 nM	86.5 nM

Table 4: Comparative table of Ega3 EC<sub>50</sub> from different organisms or cell lines. Data were obtained using our standard crystal violet biofilm disruption assay against biofilms of *A. fumigatus* Af293 and *P. aeruginosa* strain PA14.

## 2- Pulmonary tolerability of HEK293-produced Ega3

Tolerability studies of Ega3 as shown in Major Task 2 were performed with Ega3 from *P. pastoris*. As we anticipated moving to the use of HEK293-produced Ega3, it was necessary to reassess the tolerability of this new GH preparation.

**Methodology:** Recombinant Ega3 was administered intratracheally at a single dose of 100 or 500 µg in immunocompetent mice. Mice were monitored for 7 days, then sacrificed to perform immunoprofiling and assess tissue injury. All assays were performed as 2 independent experiments, with groups of 5 mice per condition: 4 mice had their lungs harvested, lavaged for measurement of lactate dehydrogenase (LDH) or total protein release (using a bicinchoninic acid (BCA) assay) and digested with collagenase for pulmonary leukocyte recruitment by flow-cytometry. The lungs of the remaining mouse were analyzed by histopathology.

**Results:** Total protein levels and lactate dehydrogenase (LDH) activity in the BAL fluid of Ega3-treated mice were similar to the untreated controls, independently of the origin of the GH (Figure 39) suggesting that all three protein preparations do not induce significant pulmonary injury.

No significant increase in leukocyte recruitment was observed with HEK293-produced Ega3 (Figure 40). We again observed a trend to increased pulmonary eosinophil levels in mice treated with Ega3 produced in *P. pastoris* (as described in Major Task 2 Subtask 2 and 3), which was absent in mice treated with Ega3 produced in HEK293. Treatment with yeast-produced, but not HEK293-produced Ega3, was also associated with an increase in pulmonary macrophage numbers at a dose of 100 µg. Taken together, these results suggest that HEK293-produced Ega3 is better tolerated by mice.

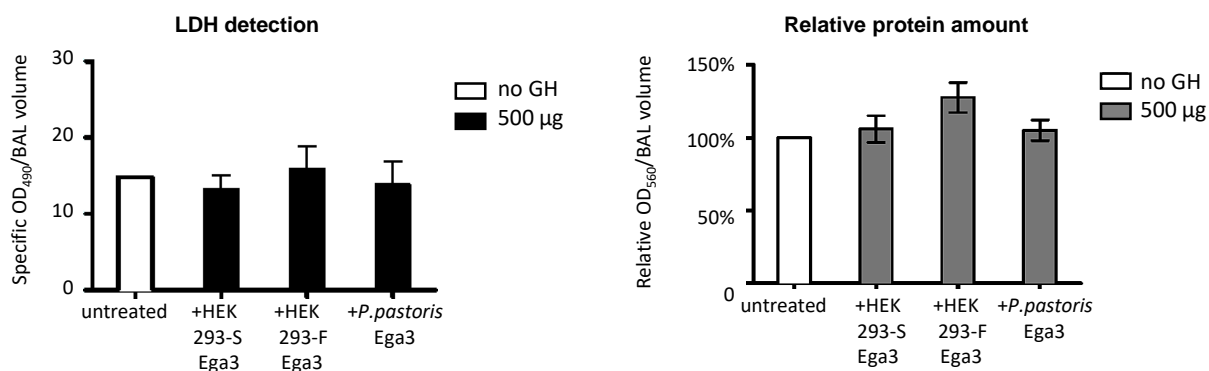


Figure 39: Lung damage, as measured by LDH activity and total protein (via BCA assay) in the BAL fluid from mice 7 days post treatment with a single dose of Ega3 produced in HEK293-S, in HEK-293-F cells or in *P. pastoris*. No significant difference was observed with the untreated group ( $p \leq 0.05$  by ANOVA). Data presented here are the average of 2 independent experiments.

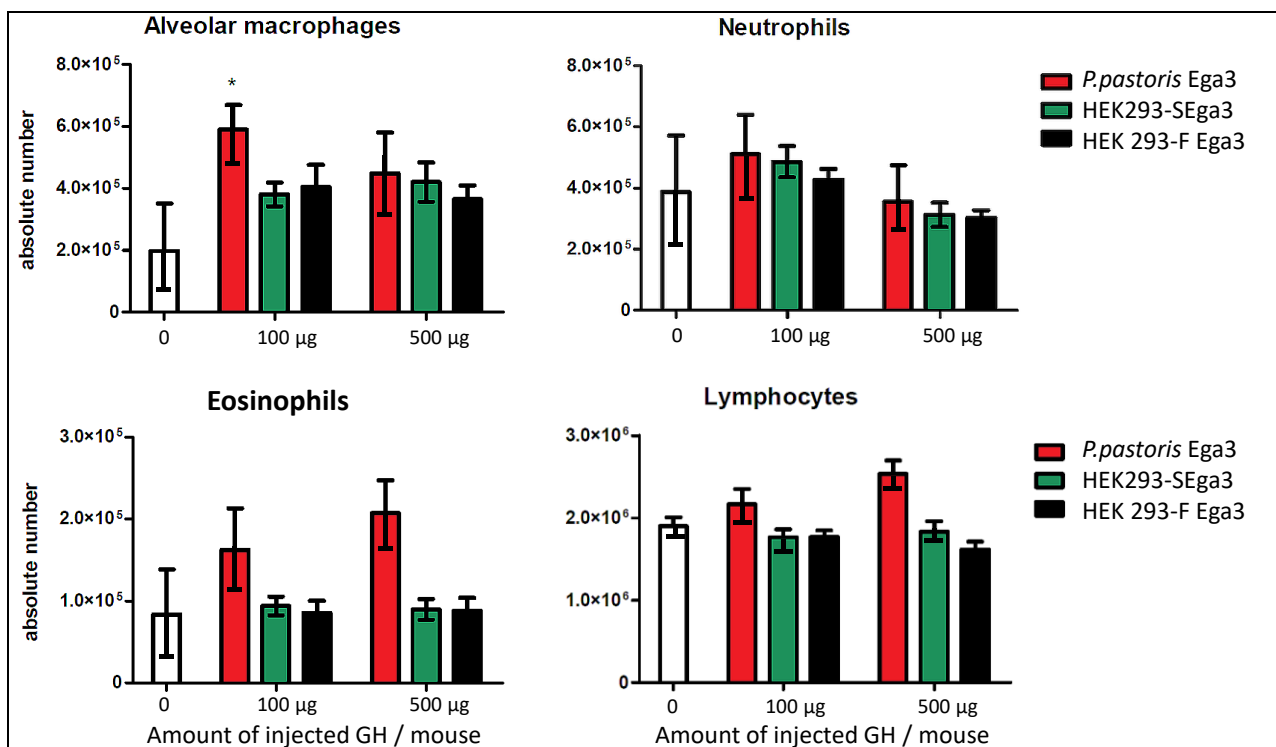


Figure 40: Absolute quantification of leukocytes populations, by flow cytometry, in mouse lung digest at 7 days post treatment with a single dose of Ega3 produced in HEK293-S, in HEK-293-F cells or in *P. pastoris*. \* indicates a significant difference with the untreated group ( $p \leq 0.05$  by ANOVA). Data presented here are the average of 2 independent experiments.

### 3- Pharmacokinetics of HEK293-produced Ega3

Pharmacokinetic studies of Ega3 as shown in Major Task 3 were performed with Ega3 from *P. pastoris*. As we anticipated moving to the use of HEK293-produced Ega3, it was necessary to reassess the pharmacokinetics of this new GH preparation.

**Methodology:** Immunocompetent mice were treated with *P. pastoris*-produced Ega3, HEK293F-Ega3 or HEK293S-Ega3, then sacrificed at different time points for Western-blot analysis of lung homogenates using our rabbit anti-Ega3 antibody. A goat-anti-rabbit-HRP antibody was used as the secondary antibody; the HRP signal was detected and analyzed by densitometry when the percent band intensity was normalized to the total band intensity at the 0h time point for each mouse. For each time-point, a minimum of 4 mice was used during the initial experiment. During the duplication, another minimum of 4 mice was used, and earlier or later time-points were added whenever needed.

**Results:** Our anti-Ega3 antibody was able to specifically recognize HEK293-produced Ega3 as well as *P. pastoris*-produced Ega3 in lung homogenates (Figure 41). The half-life of mammalian-produced Ega3 was approximately 9h, which did not differ substantially from the results obtained from the 8h half-life of Ega3 expressed in yeast (below and in Major Task 3 Subtask 2).

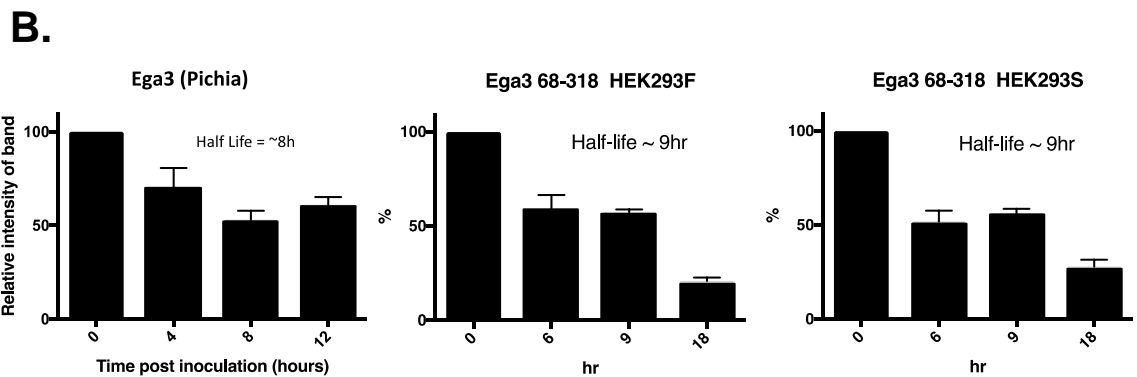
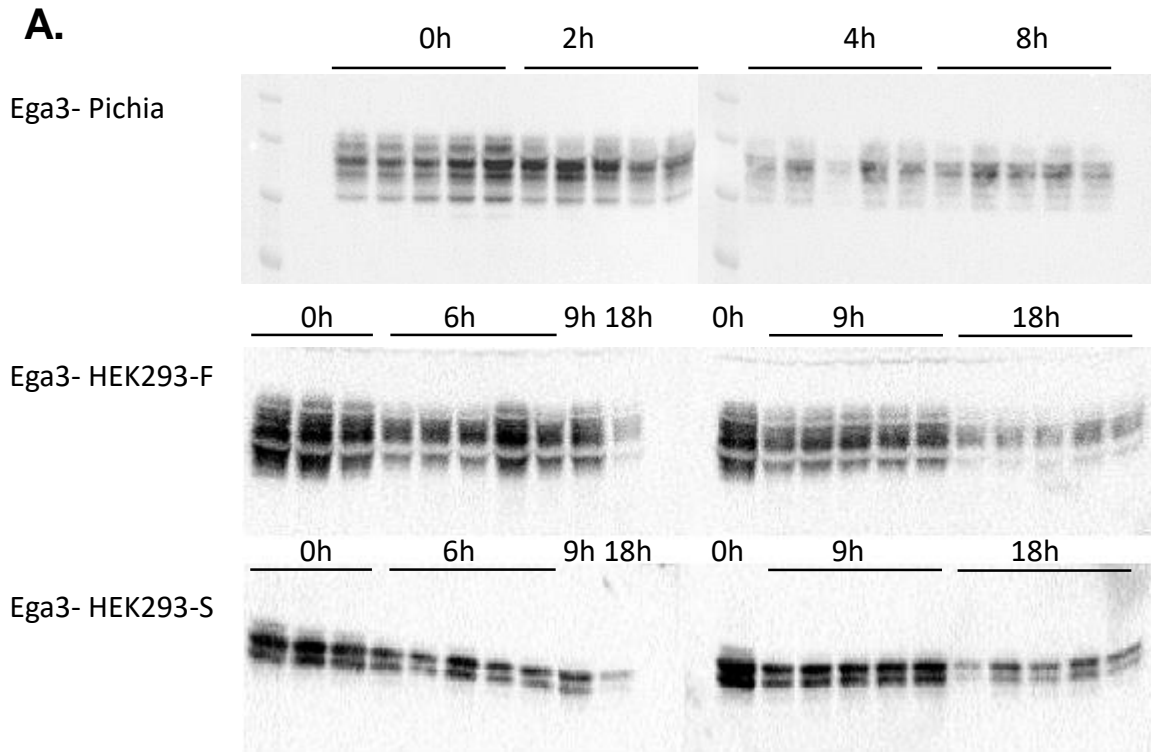


Figure 41: (A.) Western-blot analysis of mouse lung homogenates demonstrates the persistence of Ega3 for up to 18h after intratracheal administration of a single dose of protein. Each line in the Western-blot represents a single mouse. (B.) Densitometric analyses using the ImageJ software indicate a half-life of approximately 8h for Ega3 from *P. pastoris* vs. 9h for Ega3 from HEK293-F or HEK293-S.

**Conclusion:** HEK293-produced Ega3 is as active *in vitro* against biofilms of different microorganisms, exhibits similar pharmacokinetics, and is better tolerated than its yeast produced counterpart. No differences in these parameters was observed between Ega3 produced in HEK293F or HEK293S cells, and therefore HEK293S produced Ega3 was selected for all further studies.

## **B. Development of GH orthologues:**

**Rationale:** Although this Major Task 4 Subtask 5 is formally complete as it is, in an effort to improve GH pharmacokinetics, our labs have been exploring the properties of GH orthologues from other bacterial or fungal species: the Sph3 orthologues from *Aspergillus oryzae* and *Aspergillus nidulans*, and the PelA orthologue from *Bacillus cereus* (BCE5582).

### **1. Sph3 orthologue from *Aspergillus* spp.**

Sph3 demonstrated the shortest half-life ( ~1h in immunocompetent mice). Given the lack of solubility of recombinantly expressed *A. fumigatus* Sph3, so far we have been using *A. clavatus* Sph3 for our studies. To find a more stable protein we have screened Sph3 orthologues from other *Aspergillus* spp and evaluated them for stability and efficacy.

#### **a- Production of Sph3 orthologues.**

##### ***Methodology:***

Sph3 orthologue genes, identified from *Aspergillus oryzae* and *Aspergillus nidulans*, were cloned into a pET28 expression vector for expression in *E. coli*. Production of a His-tagged protein and purification using a Nickel His -trap gravity column were as described for Sph3 from *A. clavatus* (Major Task 1 Subtask 1).

**Results:** Sph3 orthologues were produced at a level of quantity and quality equivalent to *A. clavatus* Sph3, and were specifically recognized by the antibody developed against this protein (data not shown).

#### **b- Resistance of Sph3 orthologues to commercial elastase.**

**Methodology:** Similarly to what was described above (Major task 4 Subtasks 2-3), for the protease resistance assay, 1 µg of-GH was incubated at 37 °C with 60 µl of PBS with or without commercial elastase at 100 µg/mL. Samples were collected at the indicated time points. GH degradation was stopped by adding SDS-PAGE buffer and samples were analyzed by SDS-PAGE and Western-blotting.

**Results:** Sph3 orthologues from *A. oryzae* and *A. nidulans* showed a sensitivity to degradation by elastase comparable to the one of *A. clavatus* Sph3 (Figure 42). All three Sph3's were susceptible to elastase degradation within 2h of exposure to the protease. In future studies, beyond the scope of this SOW, we will look at identifying residues to mutate to generate more stable variants of the protein.

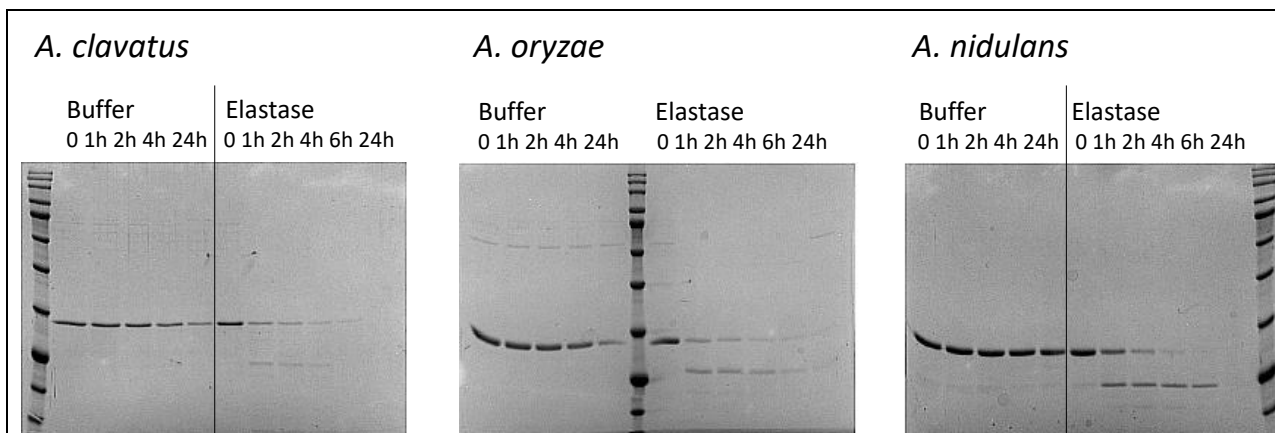


Figure 42: Western-blot monitoring of *in vitro* PelA and Sph3 orthologue persistence when incubated with elastase

Conclusion about Sph3 orthologues: Given that Sph3 orthologues resistance to elastase is not significantly better than the one of *A. clavatus* Sph3, we will not proceed further with these orthologues at present.

## 2. PelA orthologue from *Bacillus cereus*.

### a- Production of BCE5582.

*Methodology:* The gene *BCE5582* was identified in a strain of *Bacillus cereus* as coding for an orthologue of PelA. It was PCR amplified and cloned into a pET24 vector with a His tag on the C-terminal. The plasmid was transformed into Clear coli<sup>®</sup> for expression. For protein purification, cultures were grown in TB, induced with IPTG overnight and centrifuged. The bacterial pellet was sonicated, and the protein purified using nickel affinity chromatography similar to other hydrolases (Major Task 1 Subtask 1).

*Results:* BCE5582 was produced at a level of quantity and quality equivalent to and was specifically recognized by the antibody developed against *P. aeruginosa* PelA (data not shown).

### b- Activity of BCE5582 on biofilm.

*Methodology:* BCE5582 activity was measured using our standard biofilm disruption assay (Major Task 1 Subtask 3) on a mature *P. aeruginosa* PA14 biofilm exposed to either PelA, BCE5582 or to the corresponding buffer.

*Results:* *In vitro* assays showed that BCE5582 efficiently degrades established *P. aeruginosa* PA14 biofilm, with an EC<sub>50</sub> that is comparable to *Pseudomonas* PelA (Figure 43).

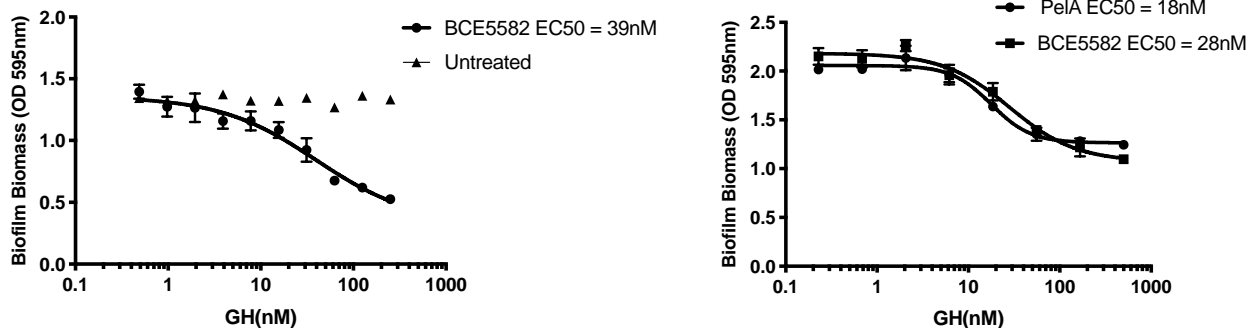


Figure 43: Biofilm disruption assay against *P. aeruginosa* PA14 biofilms was performed with PelA and BCE5582, as measured by *P. aeruginosa* biofilm disruption assay.

#### c- Mechanism of action of BCE5582.

To demonstrate that the enzyme activity of BCE5582 is specifically responsible for the disruption of biofilm, we used targeted mutation of various amino-acids, starting with the predicted catalytic residue E218, an active site residue in *Pseudomonas* PelA.

**Methodology:** To generate the E213A point variant of BCE5582, PCR mutagenesis was performed to generate a BCE5582 variant in which a residue glutamate has been replaced by an alanine at position 213 of the enzyme.

**Results:** Directed mutation in the putative catalytic site resulted in a dramatic drop in enzymatic activity (Figure 44), thus confirming that this enzyme shares a similar mechanism of action with PelA.

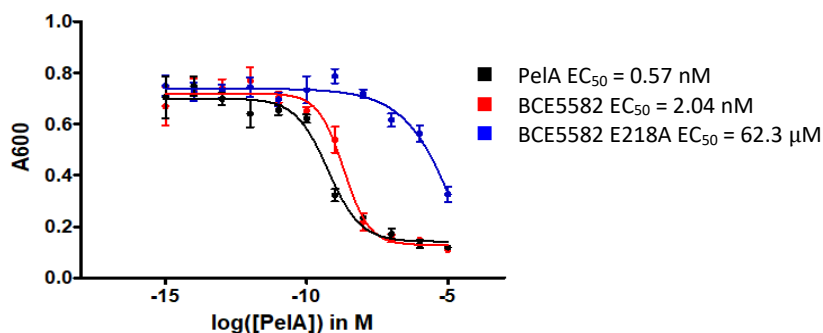


Figure 44: Enzymatic activity of PelA, BCE5582, and BCE5582 mutant (BC5582<sup>E218A</sup>) as measured by *P. aeruginosa* PA14 biofilm disruption assay.

#### 4- Resistance of BCE5582 to commercial elastase.

**Protease assay:** 1 μg of GH was incubated at 37 °C with 60 μl of phosphate buffer saline (PBS) with or without elastase. At the indicated time points, GH degradation was stopped by adding SDS-PAGE buffer and samples were analyzed by SDS-PAGE.

**Results:** the resistance of BCE5582 to elastase was significantly higher than for *Pseudomonas* PelA. BCE5582 showed no significant degradation after 6h of incubation with elastase, while degradation of PelA was observed after only 1h (Figure 45).

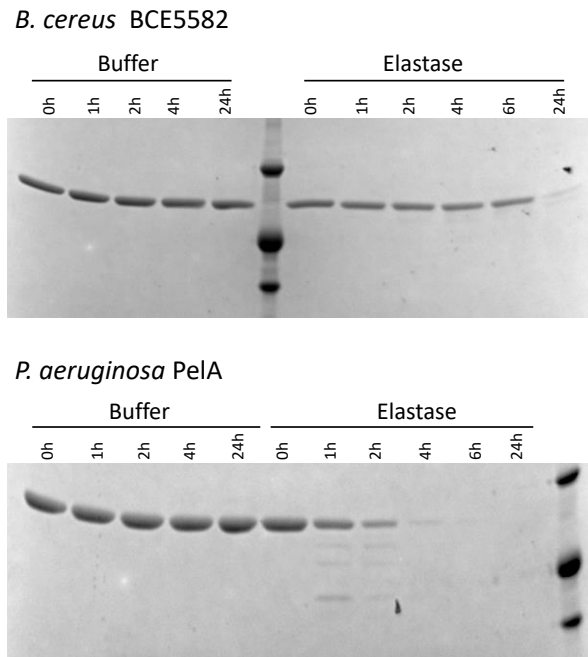


Figure 45: Western-blot monitoring of *in vitro* PelA and BCE5582 persistence when incubated with elastase.

#### 5- Tolerability of BCE5582.

**Methodology:** a single dose of 500  $\mu$ g of BCE5582 or PelA was administered intratracheally to immunocompetent mice. Mice were monitored for 7 days, then sacrificed for analysis of pulmonary injury and inflammation. The assay was performed once, with groups of 10 mice per condition: 8 mice had their lungs harvested, lavaged for measurement of lactate dehydrogenase (LDH) release and digested with collagenase for pulmonary leukocyte recruitment by flow-cytometry. The lungs of the remaining 2 mice were analyzed by histopathology.

**Results:** No significant differences in leukocyte recruitment was observed between mice treated with BCE5582 compared with those receiving PelA (Figure 46). No lung damage was detected in either group of mice by LDH quantification in BAL fluid (Figure 47) or histopathology (data not shown).

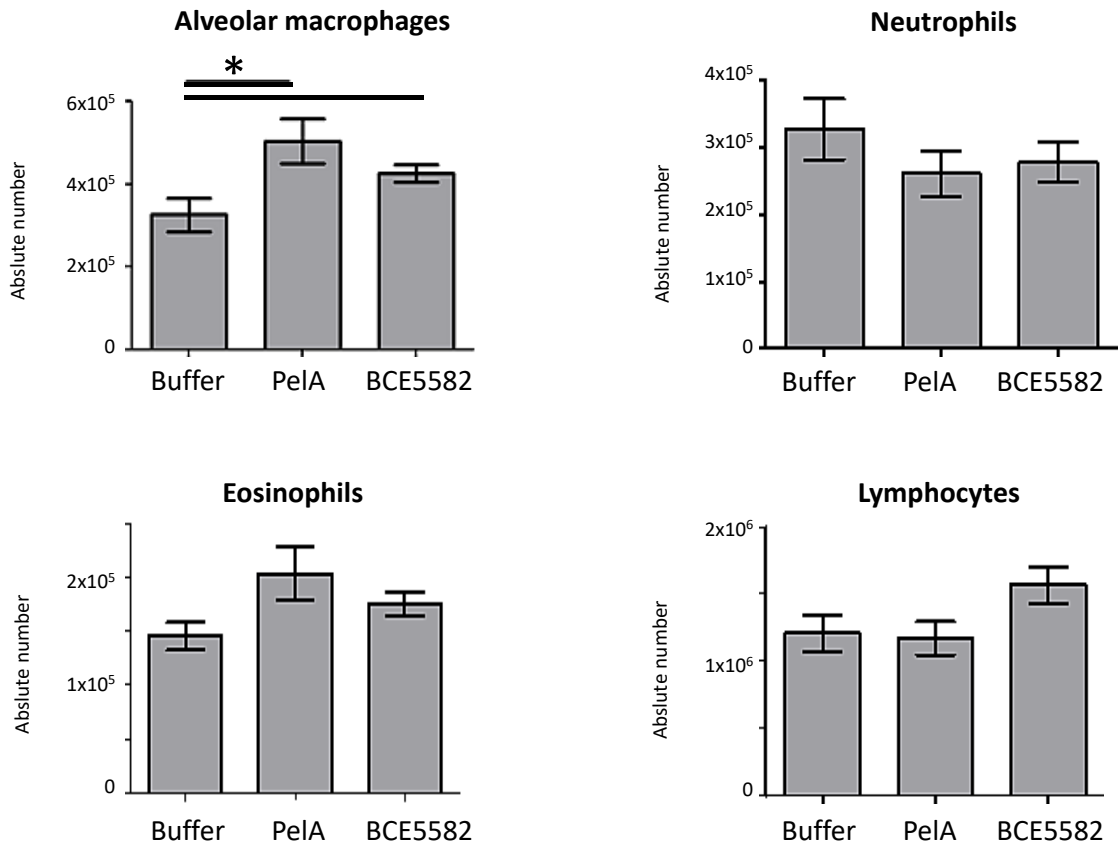


Figure 46. Absolute quantification of leukocyte populations in mouse lungs as measured by flow-cytometry performed on lung digests. Lungs were harvested 7 days following treatment with a single dose of the indicated GH combination. \* indicates a significant difference with the untreated group ( $p < 0.05$  by ANOVA).

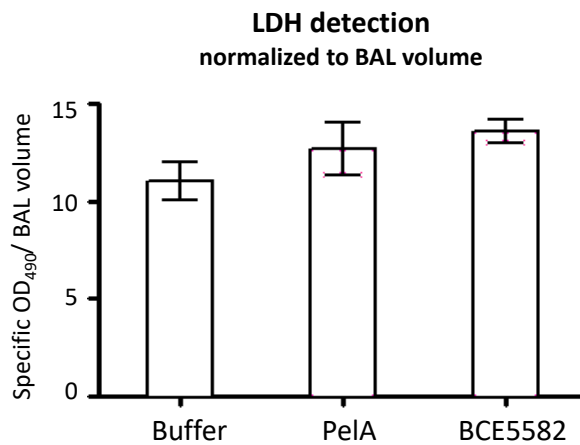


Figure 47. Quantification of lactate dehydrogenase (LDH) activity in bronchoalveolar fluid harvested from mice 7 days following treatment with a single dose of the indicated GH combination. No significant difference was observed between either treatment or the untreated group by ANOVA.

## 6- Pharmacokinetics of BCE5582.

**Methodology:** An antibody specific for BCE5582 was generated in rabbits and used to perform Western blot analyses of mouse lung homogenates following intratracheal BCE5582 administration of immunocompetent mice, as described above (Major Task 3 Subtask 2).

**Results:** The pulmonary half-life of BCE5582 was ~ 8h in immunocompetent mice (Figure 48A and Table 3, page 36), which is significantly higher than the ~3h half-life of *Pseudomonas* PelA. In immunosuppressed mice, the half-life increased to more than 24h, as compared to the 5h half-life of *Pseudomonas* PelA (Figure 48B and Table 3, page 36).

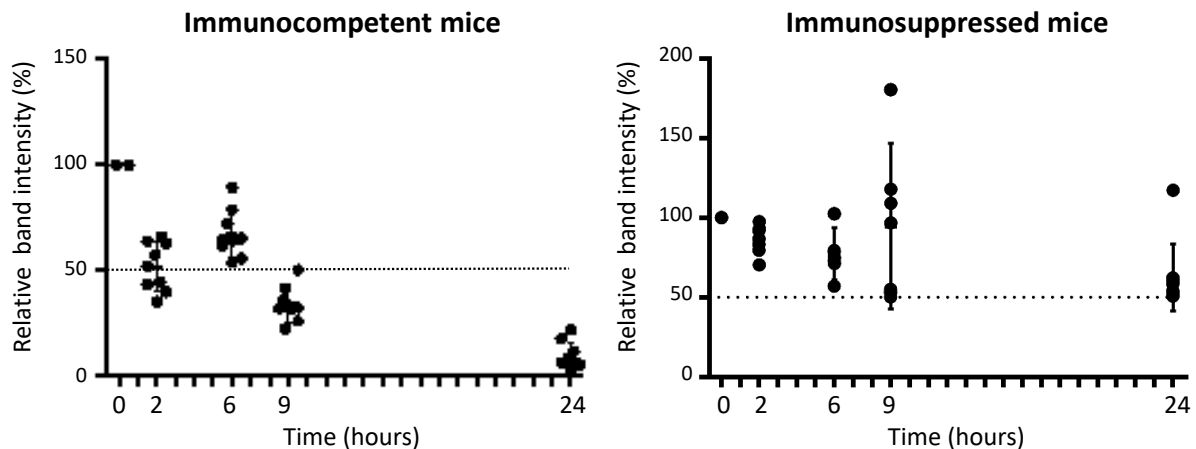


Figure 48: Determination of pulmonary GH pharmacokinetics by Western-blot analysis. 500 $\mu$ g of BCE5582 was intratracheally administered to immunocompetent (panel A) or immunosuppressed mice (panel B). Each symbol represents the densitometry value from a single mouse. Results are corrected for background signal obtained from untreated mouse lung samples and was normalized to the total band intensity at the 0h time point for each GH. Graphs represent the compilation of 2 experiments performed on separate days (n=2).

## 5- Efficacy of BCE5582.

**Methodology:** Groups of 8 mice were rendered neutropenic by treatment with anti-Ly6G antibody (200  $\mu$ g intraperitoneally every 48 hours beginning 1 day prior to infection). At day 0, a 50  $\mu$ L suspension containing  $3 \times 10^6$  Af293 conidia (wild-type *A. fumigatus*) was administered intratracheally to mice in combination with 250  $\mu$ g of BCE5582 or sterile GH buffer. Two days after infection, mice were sacrificed and their lungs were harvested for fungal burden estimation by galactomannan (GM) quantification with the commercial kit "Platelia™ Aspergillus EIA" from BioRad. The GM reading was normalized to the weight of the harvested lung and to a highly infected lung homogenate standard (our lab).

**Results:** Treatment of *Aspergillus*-infected mice with both PelA and BCE5582 resulted in a significantly lower fungal burden (Figure 49).

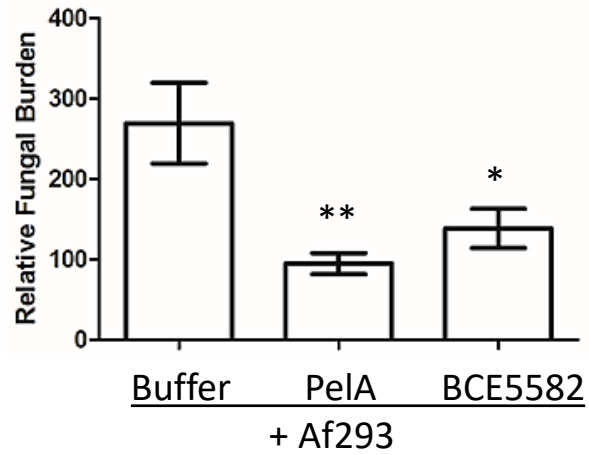


Figure 49. Pulmonary fungal burden of immunosuppressed mice intratracheally infected with  $3 \times 10^6$  conidia of *A. fumigatus* and treated with the indicated GH (250  $\mu\text{g}$  single) or the corresponding sterile buffer. \* and \*\* indicates a significant change in GM content ( $p < 0.05$  and  $p < 0.005$ , respectively, by unpaired T test). Two experiments were done with 8 mice per group each time.

**Milestone Achieved: Development of stable candidate hydrolases.**

SPECIFIC AIM 3: TO EVALUATE CANDIDATE HYDROLASES ALONE AND IN COMBINATION WITH ANTIMICROBIAL AGENTS IN THE TREATMENT OF EXPERIMENTAL *A. fumigatus* AND *P. aeruginosa* PULMONARY INFECTIONS *IN VIVO*.

#### **MAJOR TASK 5: TEST HYDROLASES FOR ACTIVITY IN ANIMAL MODELS OF ACUTE DISEASE**

**Subtask 1: Express and purify recombinant PelA and PslG for subtasks 3 – 4.** Dr Howell's lab. SOW Time Period: Months 13-30. Completion level = 100%.

As presented in Major Task 1 – Subtask 1, sufficient protein, both in quantity and quality (endotoxin-free enzyme, verified activity) was produced to meet all requirements for the other subtasks of Major Task 2.

**Subtask 2: Determine the effects of hydrolases (Sph3, Ega3, PelA) on survival of immunosuppressed mice infected with *A. fumigatus*.** Dr Sheppard's lab. SOW Time Period: Months 13-30. Completion level = 100% [10 mice per group X 8 experimental groups X 3 hydrolase regimens, AND 3 mice for histopathology all performed in duplicate = 624 mice]

##### **A. Leukopenic model.**

*Methodology:* Mice were rendered neutropenic by subcutaneous injection of 250 mg/kg of cortisone plus intraperitoneal injection of 250 mg/kg of cyclophosphamide at day -2, followed by injection of 200 mg/kg cyclophosphamide intraperitoneally at day +3. At day 0, a 50  $\mu$ L suspension containing  $5 \times 10^3$  conidia of the indicated fungal strain as well as 500  $\mu$ g of Sph3 (or sterile GH buffer) in a ratio 1:1 was administered to mice. Mice were then monitored daily and euthanized upon reaching clinical endpoints.

*Results:* Sph3 treatment resulted in a non-significant trend to increased survival during *Aspergillus* infection (Figure 50) with an increase in median survival from 7 days (Af293 alone) to 9 days (Af293 + Sph3). These results are consistent with the short half-life of 3h that was observed for Sph3 in leukopenic mice (Major Task 3 Subtask 3-4 pages 35-36) and the hyperacute nature of infection in this model. We therefore evaluated the effects of GH therapy on survival in a less acute model of invasive aspergillosis: the neutrophil-depleted mouse model (Subtask 2 part "B. Neutropenic model")

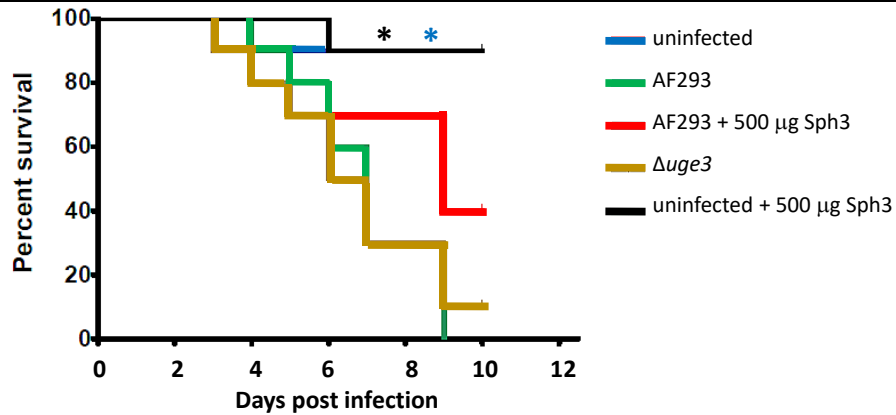
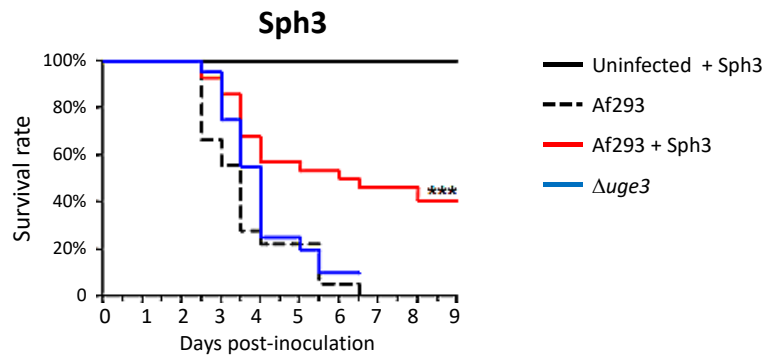


Figure 50. Survival of immunosuppressed mice intratracheally injected with a mix of conidia ( $5 \times 10^3$ ) and GH at  $500 \mu\text{g}$  1:1, or the corresponding sterile buffers. \* indicates a significant change in survival compared to mice infected with Af293 alone ( $p < 0.05$  by Wilcoxon-rank). 2 independent experiments were performed

**B. GH therapy in mice rendered neutropenic by anti-neutrophil antibody treatment.**

*Methodology:* Mice were rendered neutropenic by treatment with anti-Ly6G antibody ( $200 \mu\text{g}$  intraperitoneally every 48 hours, beginning 1 day prior to infection). Mice were then infected intratracheally with a  $50 \mu\text{L}$  suspension of  $5 \times 10^6$  Af293 or  $\Delta uge3$  conidia, or sterile conidial buffer, with or without  $500 \mu\text{g}$  of the appropriate GH. Mice were monitored daily and euthanized upon reaching clinical endpoints. Experiments were performed on two separate occasions, with groups of 8 mice per condition.

*Results:* Co-administration of PelA, Ega3 or Sph3 at the time of *A. fumigatus* infection significantly increased the survival of neutropenic mice (Figure 51).



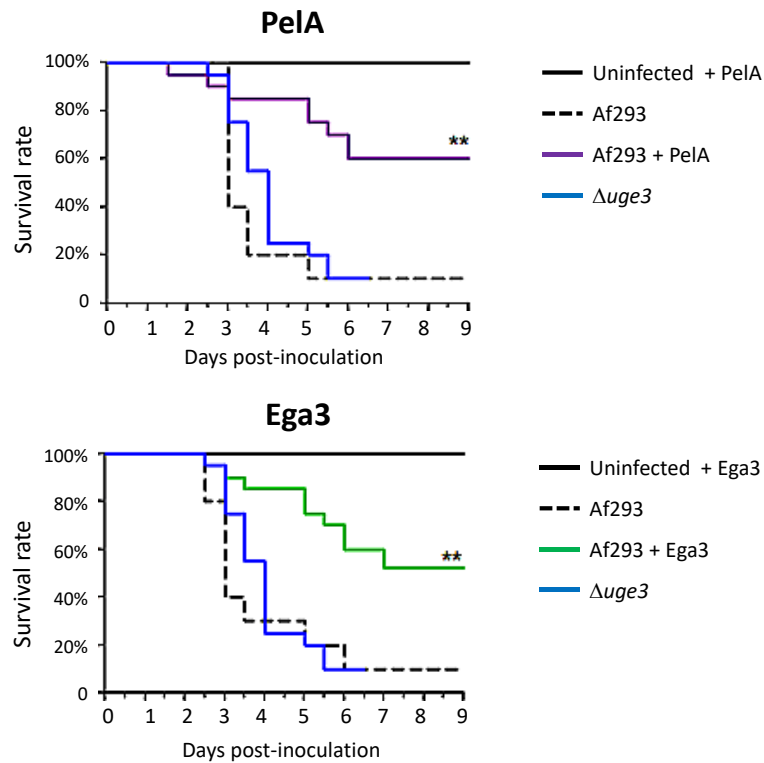


Figure 51. Survival of neutropenic mice inoculated intratracheally with a single dose of  $5 \times 10^6$  conidia of the indicated *A. fumigatus* strain or the corresponding sterile buffer in the presence or absence of 500  $\mu\text{g}$  of the indicated GH. \*\* and \*\*\* indicate a significant change in survival as compared to mice infected with Af293 alone ( $p < 0.01$  and  $< 0.001$ , respectively, by Wilcoxon-rank). Experiments were performed in triplicate for Sph3 and in duplicate for PelA and Ega3, with 8 mice per group in each experiment.

**Subtask 3: Determine the effects of hydrolases (Sph3, Ega3, PelA) on fungal burden** of mice infected with *A. fumigatus*. [10 mice per group X 8 experimental groups X 3 hydrolase regimens, all performed in duplicate = 480 mice] Dr Sheppard's lab. Months 13-30. Completion level = 100%.

**Methodology:** Mice were rendered neutropenic by subcutaneous injection of 250 mg/kg of cortisone plus intraperitoneal injection of 250 mg/kg of cyclophosphamide at day -2, followed by 200 mg/kg cyclophosphamide at day +3. At day 0, a 50  $\mu$ L suspension was administered intratracheally to each mouse. The administered suspension contained  $5 \times 10^3$  conidia of the appropriate fungal strain (or sterile conidial buffer) as well as 500  $\mu$ g of the appropriate GH (or sterile GH buffer) in a ratio 1:1. At day 4, all mice were sacrificed and their lungs were harvested for fungal burden estimation by galactomannan. This experiment has been replicated four times (n=4) for Sph3 and twice for the other GHs and GH combinations (n=2).

**Results:** Treatment of mice with 500  $\mu$ g of any of the GHs, as well as treatment with the indicated GH combinations (250  $\mu$ g of each GH), resulted in a significant reduction in pulmonary fungal burden 4 days after *A. fumigatus* challenge (Figure 52). GH therapy was associated with fungal burden levels similar to that observed in mice infected with a GAG-deficient strain of *A. fumigatus* ( $\Delta$ uge3), suggesting that these enzymes efficiently degrade GAG *in vivo* to attenuate virulence.

These results, combined with the improvement in survival associated with GH-therapy demonstrated above, provide solid pre-clinical evidence for the development of GH therapy for use in invasive aspergillosis.

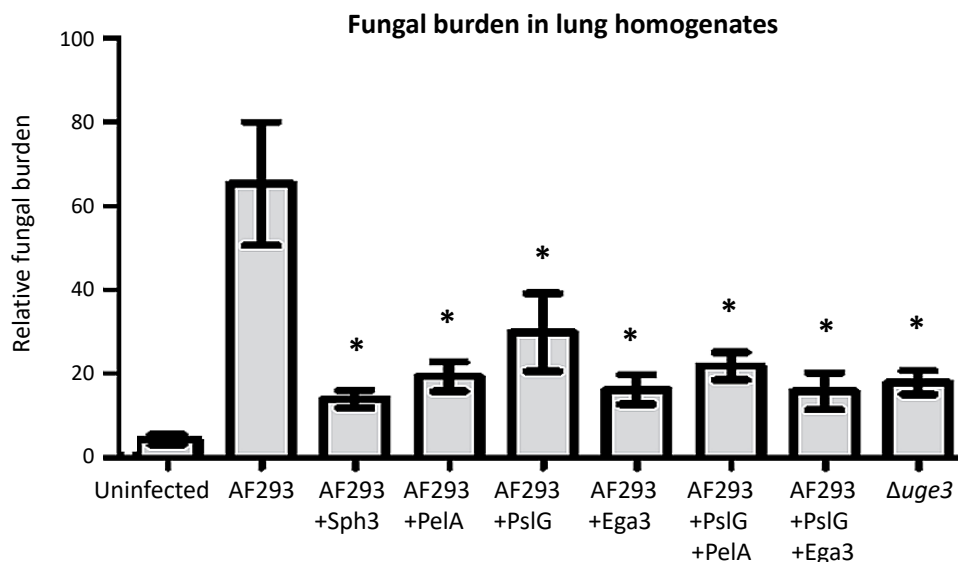


Figure 52. Fungal burden in lungs of immunosuppressed mice intratracheally infected with  $5 \times 10^3$  conidia of *A. fumigatus* and treated with the indicated GH (500  $\mu$ g single dose for monotherapy or 250  $\mu$ g of each GH for combination therapy), or the corresponding sterile buffer. \* indicates a significant difference in GM content as compared with untreated, infected mice ( $p < 0.05$  by ANOVA). 4 independent experiments were performed (n=4) for Sph3, 2 for the other GHs (n=2).

**Subtask 4: Determine the effects of hydrolases (PslG/PelA and PslG/Ega3 combinations) on bacterial burden** of mice infected with three strains of *P. aeruginosa*. Dr Sheppard's lab. Months 13-30. Completion level = 100%. [10 mice per group X 7 experimental groups X 2 hydrolase regimens X 3 strains X 2 time points AND 3 mice for histopathology X 7 groups X 2 hydrolase regimens X 3 strains at a single time point all performed in duplicate = 1932 mice]

1) Effects of PslG and PelA monotherapy on mice infected with wild-type *P. aeruginosa*.

**Methodology:** Mice were intratracheally administered a 50  $\mu$ L suspension containing  $1.5 \times 10^7$  bacteria (*Pseudomonas aeruginosa* PAO1), combined with 500  $\mu$ g PelA, PslG, an enzymatically inactive form of PslG, a 1:1 mix of PslG/PelA (250  $\mu$ g each) or the sterile GH buffer, as indicated. At 48 hours post-infection, all mice were sacrificed, BALs were performed; blood and lungs were harvested and plated for colony forming unit (quantitative culture) counting. The quantitative cultures were normalized by lung weight. Leukocyte populations in BAL fluid were analyzed by flow cytometry.

**Results:** In contrast to our findings with GH-therapy in fungal infection, mice treated with PslG or PelA exhibited a trend towards higher pulmonary bacterial burden 2 days post infection, compared to the mice that received PAO1 alone, although this was not statistically significant (Figure 53).

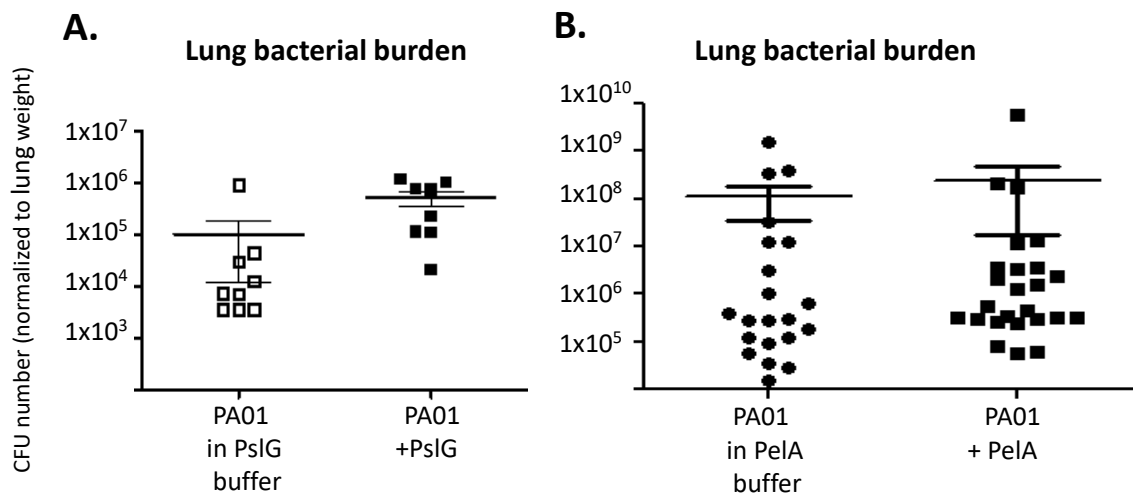


Figure 53. Effect of PslG (A.) and PelA (B.) as monotherapy on pulmonary bacterial burden, as determined by quantitative culture of lung homogenate. Results shown are from a single experiment with PslG (n=1) and three independent experiments with PelA (n=3). No significant difference between the groups was shown by ANOVA.

These data indicate that, in contrast to our findings with GH therapy for *Aspergillus*, PslG or PelA alone may not be protective against *P. aeruginosa* infection, and could even increase pulmonary dissemination. There are multiple potential explanations for this observation. For example, it is possible that PslG degradation of *P. aeruginosa* at the time of inoculation results in reduced adherence to pulmonary tissues and increased motility *P. aeruginosa*, leading to enhanced tissue invasion. This hypothesis is consistent with a recent observation that PslG therapy

can increase *P. aeruginosa* motility in vitro (Zhang *et al.*, Appl. Environ. Microbiol. doi:10.1128/AEM.00219-18). Alternately, PslG may have a direct effect on host tissue glycans that enhances tissue invasion.

Therefore, GH combination therapy was deferred in favor of mechanistic studies. For these assays, we added control groups: a catalytically inactive variant of PslG; a Psl deficient PAO1 mutant; two motility deficient mutants; a change of GH buffer.

## 2) Comparison of PslG and PslG inactive monotherapy on mice infected with wild-type *P. aeruginosa*.

**Methodology:** Mouse infections and treatments as well as lung and blood analysis were performed as described above.

**Results:** As previously, a trend towards elevated bacterial burden was observed in the lungs of mice treated with active protein (Figure 54A). Unexpectedly, this was also observed with enzymatically inactive PslG. Similarly, the bacterial burden in blood was significantly higher in the presence of either form of PslG as compared to the buffer controls, in which very little bacterial dissemination was observed (Figure 54B).

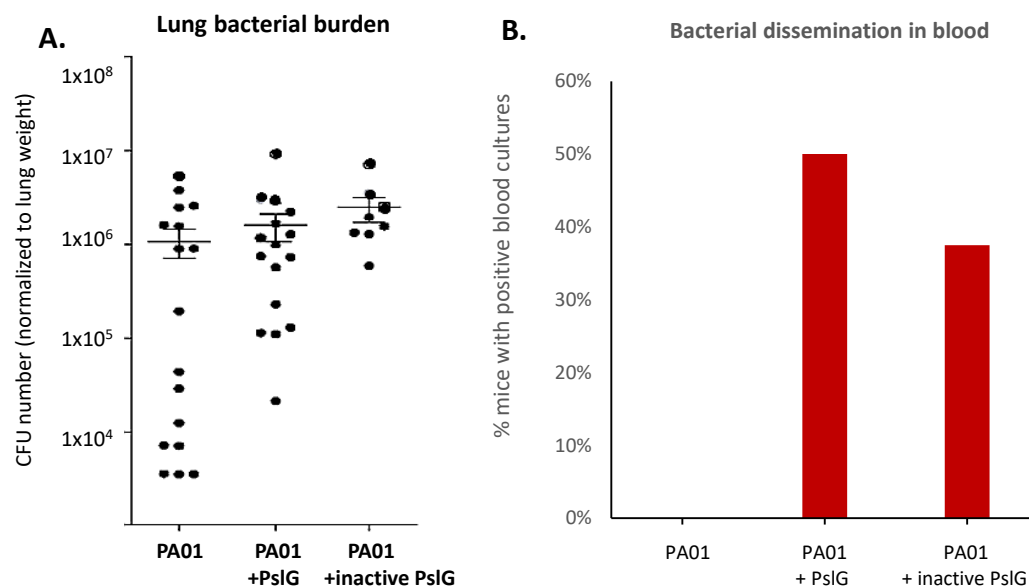


Figure 54. Effects of PslG and modified PslG (inactive PslG) on (A) pulmonary bacterial burden and (B) hematogenous dissemination of bacteria, as determined by quantitative culture of lung homogenate. No significant difference between the groups was shown by ANOVA.

These data suggest that enhanced dissemination of *P. aeruginosa* following GH-treatment is not a consequence of exopolysaccharide degradation, as similar effects were observed with catalytically inactive PslG.

### 3) Effects of PslG on mice infected with Psl deficient *P. aeruginosa*.

**Methodology:** The absence of Psl with the strain  $\Delta psI$  was validated in flow-cytometry, using the antibody Psl0096, a human monoclonal antibody conjugated to Alexa Fluor 647. Mouse infection and bacterial burden studies were performed as outlined above.

**Results:** Infection with the Psl-deficient *P. aeruginosa* strain ( $\Delta psI$ ) was associated with lower pulmonary bacterial burden than with wild-type PA01 (Figure 55A) suggesting that Psl may play a role in lung colonization. Treatment with PslG resulted in a higher bacterial burden and increased hematogenous dissemination in both mice infected with the wild-type PA01 strain and those mice infected with the  $\Delta psI$  strain (Figure 55). These data are consistent with PslG-mediated augmentation of virulence acting through a mechanism independent of its hydrolase activity on Psl.

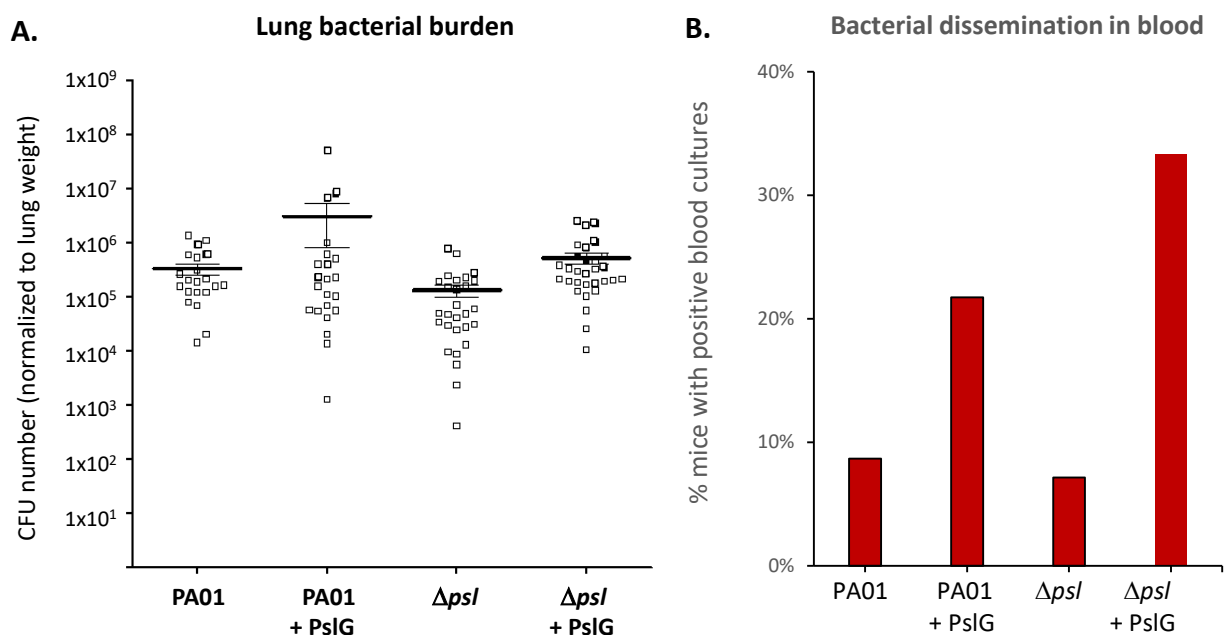


Figure 55. Effects of PslG on pulmonary bacterial burden and hematogenous dissemination of bacteria as determined by quantitative culture of lung homogenate and blood, respectively. The strain *P. aeruginosa*  $\Delta psI$  is a Psl-deficient mutant of the wild-type PA01 strain. Results shown are the aggregate of three independent experiments. No significant difference between the groups was shown by ANOVA.

### 4) Effects of PslG on *P. aeruginosa* motility.

**Methodology:** 1% LB-agar with or without PslG (0.05 or 2  $\mu$ M as final concentration) were stab inoculated with approximately  $4 \times 10^8$  of each bacterial strain. After 24 hours of incubation at 37°C, petri dishes were stained with crystal violet and washed. The diameter of the halos formed by bacteria was measured. Four bacterial strains were assayed: two different wild-type strains obtained from different sources, and two motility deficient mutants:  $\Delta pilT$ , and  $\Delta pilA$ .

**Results:** Non-motile mutants exhibited reduced growth diameter as compared to motile strains (Figure 56). Exposure to PslG significantly increased the spreading of motile bacteria in a dose

dependent manner, but had no effect on non-motile strains. These results suggest that PslG treatment increases the motility of *P. aeruginosa*.

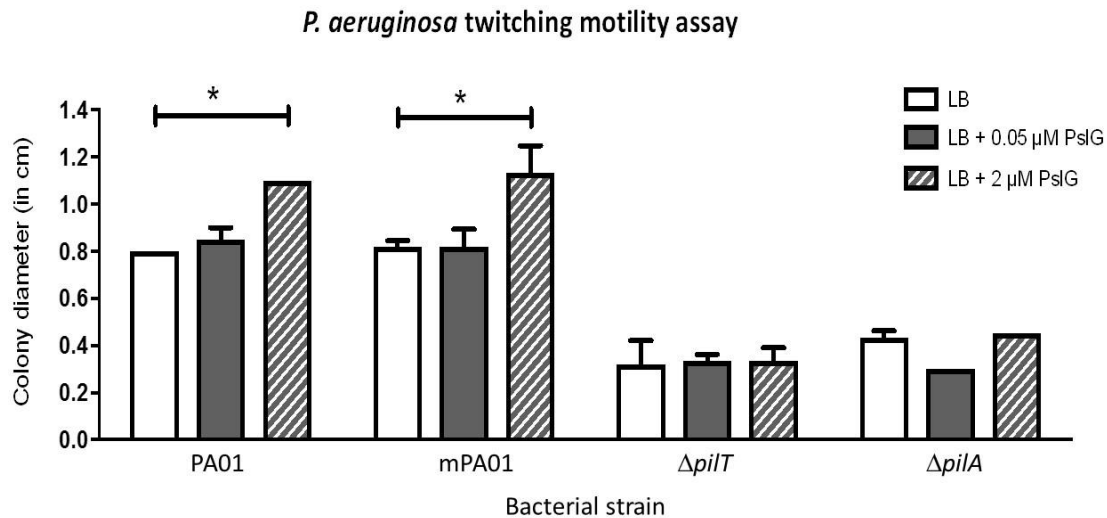


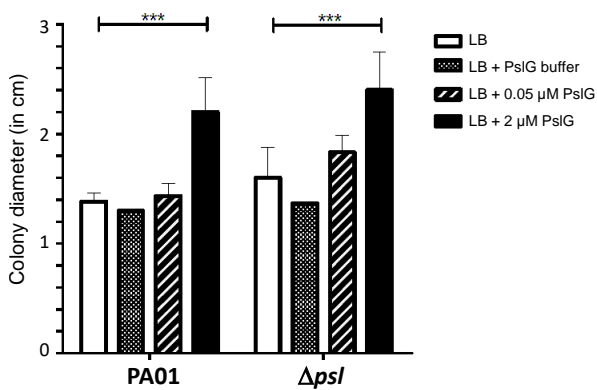
Figure 56. Effect of PslG on the motility of *P. aeruginosa*. Motile and non-motile bacterial strains were point-inoculated on a nutritive agar plate enriched or not with PslG at 0.05 or 2  $\mu$ M. Bacterial spreading was measured as proportional to the diameter of the biofilm attached to the plastic of the plate. \* indicates a significant difference with the untreated group ( $p < 0.05$  by ANOVA).

##### 5) Effects of PslG treatment on twitching motility of Psl deficient *P. aeruginosa* strains *in vitro*.

**Methodology:** 1% LB-agar with or without PslG (0.05 or 2  $\mu$ M as final concentration) were stab inoculated with approximately  $4 \times 10^8$  of each bacterial strain. After 24 hours of incubation at 37°C, petri dishes were stained with crystal violet and washed. The degree of bacterial spread was measured as an indication of twitching motility.

**Results:** Consistent with our *in vivo* findings, PslG treatment enhanced motility of both Psl-producing and Psl-deficient strains in a dose-dependent manner (Figure 57). Moreover, treatment of both strains with Sph3, which has no activity against *P. aeruginosa* Psl, also enhanced the motility of *P. aeruginosa*, again suggesting that the effect of GH enzymes on motility is independent of their catalytic activity. This finding was consistent with our observation that both active and catalytically inactive PslG treatment resulted in similar levels of increased pulmonary bacterial burden and haematogenous dissemination, and that PslG treatment increased dissemination during infection with a Psl-deficient strain.

Effect of PslG on *P. aeruginosa* twitching motility



Effect of Sph3 on *P. aeruginosa* twitching motility

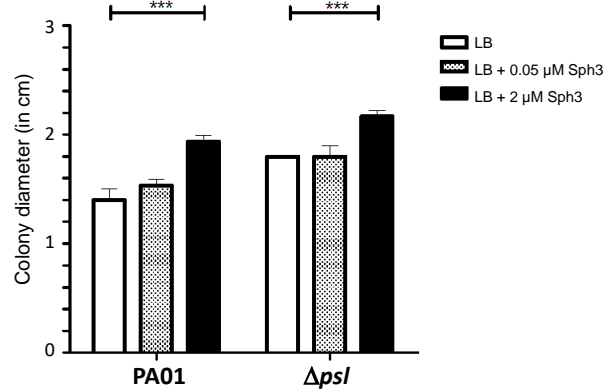


Figure 57. Effect of PslG and Sph3 on the motility of *P. aeruginosa*. Bacterial strains were point-inoculated on a nutrient agar plate with or without PslG at 0.05 or 2 μM. Bacterial spreading was measured as proportional to the diameter of the biofilm attached to the plastic of the plate. \*\*\* indicates a significant difference with the untreated group ( $p < 0.05$  by ANOVA).

#### 6) Effects of protein supplementation on *P. aeruginosa* twitching motility *in vitro*.

To determine if the GH-mediated increased motility of *P. aeruginosa* was simply a consequence of protein supplementation, the effects of BSA on bacterial motility were tested.

**Methodology:** 1% LB-agar alone, or supplemented with PslG (2 μM as final concentration, equivalent to 0.1 mg/mL) or bovine serum albumin (BSA, at 0.1 mg/mL) was stab inoculated with approximately  $4 \times 10^8$  of each bacterial strain. After 24 hours of incubation at 37°C, petri dishes were stained with crystal violet and washed. The degree of bacterial spread was measured as an indication of twitching motility.

**Results:** As previously seen, PslG enhanced the motility of wild-type and Psl-deficient *P. aeruginosa*. BSA supplementation also enhanced motility of both *P. aeruginosa* strains, although the effect was less marked than was seen with PslG (Figure 58).

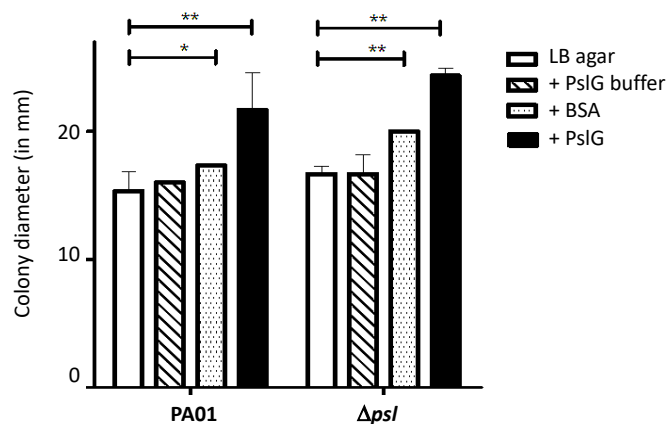


Figure 58. Effect of PslG and BSA supplementation on the motility of Psl-producing and Psl-deficient *P. aeruginosa*. Bacterial strains were point-inoculated on a nutritive agar plate with or without 0.1 mg/mL PslG or BSA. Bacterial spreading was quantified by measuring the diameter of the resulting colonial

growth. \* and \*\* indicate a significant difference with the untreated group ( $p < 0.05$  and  $p < 0.01$ , respectively, by ANOVA).

Taken together, results of these experiments suggest that GH-media augmentation in motility is independent of GH catalytic activity and may be a generalized bacterial response to extracellular proteins.

7) Effects of PslG and PelA monotherapies on the virulence of wild-type and motility-deficient, pilus-deficient *P. aeruginosa* strains in vivo.

**Methodology:** Mice were treated intratracheally with a 50  $\mu$ L suspension containing  $1.5 \times 10^7$  bacteria (*P. aeruginosa* PAO1, or pilus-deficient *P. aeruginosa*), combined with 500  $\mu$ g PslG, or PelA, or the sterile GH buffer, as indicated. At 48 hours post-infection, all mice were sacrificed and blood and lungs were harvested and plated for quantitative culture.

**Results:** Unlike previous experiments, PslG and PelA treatments did not result in increased pulmonary bacterial burden or hematogenous dissemination of wild-type *P. aeruginosa* (Figure 60). In contrast, while PslG treatment did not increase pulmonary bacterial burden of the pilus-deficient strain of *P. aeruginosa*, increased hematogenous dissemination was observed, suggesting that bacterial motility is dispensable for GH-mediated hematogenous dissemination.

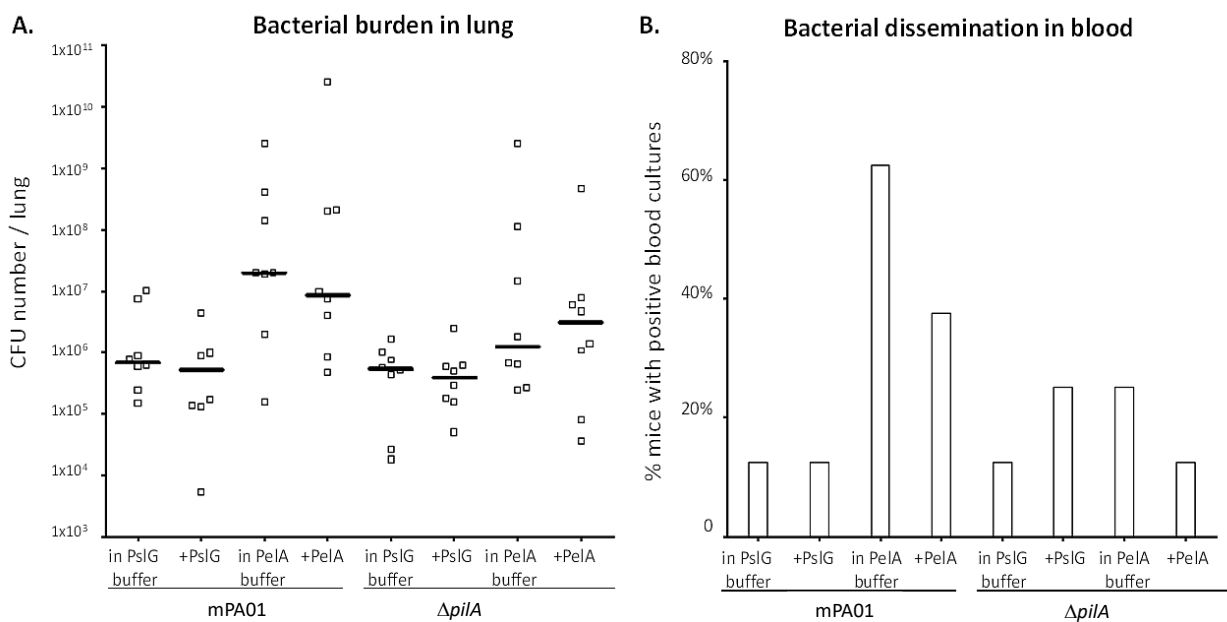


Figure 60. Effect of PslG and PelA on (A.) pulmonary bacterial burden and (B.) hematogenous dissemination of bacteria as determined by quantitative culture of lung homogenate and blood, respectively. Results shown are from a single experiment with 8 mice per condition. Horizontal lines indicated the median of each experimental group. No significant difference between the groups was shown by ANOVA.

Summary:

Treatment of mice infected with *P. aeruginosa* PAO1 with intratracheal PslG (or PelA) compared to the mice that received PAO1 alone. PslG treatment was also associated with dissemination of the bacteria in blood (not observed with PAO1 alone). Similar findings were observed in response to

treatment with a catalytically inactive PslG as well as when *P. aeruginosa* PA01 was replaced by a bacterial strain deficient in Psl production (i.e. lacked the PslG substrate). In vitro, PslG exposure increased the spreading of motile bacteria (twitching motility assay) in a dose-dependent manner, but had no effect on non-motile strains.

In conclusion, these experiments suggest that although Psl plays a role in lung colonization by *P. aeruginosa*, PslG alone (or PelA alone) is not protective against *P. aeruginosa* infection, likely through directly enhancing bacterial motility and dissemination. Since GH therapy alone did not result in significant improvement in the natural history of acute *P. aeruginosa* infection, we elected to focus our future studies on GH-antibiotic combination therapy as outlined in Major Task 7.

**Milestone Achieved: Determination of the efficacy of candidate hydrolase regimens in the treatment of acute infection with *A. fumigatus* and *P. aeruginosa*.**

## **MAJOR TASK 6: TEST HYDROLASES FOR ACTIVITY IN ANIMAL MODELS OF CHRONIC DISEASE**

**Subtask 1: Express and purify recombinant PelA and PsIG for subtasks 3 – 4.** Dr Howell's lab. SOW  
Time Period: Months 13-30. Completion level = 100%.

As presented in Major Task 1 – Subtask 1, sufficient protein, both in quantity and quality (endotoxin-free enzyme, verified activity) was produced to meet all requirements for the other subtasks of Major Task 2.

**Subtask 2: Determine the effects of candidate hydrolases (Ega3) on fungal burden of immunocompetent mice chronically infected with *A. fumigatus*.** [10 mice per group X 6 experimental groups X 1 hydrolase regimens X 2 time points AND 3 mice for histopathology at a single time point X 6 groups X 1 hydrolase regimens performed in duplicate = 276 mice] Dr Sheppard's lab. Months 13-30. Completion level = 100%.

### Background:

As detailed above (Major Task 1 Subtask 1), *in vivo* studies using Ega3 were delayed while we optimized formulation of this enzyme. In the interim, we performed *in vivo* studies using Sph3 as a proof of principle GH in chronic aspergillosis. Then, we completed the subtask by studying PelA and Ega3.

### Accomplishments:

**Methodology:** A 50  $\mu$ L suspension of agarose beads with or without  $1.25 \times 10^6$  conidia of *A. fumigatus* strain Af293 was administered intratracheally to immunocompetent female BALB/c mice. Beads were suspended in a solution containing 500  $\mu$ g of GH, or sterile buffer. At days 2 and 7, mice were sacrificed and their lungs were harvested and homogenized to assay for fungal burden as assayed by galactomannan (GM) analysis with the commercial kit "Platelia™ Aspergillus EIA" from BioRad. GM readings were normalized to the weight of the harvested lung and to a highly infected lung homogenate standard. Lungs were also processed for histopathology examination to determine inflammatory responses and for immunostaining for exopolysaccharides. Experiments were performed on two separate occasions, on groups of 8 mice per condition.

### **Results:**

In contrast to acute invasive aspergillosis, no differences in pulmonary fungal burden were observed between GH-treated and untreated mice (Figure 61), suggesting that GH therapy is not effective in the bead model of chronic pulmonary *Aspergillus* infection.

Interestingly, in these experiment, there was also no significant difference between the pulmonary fungal burden of mice infected with wild-type and the GAG-deficient  $\Delta$ *uge3* mutant. It is likely that the use of agar beads allows retention of fungi within the airways despite the absence of GAG.

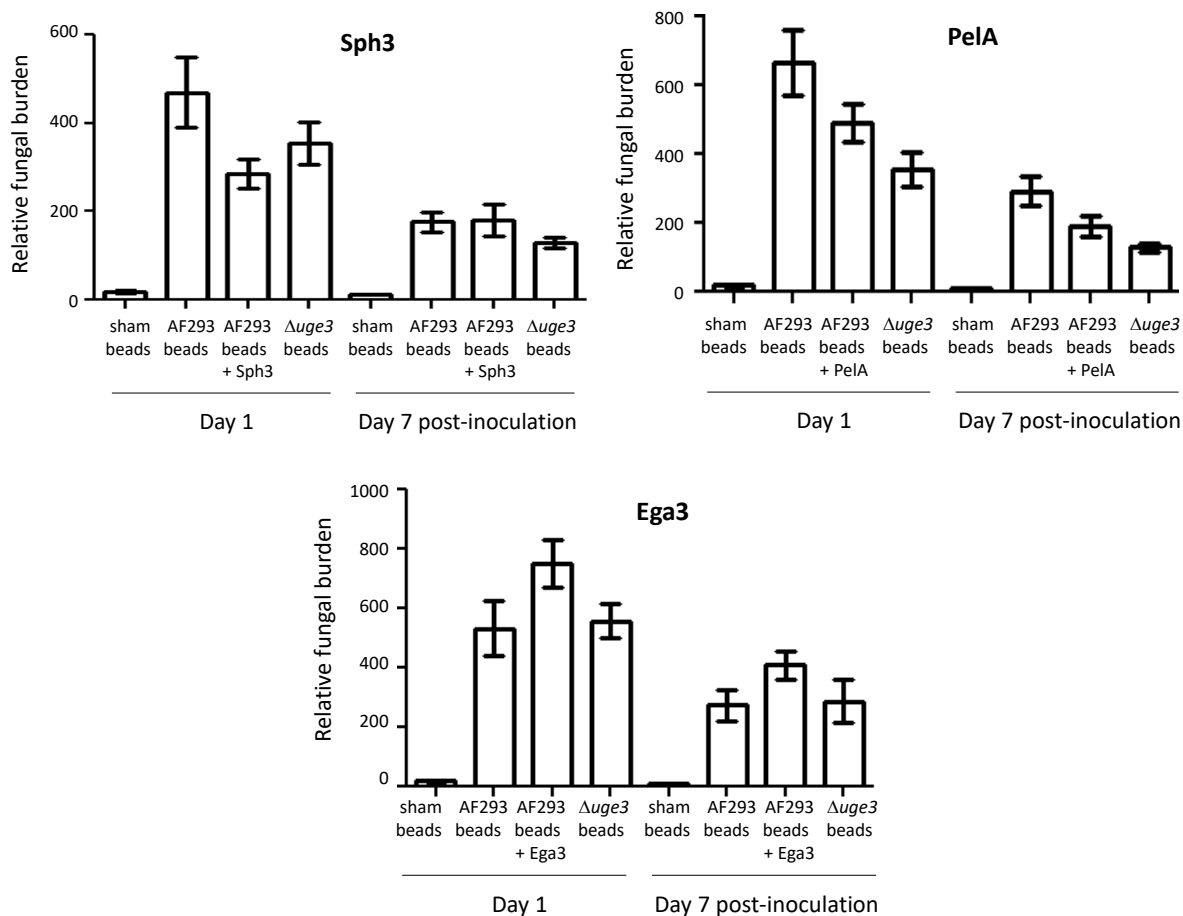


Figure 61: Relative fungal burden in lungs of immunocompetent mice intratracheally infected with a single dose of agar beads containing buffer only (sham) or  $1.25 \times 10^6$  conidia of Af293, suspended in sterile buffer with or without 500 of the indicated GH. Fungal burden was determined by galactomannan content quantification (Platelia® Aspergillus EIA) of lung homogenates.

**Subtask 3: Determine the effects of candidate hydrolases (PslG/PelA and PslG/Ega3 combinations) on bacterial burden of immunocompetent mice chronically infected with *P. aeruginosa*.** [10 mice per group X 6 experimental groups X 2 hydrolase regimens X 3 strains X 2 time points AND 3 mice for histopathology X 6 groups X 2 hydrolase regimens X 3 strains at a single time point all performed in duplicate = 1656 mice] Dr Sheppard's lab. Months 18-30. Completion level = 100%.

### 1) Inoculum optimization.

**Methodology:** Immunocompetent female BALB/c mice were infected intratracheally with a 50  $\mu$ L suspension containing  $1 \times 10^6$ ,  $2 \times 10^6$  or  $3 \times 10^6$  beads of *P. aeruginosa*-containing agar beads. Agarose beads were generated by mixing an equal volume of molten agarose solution and bacterial suspension of *P. aeruginosa* strain PA01 ( $OD_{600nm} = 0.6$ ). At days 2 and 7 post-injection, mice were sacrificed and their lungs were harvested, homogenized and quantitative culture was performed. Lungs were also processed for histopathology studies to examine the inflammatory

responses. Experiments were performed on, at least, two separate occasions, on groups of 8 mice per condition.

**Results:** High dose *P. aeruginosa* bead infection ( $3 \times 10^6$  organisms per mouse) resulted in an initially high pulmonary bacterial burden that rapidly declined by 7 days after infection (Figure 62), and was associated with mortality (2/15 mice). Further experiments were therefore not performed with this inoculation dose (in particular, day 4 was not performed in order to limit mouse use). Low dose infection ( $1 \times 10^6$  organisms/mouse) resulted in stable, low level infection in the majority of mice, but infection was not established in 100% of animals. Infection with  $2 \times 10^6$  organisms/mouse produced reliable levels of infection with a slow decrease in bacterial burden over seven days. Future experiments evaluating the activity of GH therapy therefore used this  $2 \times 10^6$  dose to establish a non-lethal persistent bacterial infection.

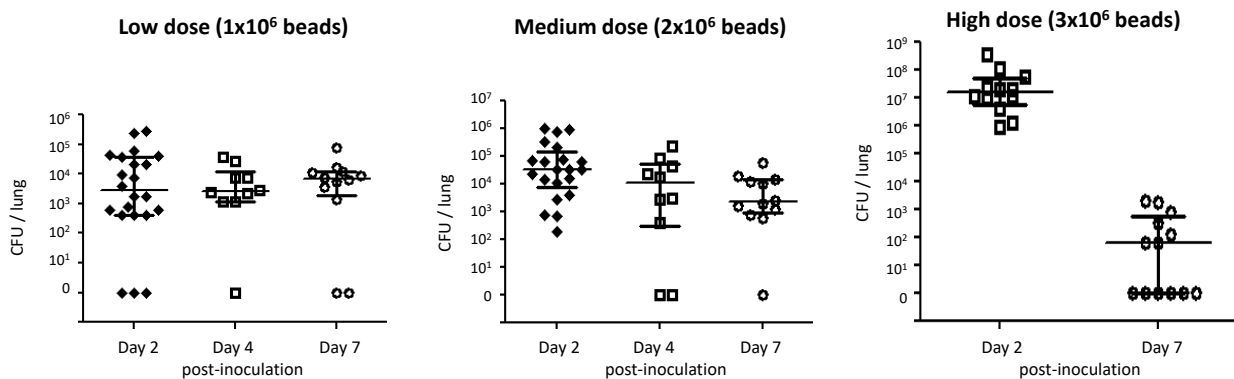


Figure 62. Pulmonary bacterial burden as determined by quantitative culture of lung homogenates. Horizontal lines indicate the median of each experimental group, error bars represent the 75<sup>th</sup>- and 25<sup>th</sup>-percentile. The experiment has been performed with groups of a minimum of 6 mice per condition. Low and medium doses were tested in triplicate, and high dose in duplicate.

## 2) Effect of hydrolases on the natural history of *P. aeruginosa* chronic infection.

**Methodology:** Mice were infected with *P. aeruginosa* beads as outlined above, and treated intratracheally with a combination of 250  $\mu$ g of PslG and 250  $\mu$ g PelA at the time of infection.

**Results:** GH treatment of mice infected with *P. aeruginosa* PA01 beads did not result in a significant reduction of bacterial burden at day 7 (Figure 63). Given the lack of efficacy of GH therapy in both fungal and bacterial infection, and the lack of efficacy of GH-therapy alone in acute bacterial infection we therefore elected to focus our efforts on studying the potentiation of antibiotics by GHs in this model as we did with acute bacterial infection (as reported in Major Task 7, Subtask 3).

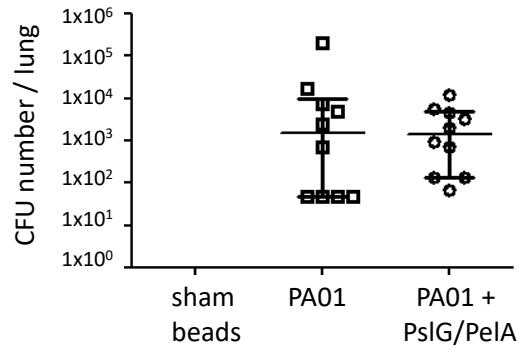


Figure 63. Pulmonary bacterial burden as determined by quantitative culture of lung homogenates, in mice infected by sterile agar beads, and *P. aeruginosa*-containing agar beads with and without PslG/PelA at 250  $\mu$ g each. Horizontal lines indicate the median of each experimental group, error bars represent the 75<sup>th</sup>- and 25<sup>th</sup>-percentile. The experiment was performed once, with groups of a minimum of 6 mice per condition. No significant change was observed between groups with or without GH by Mann-Whitney.

**Milestone Achieved: Determine efficacy of candidate hydrolase regimens in the treatment of chronic infection with *A. fumigatus* and *P. aeruginosa*.**

## **MAJOR TASK 7: TEST HYDROLASES FOR SYNERGY WITH ANTIMICROBIALS.**

**Subtask 1: Express and purify recombinant PelA and PslG for subtasks 3 – 4.** Dr Howell's lab. SOW Time Period: Months 25-36. Completion level = 100%.

As presented in Major Task 1 – Subtask 1, sufficient protein, both in quantity and quality (endotoxin-free enzyme, verified activity) was produced to meet all requirements for the other subtasks of Major Task 2.

**Subtask 2: Determine the effects of hydrolase (Sph3, Ega3, PelA)-antifungal combinations on fungal burden of mice infected with *A. fumigatus*.** [10 mice per group X 6 experimental groups X 2 hydrolase antifungal combinations X 2 time points AND 3 mice for histopathology X 6 groups X 2 hydrolase antifungal combinations at a single time point all performed in duplicate = 552 mice] Dr Sheppard's lab. Months 25-36. Completion level = 100%.

### Rationale:

Our *in vitro* assays for potentiation of antifungal drugs by GHs (Major Task 1), we identified posaconazole/Sph3 and caspofungin/PelA as the most promising antifungal/GH combinations. Since posaconazole and caspofungin showed comparable potentiation results when assayed *in vitro* with Sph3 as well as with PelA (Major Task 1 Subtask 2), to fulfill the SOW requirements, we initially elected to assay posaconazole with both GHs. As our previous experiments demonstrated that GH-dependent effects on fungal burden are lost over time, we elected to test two different antifungal/GH combinations using 2 different antifungal concentrations at a single time-point.

### Accomplishments:

#### **1) Potentiation of the effect of posaconazole.**

*Methodology:* For the severely immunosuppressed mouse model (leukopenic model), mice were treated by subcutaneous injection of 250 mg/kg of cortisone plus intraperitoneal injection of 250 mg/kg of cyclophosphamide at day -2, followed by injection of 200 mg/kg cyclophosphamide and 250mg /kg of cortisone intraperitoneally at day +3. For the less acute immunosuppressed mouse model (neutrophil-depleted model), mice were treated with an antibody targeting the neutrophil-specific surface molecule Ly6G, by intraperitoneal injection of 200 µg of the antibody every 48h, beginning 1 day prior to infection.

At day 0, mice from both models were endotracheally infected with a 50 µL suspension containing 0 or 500 µg of Sph3 or PelA and 0 or 5x10<sup>6</sup> conidia of Af293 *A. fumigatus*. Mice were then treated every 12 hours with the indicated dose of posaconazole by oral gavage and monitored for health status. For fungal burden, the lungs were harvested and homogenized in PBS. Lung homogenates were assayed by galactomannan assay using the Platelia® Aspergillus EIA (BioRad); GM values were then normalized to a highly infected lung homogenate standard.

**Results:**

**a) Antifungal dose determination.**

Dose-ranging studies were performed to determine an appropriate sub-therapeutic antifungal dose. In the leukopenic model (cortisone + cyclophosphamide), no effect of the posaconazole on the fungal burden could be observed at any dose tested (Figure 64).

**Effect of posaconazole injection on fungal burden**

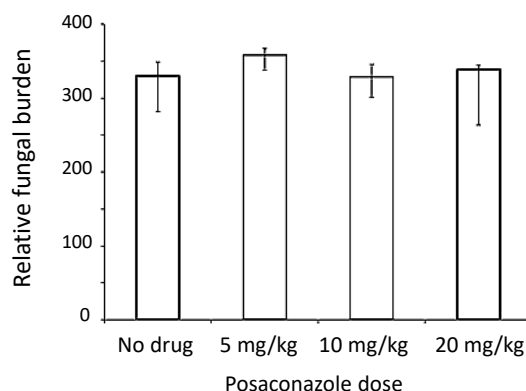


Figure 64: Fungal burden at day +4 in lungs of immunosuppressed mice intratracheally infected with  $5 \times 10^3$  conidia of *A. fumigatus* and treated orally every 12 hours with the indicated dose of posaconazole.

We therefore decided to move to the neutrophil-depleted model (Ly6G). Survival was used as an endpoint in these dose-optimization studies. In this model, 5 mg of posaconazole/kg of mice produced a significant but not maximal therapeutic effect (Figure 65). Posaconazole doses of 5 mg/kg and 2.5mg/kg were therefore selected for further study in combination with GH therapy.

**Effect of posaconazole on mouse survival**

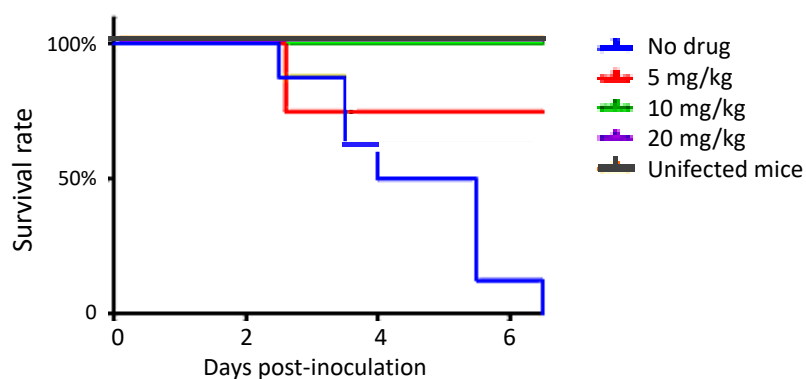


Figure 65. Survival of neutropenic mice infected with a single dose of *A. fumigatus* strain Af293 conidia ( $5 \times 10^6$ ) and treated orally with posaconazole every 12 hours. 8 mice per group in a single experiment.

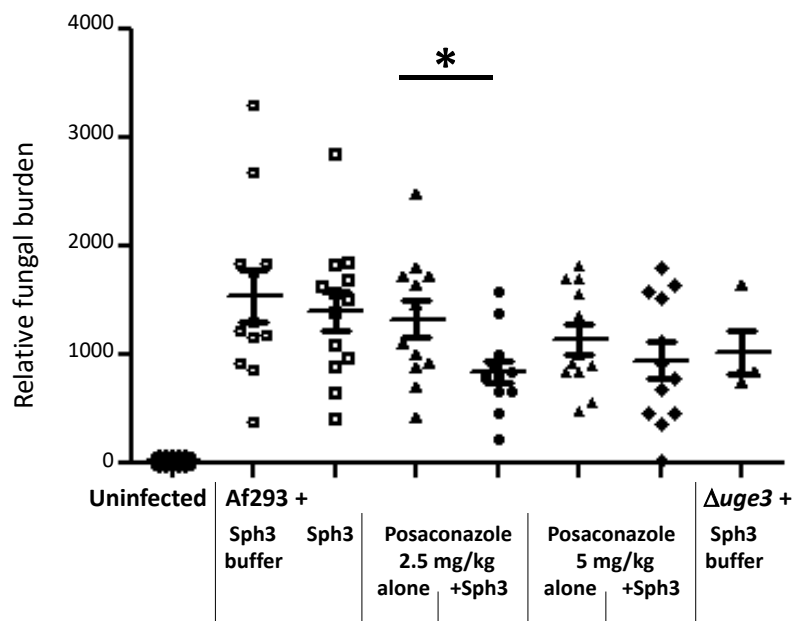
**b) Potentiation of posaconazole by Sph3 and PelA.**

Posaconazole monotherapy at 5 or 2.5mg/kg/day had no significant effect on pulmonary fungal burden (Figure 66A and 66B) in neutrophil depleted mice. The combination of Sph3 to 2.5 mg/kg

posaconazole resulted in a significant reduction of fungal pulmonary fungal burden as compared with posaconazole alone or Sph3 therapy alone. As expected, Sph3 monotherapy resulted in a trend to reduced pulmonary fungal burden at 2 days of infection in the neutrophil depletion model (Figure 66A) that was less marked than the effect observed in our previous studies at 4 days of infection in the cortisone acetate-cyclophosphamide model (Figure 52). A trend towards reduced fungal burden was also observed when Sph3 was combined with the 5 mg/kg dose of posaconazole, but this was not statistically significant, in part due to a greater antifungal effect of this dose of posaconazole monotherapy.

The addition of PelA alone resulted in a dramatic reduction in pulmonary fungal burden (Figure 66B) which precluded the assessment of PelA - posaconazole synergy.

**A. Effect on fungal burden of posaconazole in combination with Sph3**



## B. Effect on fungal burden of posaconazole in combination with PelA

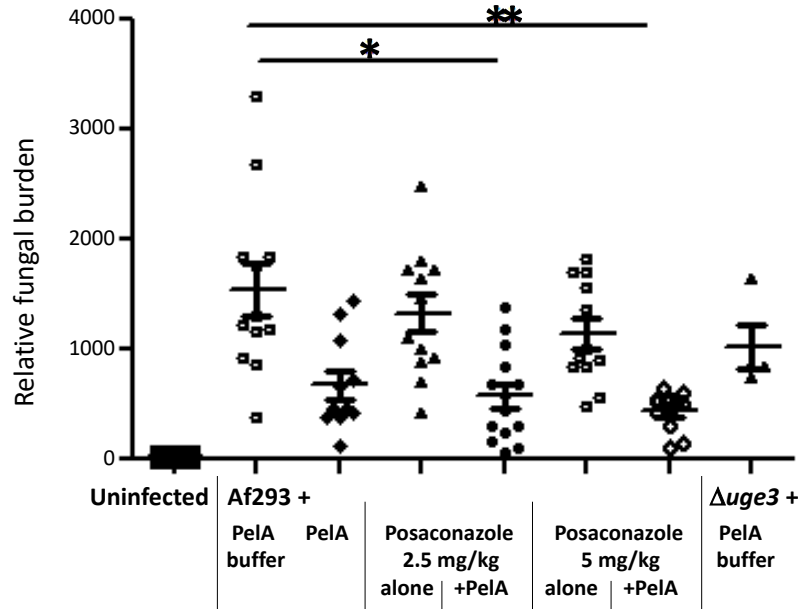


Figure 66. Pulmonary fungal burden of immunosuppressed mice intratracheally inoculated with  $5 \times 10^3$  conidia of the indicated *A. fumigatus* strain with or without 500  $\mu$ g of Sph3 (A.) or PelA (B.), and then treated with the indicated dose of posaconazole every 12h for 2 days. Fungal burden was determined by galactomannan quantification (Platelia Aspergillus EIA) of lung homogenates. The experiment was performed with groups of 8 mice per condition, on 2 separate occasions ( $n=2$ ). \* and \*\* indicate a significant difference in GM content as compared with untreated, infected mice ( $p < 0.05$  and  $< 0.01$ , respectively, by Kruskal-Wallis with Dunn's multiple comparison).

Beyond the initial SOW, we also tested the potentiation of an echinocandin drug (caspofungin) with PelA.

## 2- Potentiation of caspofungin.

### a) Antifungal dose determination.

**Methodology:** Mice were immunosuppressed, infected and treated as described above. Our standard assay of pulmonary GM quantification is not suitable for studies of caspofungin treatment, as treatment with this agent can induce spurious elevations of GM. Therefore, fungal burden was quantified by quantitative PCR, using the Taqman system and oligonucleotides and probe specific for *A. fumigatus* 18S RNA coding gene.

**Results:** Dose finding experiments were performed to identify a subtherapeutic dose of caspofungin suitable for GH-antifungal combination assays. As has been reported by others, we were unable to identify a pulmonary fungal burden dose-response curve with caspofungin, even at suprathreshold doses (Figure 67).

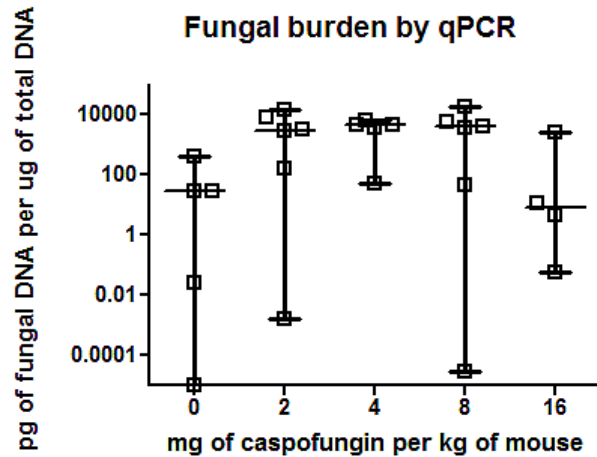


Figure 67. Fungal burden in lungs of immunosuppressed mice intratracheally infected with  $5 \times 10^6$  conidia of *A. fumigatus* and treated with the indicated doses of caspofungin. Results shown are from a single experiment with 8 mice per condition. Horizontal lines indicated the median of each experimental group, error bars represent the 75<sup>th</sup>- and 25<sup>th</sup>-percentile. No significant change was observed between groups, by Mann-Whitney.

We therefore turned to the use of survival as a measure of antifungal effect. A dose of 0.5 and 1 mg/kg of caspofungin were observed to enhance the survival of mice infected with *A. fumigatus*. (Figure 68).

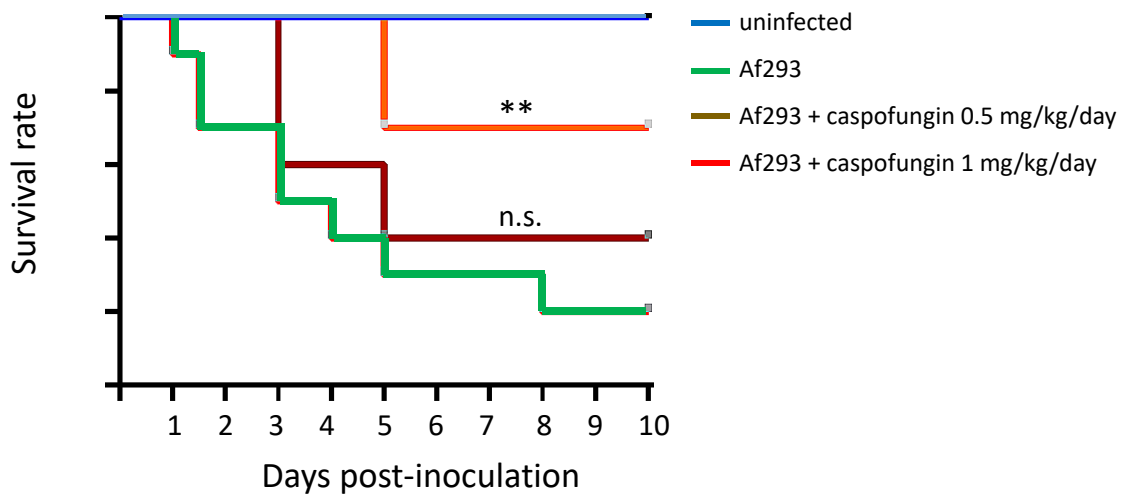


Figure 68. Mouse survival after infection with  $5 \times 10^6$  conidia of *A. fumigatus* and daily injection of various doses of caspofungin or with phosphate buffer saline. \*\* indicates significant difference for survival with the mice injected with Af293 alone ( $p < 0.01$  by Log-rank (Mantel-Cox)). n.s., indicates no significant difference.

b) Potentiation of caspofungin by PelA.

*Methodology:* Mice were immunosuppressed, infected and treated with caspofungin and PelA as described above.

*Results:* Treatment with PelA markedly potentiated the antifungal effects of both doses of caspofungin (Figure 69), reducing mouse mortality from ~70% to 10%.

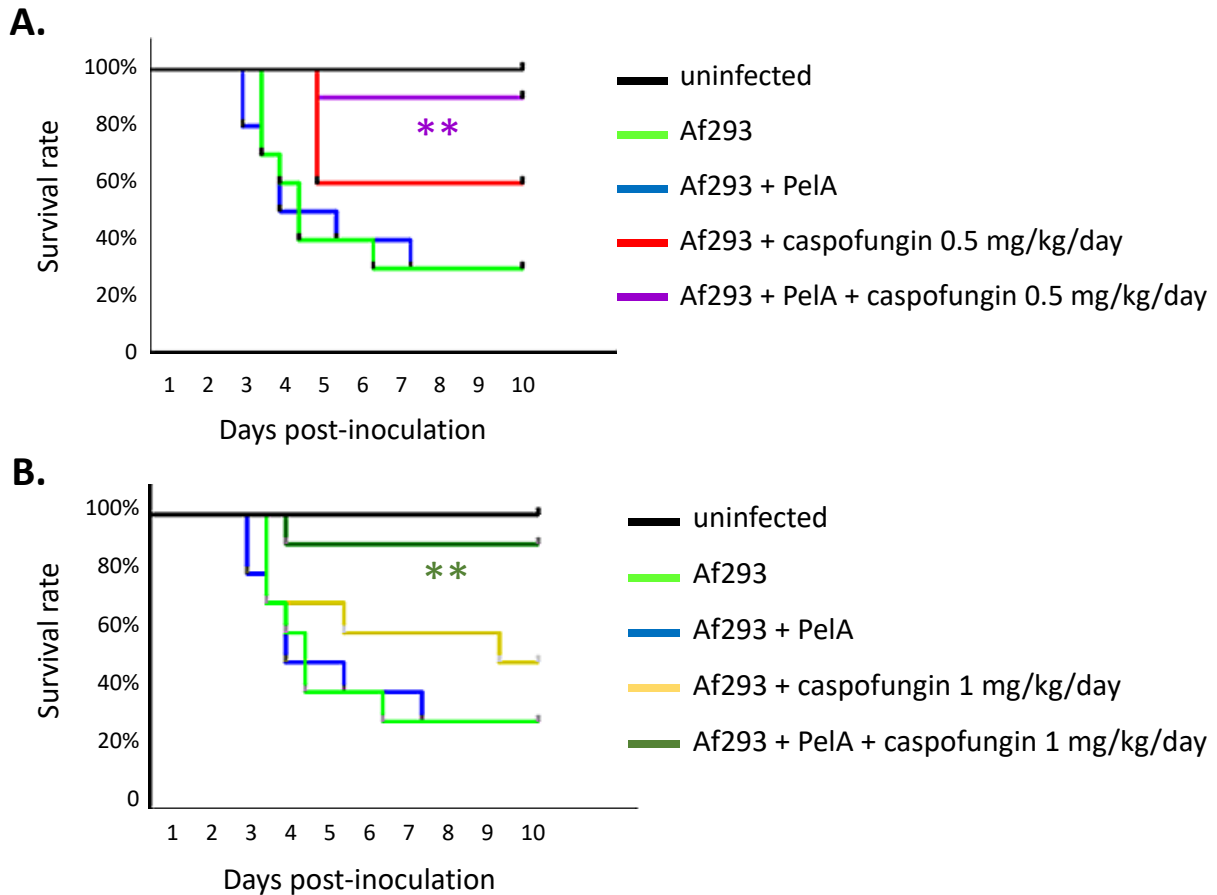


Figure 69. Mouse survival after infection with phosphate buffer saline (PBS), or  $5 \times 10^6$  conidia of *A. fumigatus*, or 500  $\mu\text{g}$  of PelA, or a combination of conidia and PelA, followed by a daily injection of 0.5 mg of caspofungin/kg of mouse (panel A) or 1 mg of caspofungin/kg (panel B). \*\* indicates significant difference for survival with the mice injected with Af293 alone ( $p < 0.01$  by Log-rank (Mantel-Cox)).

These results add to the body of evidence generated by our studies that support the use of GH therapy for the treatment of invasive aspergillosis.

**Subtask 3: Determine the effects of hydrolase (PslG/PelA and PslG/Ega3)-antibiotic combinations on bacterial burden of mice infected with *P. aeruginosa*.** [10 mice per group X 5 experimental groups X 2 hydrolase –antibiotic combinations X 2 time points AND 3 mice for histopathology X 5 groups X 2 hydrolase –antibiotic combinations at a single time point all performed in duplicate = 460 mice] Dr Sheppard’s lab. Months 25-36. Completion level = 100%.

**A- Acute model.**

**Methodology:** Mice were intratracheally infected with a 50 µL suspension containing  $1.5 \times 10^7$  bacteria (*P. aeruginosa* PAO1), in combination with 500 µg of single GH, or 250 µg of each GH if in combination, or sterile GH buffer. Ciprofloxacin, or ceftazidime, was administered intraperitoneally at 4h, 12h and 20h post-infection. At 48 hours post infection, all mice were sacrificed. Blood and lungs were harvested and plated for quantitative culture. Bacterial burden was normalized to the weight of the harvested lung. These experiments were performed in triplicate.

**Results:**

**1- Potentiation of the effect of ciprofloxacin.**

**a) Determination of ciprofloxacin dose for acute model of mouse infection by *P. aeruginosa*.**

A dose of ciprofloxacin of 10 mg/kg was determined to be the minimal dose required to result in a detectable reduction in pulmonary bacterial burden (Figure 70A) and in hematogenous dissemination (Figure 70B) in our mouse model of pulmonary *Pseudomonas* infection. These effects were minimal at doses as high as 25 mg/kg of mouse, becoming significant only at 50 mg/kg. Conversely, dissemination in blood was effectively prevented at a dose of 25 mg/kg.

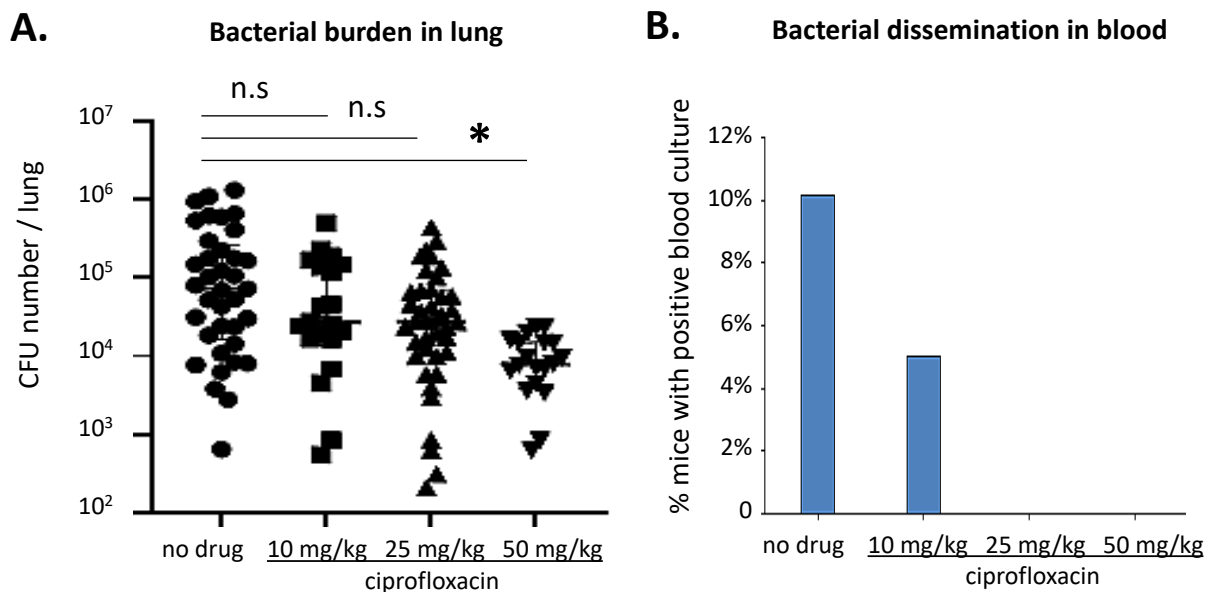


Figure 70. Effects of ciprofloxacin on pulmonary bacterial burden (A.) and on hematogenous dissemination of bacteria (B.) as determined by quantitative culture of lung homogenate or blood. Bacterial burden was normalized to the weight of the harvested lungs. Results shown are the aggregate of two to four independent experiments (n=2 for 10 mg and 50 mg/kg, n=4 for 0 and 25 mg/kg), with groups of 8 mice per condition. Horizontal lines indicate the median of each experimental group, error bars show the 75-

and 25-percentile. \* indicates a significant difference between untreated mice and those receiving ciprofloxacin ( $p < 0.01$  by Kruskal-Wallis).

b) GH monotherapy did not significantly potentiate the effect of ciprofloxacin.

**PslG:** The combined results of five experiments testing the ability of PslG to potentiate the action of ciprofloxacin failed to demonstrate a significant potentiation of ciprofloxacin by PslG monotherapy (Figure 71). While ciprofloxacin treatment prevented PslG-mediated hematogenous dissemination of *P. aeruginosa*, the combination of PslG and ciprofloxacin was not superior to ciprofloxacin alone in reducing the pulmonary bacterial burden of infected mice.

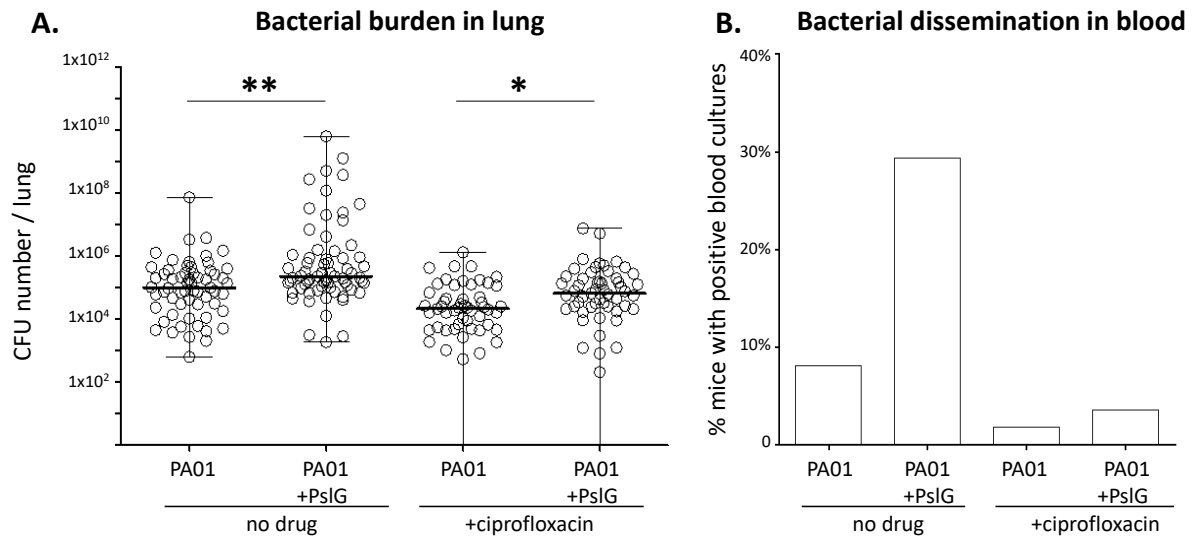


Figure 71. A. Effects of PslG and ciprofloxacin on the pulmonary bacterial burden as determined by quantitative culture of lung homogenate on LB plates. Horizontal lines indicate the median of each experimental group, error bars show the 75- and 25-percentile. B. Percentage of mice with positive blood cultures in each group. The experiment has been performed with groups of 8 mice per condition, on 5 separate occasions ( $n=5$ ). \* and \*\* indicate a significant difference between untreated mice and those receiving PslG ( $p < 0.05$  and  $< 0.01$ , respectively, by Kruskal-Wallis).

**PelA:** As with PslG monotherapy, PelA monotherapy did not potentiate the activity of ciprofloxacin (Figure 72).

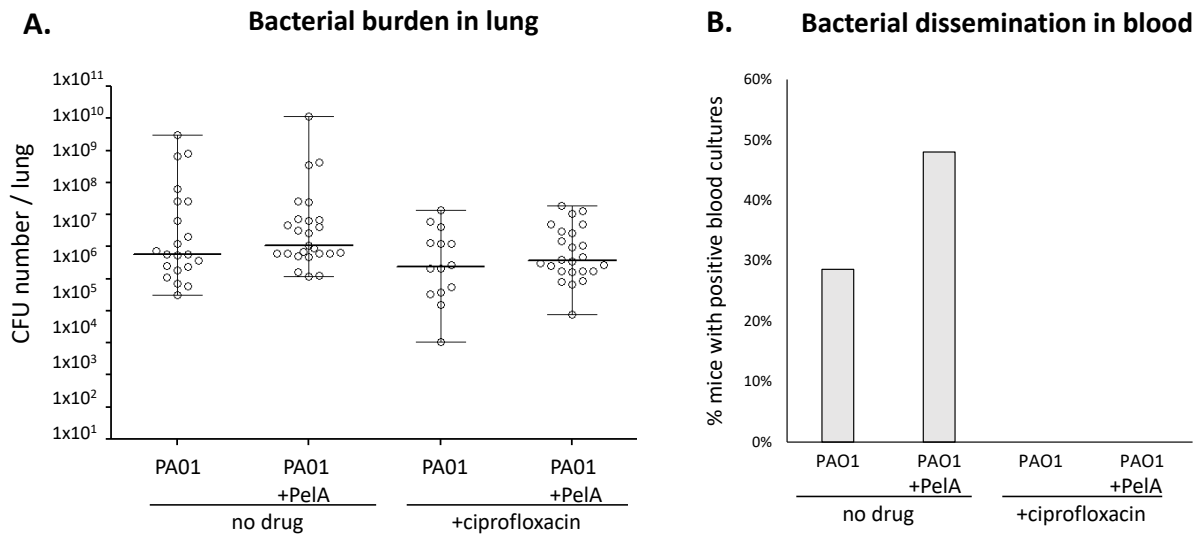


Figure 72. A. Effects of PelA and ciprofloxacin on the pulmonary bacterial burden as determined by quantitative culture of lung homogenate on LB plates. Horizontal lines indicate the median of each experimental group, error bars show the 75- and 25-percentile. B. Percentage of mice with positive blood cultures in each group. The experiment has been performed with groups of 8 mice per condition, on 3 separate occasions (n=3). There was no significant difference between untreated mice and those receiving PelA, by Kruskal-Wallis.

**Ega3:** As with other GH therapy, Ega3 monotherapy did not potentiate ciprofloxacin activity (Figure 73). In contrast to PslG and PelA however, Ega3 monotherapy did not result in increased hematogenous dissemination of bacteria.

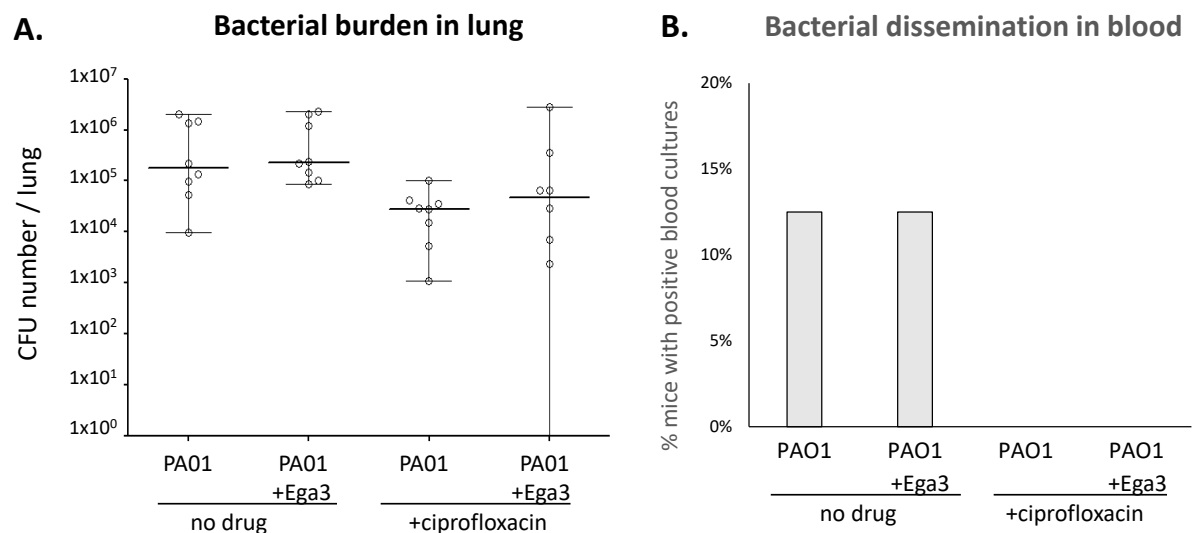


Figure 73. A. Effects of Ega3 and ciprofloxacin on the pulmonary bacterial burden of *P. aeruginosa* infected mice as determined by quantitative culture of lung homogenate on LB plates. B. Percentage of mice with positive blood cultures in each group. Horizontal lines indicate the median of each experimental group,

error bars show the 75- and 25-percentile. The experiment has been performed once with groups of 8 mice per condition (n=1). There was no significant difference between untreated mice and those receiving Ega3, by Kruskal-Wallis.

Collectively these data suggest that therapy with a single GH does not potentiate ciprofloxacin. As *P. aeruginosa* can produce both Pel and Psl, it is possible that degrading both polymers is required to augment antibiotic efficacy *in vivo*. We therefore turned to the evaluation of combination GH therapy (PslG/Ega3 and PslG/PelA) to potentiate ciprofloxacin.

c) PslG/PelA combination therapy potentiates the effect of ciprofloxacin

The addition of PslG/PelA to ciprofloxacin was associated with a reduction in pulmonary bacterial burden as compared with ciprofloxacin or PslG/PelA therapy alone (Figure 74). As observed previously, GH treatment alone was associated with an increased rate of bacteremia, however this was not seen in ciprofloxacin-treated mice.

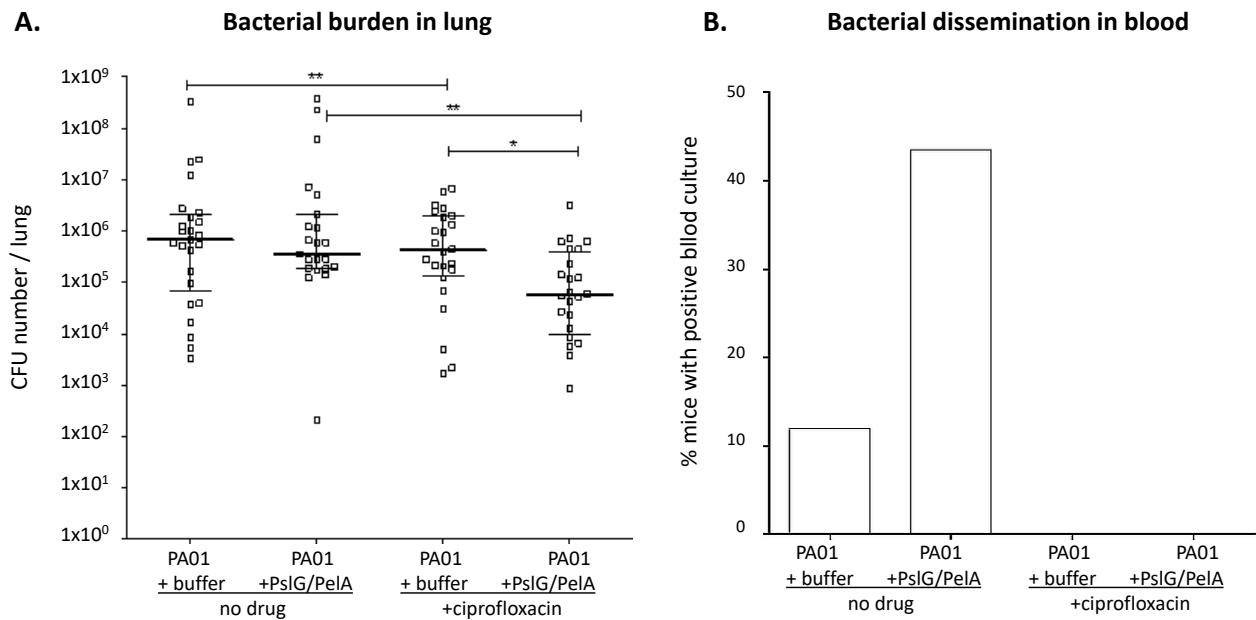


Figure 74. A. Effects of PslG/PelA and ciprofloxacin on the pulmonary bacterial burden of *P. aeruginosa* infected mice as determined by quantitative culture. B. Percentage of mice with positive blood cultures in each group. Horizontal lines indicate the median of each experimental group, error bars show the 75<sup>th</sup>- and 25<sup>th</sup>-percentile. Experiments were performed on three separate occasions, on groups of 8 mice per condition (n=3). \* and \*\* indicate a significant difference in pulmonary bacterial burden between indicated groups ( $p < 0.05$  and  $< 0.01$ , respectively, by Kruskal-Wallis).

d) PslG/Ega3 combination therapy does not significantly potentiate the effect of ciprofloxacin.

The addition of PslG/Ega3 to ciprofloxacin was associated with a trend to reduced pulmonary bacterial burden as compared with ciprofloxacin alone, but this was not statistically significant (Figure 75). PA01 with PslG/PelA, GH therapy alone resulted in increased bacteremia, but the use of ciprofloxacin protected mice from this effect.

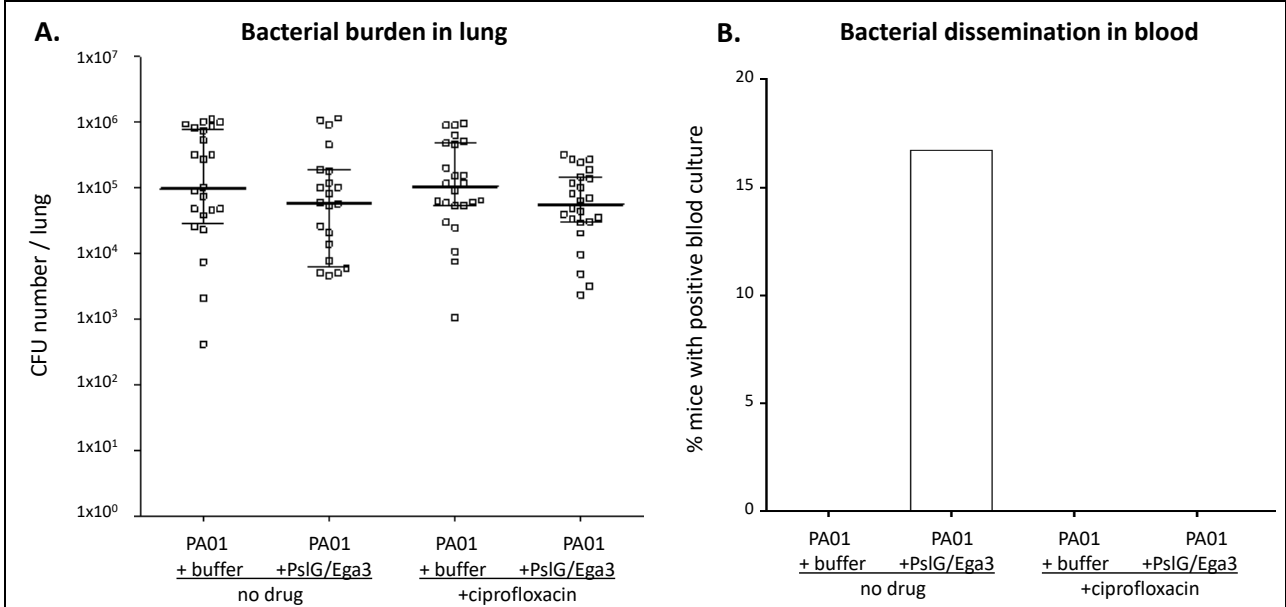


Figure 75. A. Effects of PsIG/Ega3 and ciprofloxacin on the pulmonary bacterial burden of *P. aeruginosa* infected mice as determined by quantitative culture. B. Percentage of mice with positive blood cultures in each group. Horizontal lines indicate the median of each experimental group, error bars show the 75<sup>th</sup>- and 25<sup>th</sup>-percentile. Experiments were performed on three separate occasions, on groups of 8 mice per condition (n=3). \* and \*\* indicate a significant difference in pulmonary bacterial burden between indicated groups ( $p < 0.05$  and  $< 0.01$ , respectively, by Kruskal-Wallis).

**2- Potential of the effect of ceftazidime.**

a) Determination of ceftazidime dose for acute model of mouse infection by *P. aeruginosa*.

A dose of 25 mg/kg of mouse injected subcutaneously produced a reproducible minimal reduction in bacterial burden, while doses of 50mg/kg and higher resulted in a dramatic reduction in bacterial burden (Figure 76). We therefore selected a dose of 25mg/kg for testing in combination with GH therapy to ensure that a potentiation of antimicrobial activity would be detectable.

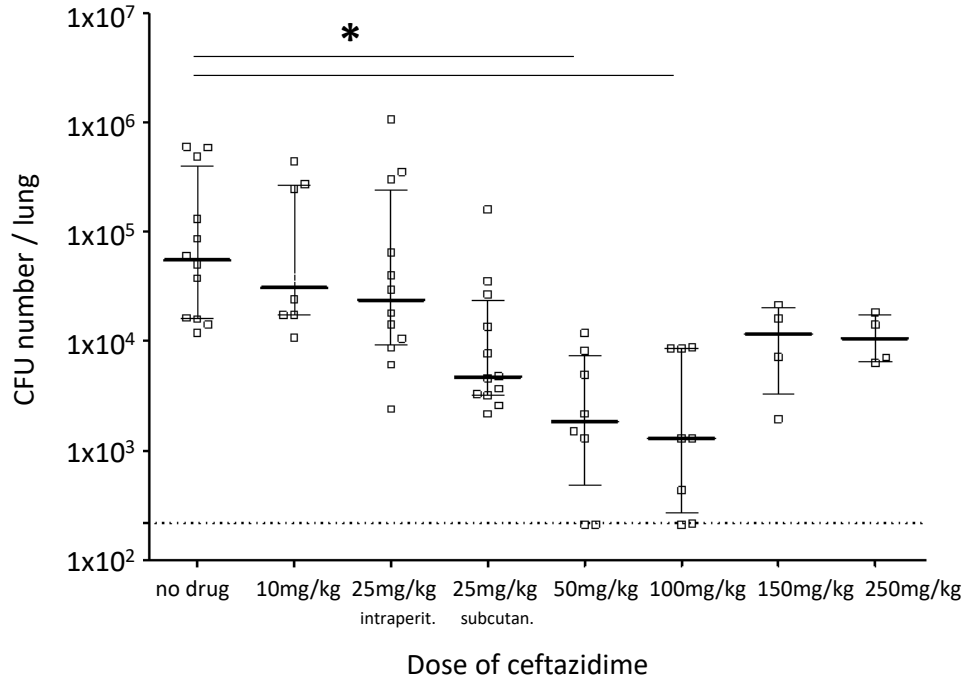


Figure 76. Effect of the indicated doses of ceftazidime on pulmonary bacterial burden as determined by quantitative culture. Ceftazidime was administered at 4h, 12h and 20h post infection by intraperitoneal injection (intraperit) or subcutaneously (subcutan) as indicated. Horizontal lines indicate the median of each experimental group, error bars indicate the 75<sup>th</sup>- and 25<sup>th</sup>-percentile. Experiments were performed on three separate occasions, on groups of 6 mice per condition (n=3). \* indicates a significant difference in pulmonary bacterial burden between indicated groups ( $p < 0.05$  by Kruskal-Wallis).

**b) PslG/PelA and PslG/Ega3 combination therapy do not significantly potentiate the effect of ceftazidime.**

Treatment with ceftazidime was associated with a reduction in pulmonary bacterial burden (Figure 77A). In contrast to the findings with ciprofloxacin, the combination of PslG/PelA or PslG/Ega3 did not potentiate the antibacterial action of ceftazidime (Figure 77). Taken as a whole, these findings suggest the ability of GH-therapy to augment antibacterials is likely drug-specific.

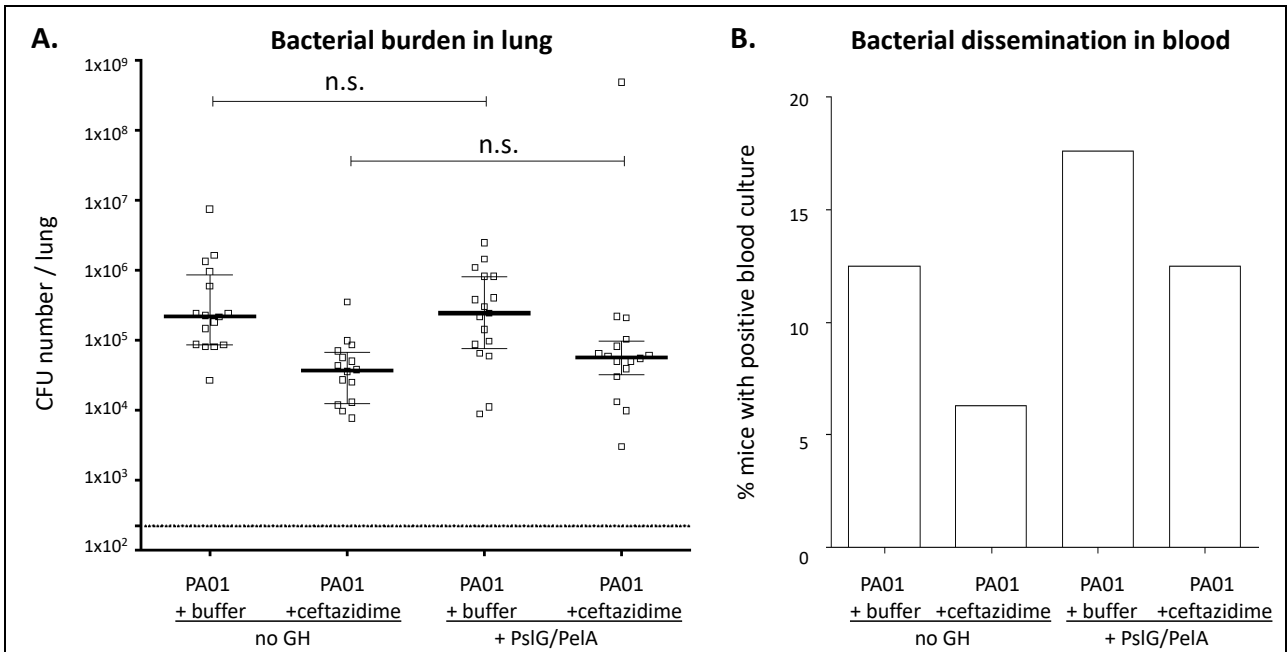


Figure 77. A. Effects of PsIG/PelA and ceftazidime on the pulmonary bacterial burden of *P. aeruginosa* infected mice as determined by quantitative culture. B. Percentage of mice with positive blood cultures, in each group. Horizontal lines indicate the median of each experimental group, error bars show the 75<sup>th</sup>- and 25<sup>th</sup>-percentile. Experiments were performed on two separate occasions, on groups of 8 mice per condition in each experiment (n=2). n.s. indicate an absence of significant difference in pulmonary bacterial burden between indicated groups, by Kruskal-Wallis.

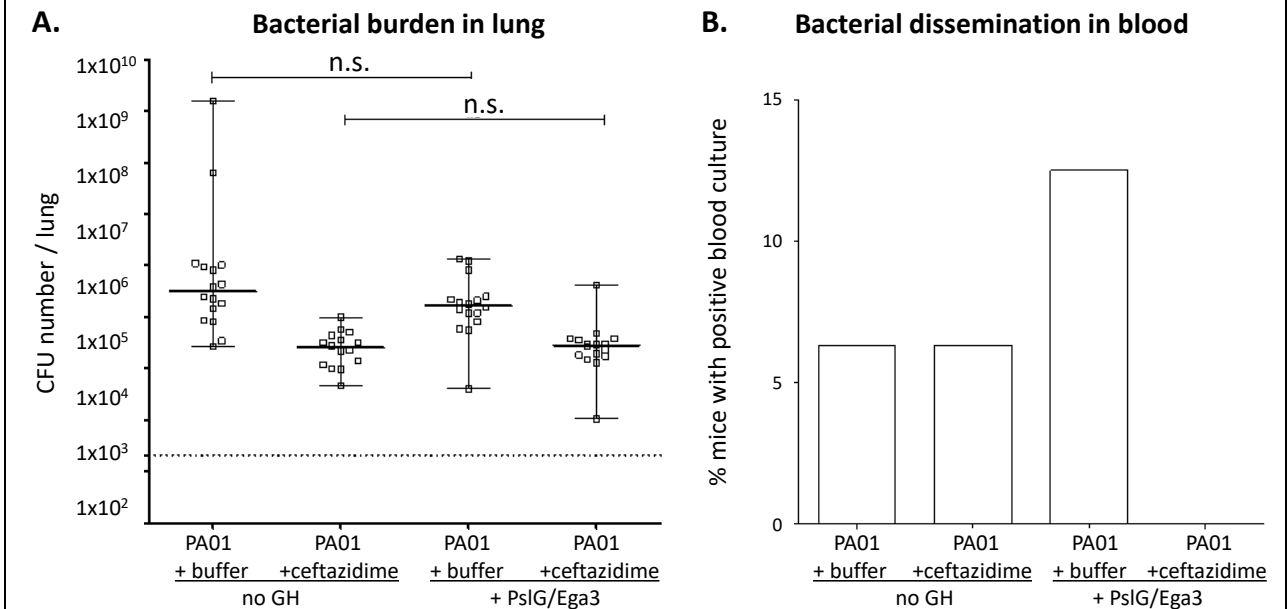


Figure 78. A. Effects of PsIG/Ega3 and ceftazidime on the pulmonary bacterial burden of *P. aeruginosa* infected mice as determined by quantitative culture. B. Percentage of mice with positive blood cultures, in each group. Horizontal lines indicate the median of each experimental group, error bars show the 75<sup>th</sup>- and 25<sup>th</sup>-percentile. Experiments were performed once, on groups of 8 mice per condition (n=1). n.s. indicates a non-significant difference in pulmonary bacterial burden between indicated groups, by Kruskal-Wallis.



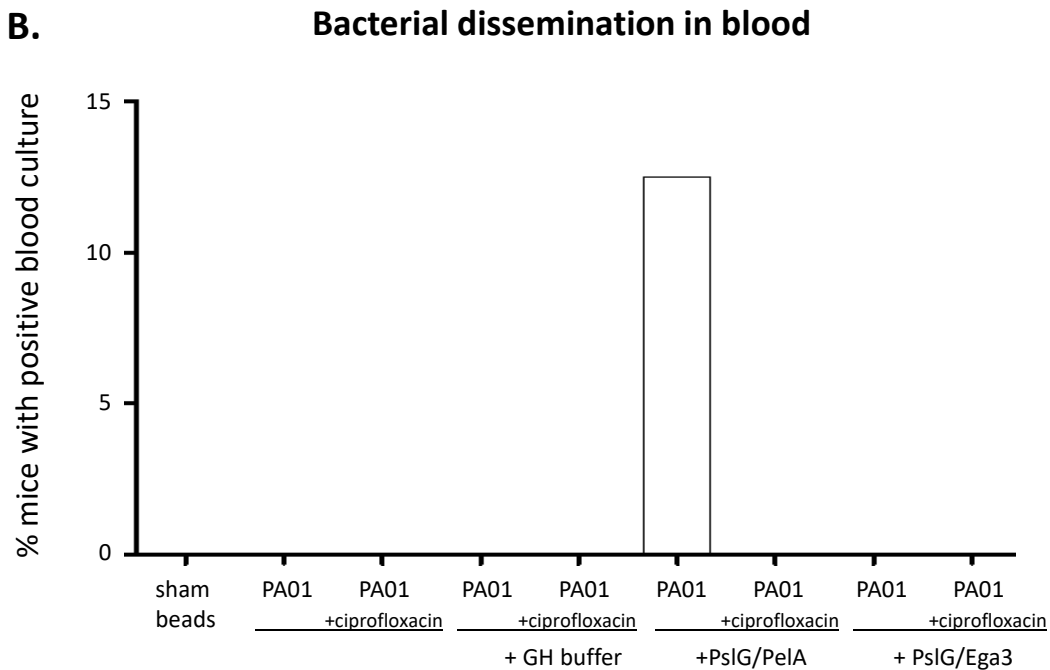


Figure 79. A. Effects of PslG/PelA or PslG/Ega3 and ciprofloxacin on the pulmonary bacterial burden of *P. aeruginosa* infected mice as determined by quantitative culture. B. Percentage of mice with positive blood cultures, in each group. Horizontal lines indicate the median of each experimental group, error bars show the 75<sup>th</sup>- and 25<sup>th</sup>-percentile. Experiments were performed on two separate occasions, on groups of 8 mice per condition. No significant difference in pulmonary bacterial burden between groups was identified, by Kruskal-Wallis.

**Milestone Achieved: Show a proof-of-concept for candidate hydrolases for use in treatment of *A. fumigatus* and *P. aeruginosa*. To make ready to initiate trials of delivery systems and detailed pharmacodynamics experiments as a prelude to Phase I clinical trials.**

### **What opportunities for training and professional development has the project provided?**

Rachel Corsini, Mai Nguyen and James Stewart were trained by Melanie Lehoux in regard of animal care. They therefore learned to perform intratracheal injection of GHs in mice, as well as mouse infection with pathogens. They also learned to isolate *P. aeruginosa* from lung tissues and monitor this population.

Brian Hicks and Piyanka Sivarajah were trained by Ira Lacdao in modern biochemical techniques, specifically protein expression and purification.

Ira Lacdao, Natalie Bamford, Perrin Baker, Brendan Snarr, Caitlin Zacharias and François LeMauff presented their results in relation to this grant at several conferences (see section “Products”), thus improving their presentation skills.

### **How were the results disseminated to communities of interest?**

Results of our GH studies published in the Proceedings of the National Academy of Sciences (USA) were the subject of a numerous media interviews and reports including: CTV National and local television news as well as TéléQuébec: Les Electrons Libres; newspaper articles in Le Devoir and LaPresse; radio interviews on CBC and CJAD radio; and internet feature articles on CBC and RCI.net. Our work was also chosen to be amongst the 10 scientific projects of the year in the review Quebec Science.

Besides, results as a whole were presented at peer conferences, as listed in section “6. PRODUCTS”

### **What do you plan to do during the next reporting period to accomplish the goals?**

This is a final report.

## **4. IMPACT**

### **What was the impact on the development of the principal discipline(s) of the project?**

Our demonstration that microbial GHs can disrupt biofilms has generated significant interest in the scientific community. We were invited to submit a “Pearl manuscript” in PLOs Pathogens in 2019 and to submit an editorial, in Future Microbiology, describing the potential of these therapeutics in the fight against antimicrobial resistant organisms.

Other groups have now begun to evaluate microbial enzymes as potential anti-biofilm therapeutics, as illustrated in a review published in Nature Microbiology Reviews highlighting the potential of GH therapy.

### **What was the impact on other disciplines?**

**XTT metabolic assay**

This assay is a commonly used method to study fungal biofilms and the activity of antimicrobial agents against biofilm-grown fungi. Our finding that loss of exopolysaccharide matrix can lead to artificially high metabolic readings suggests an important limitation to this assay that was previously unknown.

**What was the impact on technology transfer?**

The results of the studies described in this report add value to our existing intellectual property and patent describing the use of microbial GHs as anti-biofilm therapeutics.

**What was the impact on society beyond science and technology?**

Nothing to report

**5. CHANGES/PROBLEMS.**

**Changes in approach and reasons for change**

**Major Task 1, Subtask 4:**

We successfully developed a method to grow *A. fumigatus* and *P. aeruginosa* under flow biofilm conditions. Consistent with the anti-GAG activity of PslG and Sph3, GH-treated biofilms (at 2  $\mu$ M for 2h) exhibited reduced SBA staining of *A. fumigatus* wild-type compared to the untreated sample. However, given that pulmonary biofilms are not subjected to flow conditions, and the activity of hydrolases has not proven different under flow and static conditions, we elected to not pursue these experiments further and to focus our studies on static conditions and more relevant *in vivo* models of biofilm infection.

**Major Task 5, Subtask 4:**

Our experiments suggest that, although Psl plays a role in lung colonization by *P. aeruginosa*, PslG alone (or PelA alone) is not protective against *P. aeruginosa* infection. Our data suggest that when given as monotherapy, GH enzymes can increase bacterial motility and virulence via a catalytically-independent mechanism. We therefore elected to focus our future studies on GH-antibiotic combination therapy as outlined in Major Task 7.

**Actual or anticipated problems or delays and actions or plans to resolve them**

N/A

**Changes that had a significant impact on expenditures**

Nothing to Report

**Significant changes in use or care of human subjects, vertebrate animals, biohazards, and/or select agents**

**Significant changes in use or care of human subjects**

No use of human subjects in this grant

**Significant changes in use or care of vertebrate animals.**

Nothing to Report

**Significant changes in use of biohazards and/or select agents**

Nothing to Report

**6. PRODUCTS.**

**Journal publications**

**NB: all publication front pages are displayed in section "9. APPENDICES"**

2017:

Snarr BD, Baker P, Bamford NC, Sato Y, Liu H, Lehoux M, Gravelat FN, Ostapska H, Baistrocchi SR, Cerone RP, Filler EE, Parsek MR, Filler SG, Howell PL, and Sheppard DC. (2017) *Microbial glycoside hydrolases as antibiofilm agents with cross-kingdom activity*. PNAS. doi: 10.1073/pnas.1702798114.

Zhang S, Chen Y, Ma Z, Chen Q, Ostapska H, Gravelat FN, Lu L, Sheppard DC. (2017) *PtaB, a lim-domain binding protein in Aspergillus fumigatus regulates biofilm formation and conidiation through distinct pathways*. Cell Microbiol. doi: 10.1111/cmi.12799.

2018:

Asker D, Awad TS, Baker P, Howell PL, Hatton BD. (2018) *Non-eluting, surface bound enzymes disrupt surface attachment of bacteria by continuous biofilm polysaccharide degradation*. Biomaterials. doi: 10.1016/j.biomaterials.2018.03.016

Little DJ, Pfoh R, Le Mauff F, Bamford NC, Notte C, Baker P, Guragain M, Robinson H, Pier GB, Nitz M, Deora R, Sheppard DC, Howell PL. (2018) *PgaB orthologues contain a glycoside hydrolase domain that cleaves deacetylated poly- $\beta$ (1,6)-N-acetylglucosamine and can disrupt bacterial biofilms*. Plos Pathogens. doi: 10.1371/journal.ppat.1006998.

Low KE, Howell PL. (2018) *Carbohydrate active enzymes involved in exopolysaccharide biosynthesis in Gram-negative bacteria*. Curr Opin in Struct Biol. 53, 32-44.

Snarr BD, Howell PL, Sheppard DC. (2018) *Hoisted by their own petard: do microbial enzymes hold the solution to treating and preventing biofilm infections?* Future Microbiology 13:395-39. doi: 10.2217/fmb-2017-0243.

**2019:**

Bamford, NC., Le Mauff, F., Subramanian, AS., Yip, P., Millan, C., Zhang, Y., Zacharias, C., Forman, A., Nitz, M., Codee, JDC., Uson, I., Sheppard, DC., and Howell, PL. (2019) *Ega3 from the fungal pathogen Aspergillus fumigatus is an endo-alpha-1,4-galactosaminidase that disrupts microbial biofilms*. Journal of Biological Chemistry – **Editor’s pick**. 2019. doi:10.1074/jbc.RA119.009910

Le Mauff F, Bamford NC, Alnabelseya N, Zhang Y, Baker P, Robinson H, Codée JDC, Howell PL, Sheppard DC. (2019) *Molecular mechanism of Aspergillus fumigatus biofilm disruption by fungal and bacterial glycoside hydrolases*. Journal of Biochemical Chemistry. doi: 10.1074/jbc.RA119.008511

Ostapska H, Howell PL, Sheppard DC. (2019) *Deacetylated microbial biofilm exopolysaccharides: It pays to be positive*. PLOS Pathogens. doi: 10.1371/journal.ppat.1007411

Speth C, Rambach G, Lass-Flörl C, Howell PL, Sheppard DC. (2019) *Galactosaminogalactan (GAG) and its multiple roles in Aspergillus pathogenesis*. Virulence. doi: 10.1080/21505594.2019.1568174.

Zacharias CA, Sheppard DC. (2019) *The role of Aspergillus fumigatus polysaccharides in host-pathogen interactions*. Curr Opin Microbiol. doi: 10.1016/j.mib.2019.04.006. Review

**2020:**

Bamford NC, Le Mauff F, Van Loon JC, Ostapska H, Snarr BD, Zhang Y, Kitova EN, Kalsen JS, Codee JDC, Sheppard DC, Howell PL. *Structural and biochemical characterization of the exopolysaccharide deacetylase Agd3 required for Aspergillus fumigatus biofilm formation*. Nat Commun 11:2450. doi: 10.1038/s41467-020-16144-5.

Ostapska H, Raju D, Lehoux M, Lacdao I, Gilbert G, Sivarajah P, Bamford B, Baker P, Gravelat F, Dr. Howell PL, Sheppard DC. *Pre-clinical evaluation of recombinant microbial glycoside hydrolases as anti-biofilm agents in experimental invasive aspergillosis*. In revision, NPG Biofilms and Microbiomes.

**Books or other non-periodical, one-time publications.**

No publication in books or other non-periodical to be reported

**Other publications, conference papers, and presentations.**

**Presentations**

**2016:**

Sheppard DC, Invited Speaker, Immunocompromised Host Society Meeting, Santiago, Chile. *Enhancing delivery of antifungals to pulmonary lesions – intracellular antifungals and antibiofilm therapeutics*. Nov 14, 2016.

Sheppard DC, Invited Speaker, IUBMB Frontiers in Glycoscience: Host-pathogen interactions. Taipei, Taiwan. *Biofilm exopolysaccharides at the host-pathogen interphase*. Dec 12, 2016

**2017:**

Sheppard DC, Invited Speaker, 29th Fungal Genetics Conference. Asilomar, California. *Breaking the mold: From host-pathogen interactions to novel therapeutics for Aspergillus disease*. March 17 2017

Sheppard DC. *Aspergillus biofilm exopolysaccharide – from virulence factor to therapeutic target*. 29th Fungal Genetics Conference, Asilomar, California, March 19, 2017.

Sheppard DC. *Glycoside GHs as novel antibiofilm therapeutics*. US Department of Defense, CMDRP, Fort Detrick, Maryland, April 4, 2017.

Sheppard DC. *Glycoside GHs as novel antibiofilm therapeutics*. GlycoNET Network Centre of Excellence Annual General Meeting, Banff, Alberta, May 12, 2017.

Howell PL. *Microbial biofilms: Mechanisms to therapeutics*. Understanding Biology through Structure, Santa Fe, New Mexico, May 13-17, 2017.

Howell PL. *Microbial biofilms: Mechanisms to therapeutics*. Ontario Public Health, Toronto, Ontario, May 22, 2017.

Howell PL. *Microbial biofilms: Mechanisms to therapeutics*. SickKids Summer Student Seminar Program, Toronto, Ontario, June 22, 2017

Howell PL. *Glycoside hydrolases as therapeutics*. Gordon Research Conference, Cellulases and other carbohydrate active enzymes, New Hampshire, July 24-28, 2017.

Howell PL. *Microbial Biofilms: Molecular Mechanisms to Potential Therapeutics*. Genetech Inc, San Francisco, Nov 6-8, 2017.

**2018:**

Sheppard DC. Invited Seminar at Faculty of Veterinary Medicine, University of Montreal, Canada. *Breaking the mold – from bench to bedside, novel therapeutics for Aspergillus infections*. Feb 21, 2018.

Sheppard DC. *Breaking the mold – from bench to bedside, novel therapeutics for Aspergillus infections*. Keynote lecture, 16<sup>th</sup> Echinocandin Forum, Tokyo, Japan. March 10, 2018.

Sheppard DC. Keynote lecture at 16th Echinocandin Forum, Tokyo Japan. *Breaking the mold – from bench to bedside, novel therapeutics for Aspergillus infections*. March 10, 2018.

Sheppard DC. *Glycoside hydrolases as novel antibiofilm therapeutics*. Invited Speaker, US Department of Defence, JCP-2 Update, Fort Detrick, Maryland. May 20, 2018.

Sheppard DC. Invited Speaker, Banff Conference on Infectious Diseases, Alberta, Canada. *Breaking the mold – targeting biofilms of Aspergillus fumigatus*. May 25, 2018

Sheppard DC. Invited Speaker. Division of Infectious Diseases, Centre Hospitalier Universite de Montreal, Canada. *Breaking the mold: Development of new therapies to manage refractory fungal infections*. June 4, 2018.

Zacharias C, Lehoux M, Bamford N, Sheppard DC. *The role of the immune response in hydrolase mediated prophylaxis of fungal infections*. McGill Department of Microbiology and Immunology Research Day, Montreal, Canada. June 08, 2018.

Sheppard DC. Invited speaker, McGill Research Centre for Complex Traits Symposium, Montreal, Canada. *Breaking the mold: Aspergillus galactosaminogalactan*. June 11, 2018.

Howell PL. *Microbial Biofilms: Mechanisms to potential therapeutics*. FASEB Meeting, Phoenix, USA. June 17-22, 2018.

Sheppard DC. *Translational studies in antifungal prophylaxis*. Invited Speaker, Hematology Seminar Series Yonsei University Wonju Christian Hospital, Seoul, Korea. June 20, 2018.

Sheppard DC. Invited Speaker, Hematology Seminar Series Asan Medical Center, Seoul, Korea. *Translational studies in antifungal prophylaxis*. June 21, 2018.

Sheppard DC. *Translational Mycology – from bench to bedside*. Keynote Speaker, 20th Congress of the International Society of Human and Animal Mycology. Amsterdam, Netherlands. July 2, 2018.

Howell PL. *Microbial Biofilms: Mechanisms to potential therapeutics*. July 17-22, American Crystallographic Association Annual Meeting, Toronto, Canada. July 21-25, 2018.

Howell PL. *Microbiology: Microbes & the Body*. Youth Summer Program, Faculty of Medicine, University of Toronto, Canada. Aug 3, 2018.

Sheppard DC. *Biofilm exopolysaccharides – virulence factors and drug targets*. Faculty in Residence, Molecular Mycology of Pathogenic Fungi Summer Course, Marine Biology Laboratories, Woods Hole, Massachusetts. Aug 3, 2018.

Sheppard DC. *The science behind antifungal prophylaxis*, Invited Speaker, 17th Asia-Pacific Congress of Clinical Microbiology and Infection, Sept 1, 2018.

Sheppard DC. *Translational Mycology – from bench to bedside*. Keynote Speaker, 3rd Annual MycoCon and Fungal Infections Study Forum, New Delhi, India. Sept 22, 2018.

**2019:**

Howell PL, Keynote Speaker: *Microbial Biofilms: mechanisms to potential therapeutics*. Annual Tri-University Symposium, University Guelph, May 7, 2019.

Le Mauff F, Sheppard DC: *Galactosaminogalactan synthesis is mediated by the cooperative activity of two glycosyl transferases*. Canadian Glycomics symposium, Banff, May 15-17, 2019.

Sheppard DC: *New science behind invasive aspergillosis*. Invited Speaker, ID week 2019, Washington DC. Oct 6, 2019.

Sheppard DC: *Fungal Kingdom, Threats and Opportunities. Novel therapies for fungal infections through a glycobiology lens*. Invited Speaker, CIFAR Program, Toronto. Nov 17, 2019

**2020:**

Sheppard DC. *Novel Antifungal therapies*. Invited Speaker, Cidara Expert Insight Series, San Diego, California. Jan 21, 2020

Sheppard DC. *Aspergillus biofilms: informing new therapies*. Invited Speaker, Advances against Aspergillosis and Mucormycosis, Lugano, Switzerland. March 3, 2020.

P.L. Howell. Microbial Exopolysaccharide biosynthesis: Molecular mechanisms to potential therapeutics. European Glycoscience Community webinar series, September 11, 2020.

**Posters**

**2017:**

Snarr BD, Baker P, Bamford NC, Sato Y, Lui H, Lehoux M, Baistrocchi SR, Filler SG, Howell PL, Sheppard DC. *Microbial glycoside hydrolases as antibiofilm agents with cross-kingdom activity against both bacteria and fungi*. RI-MUHC IDIGH Research Day 2017, Montreal, Quebec, April 21, 2017.

Baker P, Silver H, Hill PJ, Pestrak MJ, Litvak M, Post M, Parsek MR, Wozniak DJ, Howell PL. *Developing enzyme-based bacterial biofilm disruptors by targeting exopolysaccharides*. Canadian Glycomics Symposium 2017, Banff, Alberta, May 10-12, 2017.

Bamford NC, Snarr BD, Gravelat FN, Little DJ, Le Mauff F, Lee MJ, Robinson H, Sheppard DC, Howell PL. *A novel glycoside hydrolase is required for galactosaminogalactan biosynthesis by Aspergillus fumigatus*. Canadian Glycomics Symposium 2017, Banff, Alberta, May 10-12, 2017.

Snarr BD, Baker P, Bamford NC, Sato Y, Lui H, Lehoux M, Gravelat FN, Baistrocchi SR, Parsek MR, Filler SG, Howell PL, Sheppard DC. *Microbial glycoside hydrolases as antibiofilm agents with cross-kingdom activity*. Trends in Medical Mycology Congress. Belgrade, Serbia. October 7, 2017

**2018:**

Le Mauff F, Bamford N, Alnabelseya N, Howell PL, Sheppard DC. *Molecular mechanism of Aspergillus biofilm disruption by fungal and bacterial glycoside hydrolases*. 8<sup>th</sup> Advances Against Aspergillosis Meeting, Lisbon, Portugal. Feb 1-3, 2018.

Lacdao I, Hicks B, Bamford N, Baker P, Sheppard DC, Howell PL. *Optimizing microbial glycoside hydrolase expression and purification for therapy development against bacterial and fungal biofilms*. Canadian Glycomics Symposium, Banff, Alberta, Canada. May 7-9<sup>th</sup>, 2018.

Pfoh R, Little DJ, Le Mauff F, Bamford NC, Notte C, Baker P, Guragain M, Robinson H, Pier GB, Nitz M, Deora R, Sheppard DC, Howell PL. *Molecular basis for the disruption of PNAG dependent biofilms by the dual-functional deacetylase and glycoside hydrolase PgaB*. American Crystallographic Association, Toronto, Canada. July 21-25, 2018.

- **Website(s) or other Internet site(s)**

No dissemination of the results through a website to be reported

- **Technologies or techniques**

No new technology to be reported.

- **Inventions, patent applications, and/or licenses**

**Patent**

1. Howell PL, Baker P, Alnabelseya N, Sheppard DC, Bamford N, Little D, Snarr B, United States Provisional Patent application (No. 62/008,836) entitled “Soluble Bacterial and Fungal Proteins and Methods and Uses Thereof in Inhibiting and Dispersing Biofilm”. National phase filing in US, Canada, Europe, Australia and Japan occurred between Dec 2016 – Jan 2017 (Actual date depends on jurisdiction). Patent prosecution is currently ongoing in all jurisdictions.

- **Other Products**

No other product to be reported

## 7. PARTICIPANTS & OTHER COLLABORATING ORGANIZATIONS

### What individuals have worked on the project?

*Name:* P. Lynne Howell  
*Project Role:* PI  
*Researcher Identifier (e.g. ORCID ID):* 0000-0002-2776-062X  
*Nearest person month worked:* 17  
*Contribution to Project:* Responsible for the research performed at the Hospital for Sick Children.

*Name:* Perrin Baker  
*Project Role:* Post Doctoral Fellow  
*Researcher Identifier (e.g. ORCID ID):* Not available  
*Nearest person month worked:* 9  
*Contribution to Project:* Dr Baker has been responsible for the development of yeast expression constructs and protein expression and purification. Dr Baker left the Howell lab June, 2017.

*Name:* Ira Lacdao  
*Project Role:* Technician  
*Researcher Identifier (e.g. ORCID ID):* Not available  
*Nearest person month worked:* 32.25  
*Contribution to Project:* Ms Lacdao was hired in January 2017 and has been responsible for protein expression and purification since this time. Ms Lacdao left the Howell lab September, 2019.

*Name:* Deepa Raju  
*Project Role:* Research Associate  
*Researcher Identifier (e.g. ORCID ID):* Not available  
*Nearest person month worked:* 39.25  
*Contribution to Project:* Dr Raju was hired in September 2017 to replace Dr Baker and has been responsible for the development of the ELISA and antibiotic potentiation experiments.

*Name:* Stephanie Gilbert  
*Project Role:* Technician  
*Researcher Identifier (e.g. ORCID ID):* Not available  
*Nearest person month worked:* 10  
*Contribution to Project:* Ms Gilbert has been co-responsible for protein expression and purification.

*Name:* Piyanka Sivarajah  
*Project Role:* Technician

Researcher Identifier (e.g. ORCID ID): Not available  
Nearest person month worked: 19.5  
Contribution to Project: Ms Sivarajah has been co-responsible for protein expression and purification. Ms Sivarajah has joined the lab in replacement to Ms Lacdao.

*Name:* Brian Hicks  
Project Role: Undergraduate Research Assistant  
Researcher Identifier (e.g. ORCID ID): Not available  
Nearest person month worked: 4  
Contribution to Project: Mr. Hicks assisted with the protein expression and purification

*Name:* Holly Silver  
Project Role: Research Assistant  
Researcher Identifier (e.g. ORCID ID): Not available  
Nearest person month worked: 1  
Contribution to Project: Ms Silver worked for Dr. Matt Parsek (University of Washington) and assisted with the antibiotic potentiation experiments reported.

**Has there been a change in the active other support of the PD/PI(s) or senior/key personnel since the last reporting period?**

Nothing to Report.

**What other organizations were involved as partners?**

Nothing to Report.

## 8. SPECIAL REPORTING REQUIREMENTS

Award# W81XWH-16-1-0284 Log# PR150786-P1: Development of New Therapeutics Targeting Biofilm Formation by the Opportunistic Pulmonary Pathogens *Pseudomonas aeruginosa* and *Aspergillus Fumigatus*.

PI: P Lynne Howell, Hospital for Sick Children, Toronto (ON), Canada

Budget: \$972,320.00 Topic Area: Respiratory Health

Mechanism: Peer Reviewed Medical Research Program, Investigator-Initiated Research Award, Partnering PI Option, W81XWH-15-PRMRP-IIRA



Research Area(s): **Award Status:** 15-SEP-2016 to 14-SEP-2020

### Study Goals:

*A. fumigatus* and *P. aeruginosa* are two lung opportunistic pathogens that embed themselves in a biofilm, becoming therefore more resistant to drugs and host defenses. We will test the use of four therapeutic enzymes, two glycosyl hydrolases (GH) from fungal origin, two from bacterial origin, to render microorganisms more susceptible to antimicrobials *in vivo*. We will determine the concentration of hydrolases that are both efficient and well tolerated by the host. Our purpose is to conduct proof of concept studies to move these agents into early clinical trials.

### Specific Aims:

Aim 1. To characterize the ability of microbial GHs to enhance the activity of antimicrobial agents *in vitro*.

Aim 2. Perform preliminary tolerability and pharmacokinetic studies of candidate hydrolases *in vivo*.

Aim 3. To evaluate candidate hydrolases alone and in combination with antimicrobial agents in the treatment of experimental *A. fumigatus* and *P. aeruginosa* pulmonary infections *in vivo*. Demonstrate proof-of-concept for candidate hydrolases for use in treatment of *A. fumigatus* and *P. aeruginosa*.

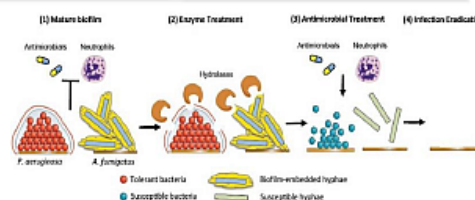
### Key Accomplishments and Outcomes:

- ☑ Routine production of recombinant GHs in sufficient quantity and quality for all experiments
- ☑ GH + antimicrobial combinations with synergistic activity against *A. fumigatus* and *P. aeruginosa* *in vitro* have been identified.
- ☑ Doses of up to 500 µg of Sph3, PeIA and PslG produced in *E. coli* and Ega3 produced in HEK293 cells are well tolerated intratracheally by mice
- ☑ Pulmonary GH half-lives vary from 1-18h (immunocompetent mice), and 3-38h (immunosuppressed mice). GH degradation may be leukocyte-dependent.
- ☑ The development and evaluation of protease-resistant GH variants allowed the identification of a *Bacillus cereus* PeIA orthologue (BCE5582) that showed similar enzymatic activity *in vitro* and similar efficacy *in vivo*, but higher tolerability and longer half-life in lung.
- ☑ Sph3, PeIA, and Ega3 monotherapy reduces *A. fumigatus* pulmonary fungal burden in lungs and improves survival while PeIA, PslG, and Ega3 alone and in combination do not reduce *P. aeruginosa* pulmonary burden and enhance hematogenous dissemination.
- ☑ In chronic infection models: no GH, in monotherapy or in GH combinations, decreased microbial burden in lungs.
- ☑ In invasive aspergillosis, Sph3 potentiated the antifungal activity of posaconazole, and both Sph3 and PeIA potentiated the antifungal effects of caspofungin. In *P. aeruginosa* infection, PslG/PeIA but not PslG/Ega3 potentiated the effect of ciprofloxacin, while neither GH combination potentiated the effect of ceftazidime. Taken as a whole, these findings suggest the ability of GH-therapy to augment anti-microbial is likely drug- and hydrolase-specific.
- ☑ Ready to initiate trials of delivery systems and detailed pharmacodynamics experiments as a prelude to Phase I clinical trials.

**Publications:** 2017: Snarr BD *et al.*, *PNAS*, 10.1073/pnas.1702798114; Zhang S *et al.*, *Cell Microbiol.* 10.1111/omi.12799. 2018: Snarr BD *et al.*, *Future Microbiology*, 0.2217/fmb-2017-0243; Little DJ *et al.*, *Plos Pathogens*, 10.1371/1006998; Asker D *et al.*, *Biomaterials*, 10.1016/j.biomaterials.2018.03.016; Low K *et al.*, *Curr Opin in Struct Biol*, 10.1016/j.sbi.2018.05.001. 2019: Speth C *et al.*, *Virulence* 10.1080/21505594.2019.1568174; Ostapska H *et al.*, *PLOS Pathogens*, 10.1371/1007411; Bamford NC *et al.*, *J Biol Chem - Editor's pick*, 10.1074/jbc.RA119.009910; Zacharias CA *et al.*, *Curr Opin Microbiol*, 10.1016/j.mib.2019.04.008; Le Mauff F *et al.*, *J Biol Chem*, 10.1074/jbc.RA119.008511. 2020: Bamford NC *et al.* *Nat Commu*, 10.1038/s41467-020-16144-5.

**Patents:** Howell PL *et al.*, United States Provisional Patent application (No. 62/008,836) entitled "Soluble Bacterial and Fungal Proteins and Methods and Uses Thereof in Inhibiting and Dispersing Biofilm".

**Funding Obtained:** 2019-2021: GlycoNET #AM25 (03/2019-02/2021; \$210,305) "Development of PslG as an anti-biofilm therapeutic for *P. aeruginosa* infections". 2020-2022: GlycoNET #ID-03 (04/2020-03/2022, \$400,000) "Anti-exopolysaccharide therapies to improve eradication of early *P. aeruginosa* infection in CF". 2021-2022: SickKids Proof of Principle Grant (02/2021-01/2022, \$100,000) "Bioactive surfaces to prevent microbial biofilms"



# Microbial glycoside hydrolases as antibiofilm agents with cross-kingdom activity

Brendan D. Snarr<sup>a,b,1</sup>, Perrin Baker<sup>c,1</sup>, Natalie C. Bamford<sup>c,d,1</sup>, Yukiko Sato<sup>a,b</sup>, Hong Liu<sup>e</sup>, Mélanie Lehoux<sup>b</sup>, Fabrice N. Gravelat<sup>b</sup>, Hanna Ostapska<sup>a,b</sup>, Shane R. Baistrocchi<sup>a,b</sup>, Robert P. Cerone<sup>a,b</sup>, Elan E. Filler<sup>e</sup>, Matthew R. Parsek<sup>f</sup>, Scott G. Filler<sup>e,g</sup>, P. Lynne Howell<sup>c,d,2</sup>, and Donald C. Sheppard<sup>a,b,2</sup>

<sup>a</sup>Department of Microbiology and Immunology, McGill University, Montreal, QC, H3A 2B4, Canada; <sup>b</sup>Department of Medicine, Infectious Diseases and Immunity in Global Health Program, Centre for Translational Biology, McGill University Health Centre, Montreal, QC, H4A 3J1, Canada; <sup>c</sup>Program in Molecular Medicine, Research Institute, The Hospital for Sick Children, Toronto, ON, M5G 1X8, Canada; <sup>d</sup>Department of Biochemistry, University of Toronto, Toronto, ON, M5S 1A8, Canada; <sup>e</sup>Los Angeles Biomedical Research Institute at Harbor-UCLA Medical Center, Torrance, CA 90502; <sup>f</sup>Department of Microbiology, University of Washington, Seattle, WA 98195; and <sup>g</sup>David Geffen School of Medicine at UCLA, University of California, Los Angeles, CA 90024

Edited by Scott J. Hultgren, Washington University School of Medicine, St. Louis, MO, and approved March 30, 2017 (received for review March 2, 2017)

Galactosaminogalactan and Pel are cationic heteropolysaccharides produced by the opportunistic pathogens *Aspergillus fumigatus* and *Pseudomonas aeruginosa*, respectively. These exopolysaccharides both contain 1,4-linked *N*-acetyl-D-galactosamine and play an important role in biofilm formation by these organisms. Proteins containing glycoside hydrolase domains have recently been identified within the biosynthetic pathway of each exopolysaccharide. Recombinant hydrolase domains from these proteins (Sph3<sub>h</sub> from *A. fumigatus* and PelA<sub>h</sub> from *P. aeruginosa*) were found to degrade their respective polysaccharides *in vitro*. We therefore hypothesized that these glycoside hydrolases could exhibit antibiofilm activity and, further, given the chemical similarity between galactosaminogalactan and Pel, that they might display cross-species activity. Treatment of *A. fumigatus* with Sph3<sub>h</sub> disrupted *A. fumigatus* biofilms with an EC<sub>50</sub> of 0.4 nM. PelA<sub>h</sub> treatment also disrupted preformed *A. fumigatus* biofilms with EC<sub>50</sub> values similar to those obtained for Sph3<sub>h</sub>. In contrast, Sph3<sub>h</sub> was unable to disrupt *P. aeruginosa* Pel-based biofilms, despite being able to bind to the exopolysaccharide. Treatment of *A. fumigatus* hyphae with either Sph3<sub>h</sub> or PelA<sub>h</sub> significantly enhanced the activity of the antifungals posaconazole, amphotericin B, and caspofungin, likely through increasing antifungal penetration of hyphae. Both enzymes were noncytotoxic and protected A549 pulmonary epithelial cells from *A. fumigatus*-induced cell damage for up to 24 h. Intratracheal administration of Sph3<sub>h</sub> was well tolerated and reduced pulmonary fungal burden in a neutropenic mouse model of invasive aspergillosis. These findings suggest that glycoside hydrolases can exhibit activity against diverse microorganisms and may be useful as therapeutic agents by degrading biofilms and attenuating virulence.

biofilm | *Aspergillus* | *Pseudomonas* | therapeutics | exopolysaccharide

The mold *Aspergillus fumigatus* and the Gram-negative bacterium *Pseudomonas aeruginosa* are opportunistic pathogens that cause pulmonary infection in immunocompromised patients and individuals who suffer from chronic lung diseases such as cystic fibrosis and bronchiectasis. *A. fumigatus* is the second most common nosocomial fungal infection (1), and ~10% of all nosocomial bacterial infections are caused by *P. aeruginosa* (2). Mortality associated with *P. aeruginosa* infections is high (3) and has increased with the emergence of multi- and even pan-resistance to antibiotics (3, 4). Similarly, invasive aspergillosis is associated with mortality rates of up to 50% (5), and increasing rates of antifungal resistance have been reported worldwide (6). These factors underscore the urgent need for new effective therapies for these infections.

Although *A. fumigatus* and *P. aeruginosa* are members of different taxonomic kingdoms, both produce biofilms that constitute a protective lifestyle for the organism. Biofilms are complex communities of microorganisms that grow embedded in an extracellular matrix composed of DNA, protein, and

exopolysaccharide (7). Biofilm formation provides a significant advantage to these organisms because the matrix mediates adherence to host cells (8, 9) and aids in the resistance to both antimicrobial agents (10, 11) and host-immune defenses (12, 13). *A. fumigatus* biofilm formation depends on the cationic polysaccharide galactosaminogalactan (GAG), a heteroglycan composed of α1,4-linked galactose and *N*-acetyl-D-galactosamine (GalNAc) that is partially deacetylated (14, 15). In comparison, *P. aeruginosa* has the genetic capacity to produce three biofilm exopolysaccharides: alginate, Psl and Pel (16). GAG shares several similarities with Pel, which has been identified as a cationic heteroglycan composed of 1,4-linked GalNAc and *N*-acetyl-D-glucosamine (GlcNAc) (17). Like GAG, the cationic nature of Pel results from partial deacetylation of the polymer (17). Most clinical and environmental isolates of *P. aeruginosa* use Pel and Psl during biofilm formation (18). Alginate is dispensable for biofilm formation and is only observed in chronic pulmonary infection when strains switch to a mucoid phenotype (18, 19).

Strains of *Aspergillus* and *P. aeruginosa* with impaired GAG, or Pel and Psl biosynthesis exhibit attenuated virulence (20, 21), suggesting that targeting these exopolysaccharides may be a

## Significance

The production of biofilms is an important strategy used by both bacteria and fungi to colonize surfaces and to enhance resistance to killing by immune cells and antimicrobial agents. We demonstrate that glycoside hydrolases derived from the opportunistic fungus *Aspergillus fumigatus* and Gram-negative bacterium *Pseudomonas aeruginosa* can be exploited to disrupt preformed fungal biofilms and reduce virulence. Additionally, these glycoside hydrolases can be used to potentiate antifungal drugs by increasing their hyphal penetration, to protect human cells from fungal-induced injury, and attenuate virulence of *A. fumigatus* in a mouse model of invasive aspergillosis. The findings of this study identify recombinant microbial glycoside hydrolases as promising therapeutics with the potential for antibiofilm activity against pathogens across different taxonomic kingdoms.

Author contributions: B.D.S., P.B., N.C.B., P.L.H., and D.C.S. designed research; B.D.S., P.B., N.C.B., Y.S., H.L., M.L., F.N.G., H.O., S.R.B., R.P.C., and E.E.F. performed research; M.R.P. contributed new reagents/analytic tools; B.D.S., P.B., N.C.B., Y.S., H.L., M.L., F.N.G., S.R.B., S.G.F., P.L.H., and D.C.S. analyzed data; and B.D.S., P.B., N.C.B., M.R.P., S.G.F., P.L.H., and D.C.S. wrote the paper.

Conflict of interest statement: A patent has been filed describing the utility of the glycoside hydrolases as antibiofilm therapeutics (CA2951152 A1, WO2015184526 A1). B.D.S., P.B., N.C.B., P.L.H., and D.C.S. are listed as inventors.

This article is a PNAS Direct Submission.

<sup>1</sup>B.D.S., P.B., and N.C.B. contributed equally to this work.

<sup>2</sup>To whom correspondence may be addressed. Email: don.sheppard@mcgill.ca or howell@ SickKids.ca.

This article contains supporting information online at [www.pnas.org/lookup/suppl/doi:10.1073/pnas.1702798114/-/DCSupplemental](http://www.pnas.org/lookup/suppl/doi:10.1073/pnas.1702798114/-/DCSupplemental).

RESEARCH ARTICLE

# PtaB, a lim-domain binding protein in *Aspergillus fumigatus* regulates biofilm formation and conidiation through distinct pathways

Shizhu Zhang<sup>1,2,3</sup>  | Yuan Chen<sup>1</sup> | Zhihua Ma<sup>1</sup> | Qiuyi Chen<sup>1</sup> | Hanna Ostapska<sup>2,3</sup> | Fabrice N. Gravelat<sup>2,3</sup> | Ling Lu<sup>1</sup> | Donald C. Sheppard<sup>2,3</sup>

<sup>1</sup>Jiangsu Key Laboratory for Microbes and Functional Genomics, Jiangsu Engineering and Technology Research Center for Microbiology, College of Life Sciences, Nanjing Normal University, Nanjing, China

<sup>2</sup>Departments of Medicine and of Microbiology and Immunology, McGill University, Montreal, Canada

<sup>3</sup>Infectious Diseases and Immunity in Global Health Program, Research Institute of the McGill University Health Centre, Montreal, Canada

## Correspondence

Ling Lu, College of Life Sciences, Nanjing Normal University, Nanjing, China.  
Email: linglu@njnu.edu.cn

Donald C. Sheppard, Departments of Medicine and of Microbiology and Immunology, McGill University, Montreal, Canada; or Infectious Diseases and Immunity in Global Health Program, Research Institute of the McGill University Health Centre, Montreal, Canada.  
Email: don.sheppard@mcgill.ca

## Funding information

National Natural Science Foundation of China, Grant/Award Number: 31470193; Fonds de Recherche Quebec Santé; Canadian Institutes of Health Research, Grant/Award Numbers: 123306 and 81361; The priority academic program development (PAPD) of Jiangsu Higher Education Institutions

## Abstract

The exopolysaccharide galactosaminogalactan (GAG) plays an important role in mediating adhesion, biofilm formation, and virulence in the pathogenic fungus *Aspergillus fumigatus*. The developmental modifiers MedA, StuA, and SomA regulate GAG biosynthesis, but the mechanisms underlying this regulation are poorly understood. PtaB is a lim-domain binding protein that interacts with the transcription factor SomA and is required for normal conidiation and biofilm formation. Disruption of *ptaB* resulted in impaired GAG production and conidiation in association with a markedly reduced expression of GAG biosynthetic genes (*uge3* and *agd3*), developmental regulators (*medA* and *stuA*), and genes involved in the core conidiation pathway. Overexpression of *medA* and dual overexpression of *uge3* and *agd3* in the  $\Delta$ *ptaB* mutant increased biofilm formation but not conidiation, whereas overexpression of core conidiation genes rescued conidiation but not biofilm formation. Overexpression of *stuA* modestly increased both conidiation and biofilm formation. Analysis of *ptaB* truncation mutants revealed that overexpression of the lim-domain binding region restored conidiation but not biofilm formation, suggesting that *ptaB* may govern these processes by interacting with different partners. These studies establish that PtaB governs GAG biosynthesis at the level of substrate availability and polymer deacetylation and that PtaB-mediated biofilm formation and conidiation are largely independent pathways.

## KEYWORDS

*Aspergillus fumigatus*, Biofilm, Conidiation, Galactosaminogalactan

## 1 | INTRODUCTION

*Aspergillus fumigatus* is an opportunistic mould that causes invasive pulmonary infections in immunosuppressed patients. Despite antifungal treatment with the currently available antifungal agents, the mortality of invasive aspergillosis (IA) remains between 50% and 95% (Abad et al., 2010). There is therefore a pressing need for novel therapeutic strategies to treat or prevent IA. A better understanding of the pathogenesis of IA is one approach that may inform the development of new therapeutic targets.

The ability of *A. fumigatus* to adhere to host cells is a key factor in the pathogenesis of IA and is required for host cell invasion and virulence (de Groot, Bader, de Boer, Weig, & Chauhan, 2010; Liu et al., 2016; Sheppard, 2011; Tronchin, Pihet, Lopes-Bezerra, & Bouchara, 2008). The adherence of *A. fumigatus* hyphae to host cells is mediated by production of the adhesive exopolysaccharide galactosaminogalactan (GAG; Briard, Muszkieta, Latge, & Fontaine, 2016; Gravelat et al., 2011). GAG is synthesised through the activity of the protein products of a five-gene cluster. These genes encode a glucose 4-epimerase (*uge3*) required for the production of UDP-

## Non-eluting, surface-bound enzymes disrupt surface attachment of bacteria by continuous biofilm polysaccharide degradation

Dalal Asker <sup>a, b</sup>, Tarek S. Awad <sup>a</sup>, Perrin Baker <sup>c</sup>, P. Lynne Howell <sup>c, d</sup>  , Benjamin D. Hatton <sup>a</sup>  

 **Show more**

<https://doi.org/10.1016/j.biomaterials.2018.03.016>

Get rights and content

### Abstract

Bacterial colonization and biofilm formation on surfaces are typically mediated by the deposition of exopolysaccharides and conditioning protein layers. *Pseudomonas aeruginosa* is a nosocomial opportunistic pathogen that utilizes strain-specific exopolysaccharides such as Psl, Pel or alginate for both initial surface attachment and biofilm formation. To generate surfaces that resist *P. aeruginosa* colonization, we covalently bound a Psl-specific glycoside hydrolase (PslG<sub>H</sub>) to several, chemically-distinct surfaces using amine functionalization (APTMS) and glutaraldehyde (GDA) linking. *In situ* quartz crystal microbalance (QCM) experiments and fluorescence microscopy demonstrated a complete lack of Psl adsorption on the PslG<sub>H</sub>-bound surfaces. Covalently-bound PslG<sub>H</sub> was also found to significantly reduce *P. aeruginosa* surface attachment and biofilm formation over extended growth periods (8 days). The PslG<sub>H</sub> surfaces showed a ~99.9% (~3-log) reduction in surface associated bacteria compared to control (untreated) surfaces, or those treated with inactive enzyme. This work demonstrates a non-eluting 'bioactive' surface that specifically targets a mechanism of cell adhesion, and that surface-bound glycoside hydrolase can significantly reduce surface colonization of bacteria through local, continuous enzymatic degradation of exopolysaccharide (Psl). These results have significant implications for the surface design of medical devices to keep bacteria in a planktonic state, and therefore susceptible to antibiotics and antimicrobials.

RESEARCH ARTICLE

# PgaB orthologues contain a glycoside hydrolase domain that cleaves deacetylated poly- $\beta$ (1,6)-N-acetylglucosamine and can disrupt bacterial biofilms

Dustin J. Little<sup>1,2</sup>, Roland Pfoh<sup>1</sup>, François Le Mauff<sup>3,4</sup>, Natalie C. Bamford<sup>1,2</sup>, Christina Notte<sup>1</sup>, Perrin Baker<sup>1</sup>, Manita Guragain<sup>5,6</sup>, Howard Robinson<sup>7</sup>, Gerald B. Pier<sup>8</sup>, Mark Nitz<sup>9</sup>, Rajendar Deora<sup>5,6</sup>, Donald C. Sheppard<sup>3,4</sup>, P. Lynne Howell<sup>1,2\*</sup>

1 Program in Molecular Medicine, The Hospital for Sick Children, Toronto, ON, Canada, 2 Department of Biochemistry, University of Toronto, Toronto, ON, Canada, 3 Departments of Medicine and of Microbiology and Immunology, McGill University, Montréal, QC, Canada, 4 Infectious Diseases and Immunity in Global Health Program, Research Institute of the McGill University Health Centre, Montréal, QC, Canada, 5 Department of Microbiology and Immunology, Wake Forest School of Medicine, Winston-Salem, NC, United States of America, 6 Department of Microbial Infection and Immunity, The Ohio State University Wexner Medical Center, Columbus, OH, United States of America, 7 Photon Sciences Division, Brookhaven National Laboratory, Upton, NY, United States of America, 8 Division of Infectious Diseases, Department of Medicine, Brigham and Women's Hospital, Harvard Medical School, Boston, MA, United States of America, 9 Department of Chemistry, University of Toronto, Toronto, ON, Canada



 OPEN ACCESS

Citation: Little DJ, Pfoh R, Le Mauff F, Bamford NC, Notte C, Baker P, et al. (2018) PgaB orthologues contain a glycoside hydrolase domain that cleaves deacetylated poly- $\beta$ (1,6)-N-acetylglucosamine and can disrupt bacterial biofilms. *PLoS Pathog* 14(4): e1006998. <https://doi.org/10.1371/journal.ppat.1006998>

Editor: David Skumik, Channing Laboratory, Brigham and Women's Hospital, UNITED STATES

Received: October 20, 2017

Accepted: March 29, 2018

Published: April 23, 2018

Copyright: ©2018 Little et al. This is an open access article distributed under the terms of the [Creative Commons Attribution License](https://creativecommons.org/licenses/by/4.0/), which permits unrestricted use, distribution, and reproduction in any medium, provided the original author and source are credited.

Data Availability Statement: Coordinates of the structure have been deposited in the Protein data bank PDB code: 6AU1.

Funding: Research described in this paper is supported by operating grants from the Canadian Institutes of Health Research (CIHR) (#43998 to PLH, #89708 to MN, and #81361 to PLH and DCS) and with Federal funds from the National Institute of Allergy and Infectious Diseases, National Institutes of Health (NIH), Department of Health

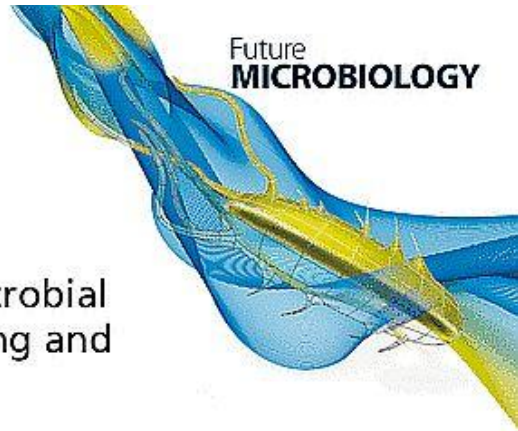
 These authors contributed equally to this work.

 Current address: Department of Biochemistry and Biomedical Sciences, McMaster University, Hamilton, ON, Canada

\* [howell@sickkids.ca](mailto:howell@sickkids.ca)

## Abstract

Poly- $\beta$ (1,6)-N-acetyl-D-glucosamine (PNAG) is a major biofilm component of many pathogenic bacteria. The production, modification, and export of PNAG in *Escherichia coli* and *Bordetella* species require the protein products encoded by the *pgaABCD* operon. PgaB is a two-domain periplasmic protein that contains an N-terminal deacetylase domain and a C-terminal PNAG binding domain that is critical for export. However, the exact function of the PgaB C-terminal domain remains unclear. Herein, we show that the C-terminal domains of *Bordetella bronchiseptica* PgaB (PgaB<sub>Bb</sub>) and *E. coli* PgaB (PgaB<sub>Ec</sub>) function as glycoside hydrolases. These enzymes hydrolyze purified deacetylated PNAG (dPNAG) from *Staphylococcus aureus*, disrupt PNAG-dependent biofilms formed by *Bordetella pertussis*, *Staphylococcus carnosus*, *Staphylococcus epidermidis*, and *E. coli*, and potentiate bacterial killing by gentamicin. Furthermore, we found that PgaB<sub>Bb</sub> was only able to hydrolyze PNAG produced in situ by the *E. coli* PgaCD synthase complex when an active deacetylase domain was present. Mass spectrometry analysis of the PgaB-hydrolyzed dPNAG substrate showed a GlcN-GlcNAc-GlcNAc motif at the new reducing end of detected fragments. Our 1.76 Å structure of the C-terminal domain of PgaB<sub>Bb</sub> reveals a central cavity within an elongated surface groove that appears ideally suited to recognize the GlcN-GlcNAc-GlcNAc motif. The structure, in conjunction with molecular modeling and site directed mutagenesis led to the identification of the dPNAG binding subsites and D474 as the probable catalytic



## Hoisted by their own petard: do microbial enzymes hold the solution to treating and preventing biofilm infections?

Brendan D Snarr<sup>1,2</sup>, P Lynne Howell<sup>\*3,4</sup> & Donald C Sheppard<sup>\*\*1,2</sup>

<sup>1</sup>Department of Microbiology & Immunology, McGill University, Montreal, QC H3A 2B4, Canada

<sup>2</sup>Department of Medicine, Infectious Diseases & Immunity in Global Health Program, Centre for Translational Biology, McGill University Health Centre, Montreal, QC H4A 3J1, Canada

<sup>3</sup>Program in Molecular Medicine, Research Institute, The Hospital for Sick Children, Toronto, Ontario, M5G 1X8, Canada

<sup>4</sup>Department of Biochemistry, University of Toronto, Toronto, Ontario, M5S 1A8, Canada

\* Author for correspondence: Tel.: +1 416 813 5378; [howell@sickkids.ca](mailto:howell@sickkids.ca)

\*\* Author for correspondence: Tel.: +1 514 934 1934; ext.: 36104; [don.sheppard@mcgill.ca](mailto:don.sheppard@mcgill.ca)

“The rising rates of antimicrobial resistance have raised the specter of a post-antibiotic era within our lifetime and highlighted the need for novel strategies to combat antimicrobial resistance.”

First draft submitted: 20 October 2017; Accepted for publication: 30 October 2017; Published online: 14 February 2018

**Keywords:** biofilm • glycoside hydrolase • therapeutics

Biofilms are microbial communities that grow within a self-produced heterogeneous extracellular matrix (ECM). The production of ECM by pathogenic bacteria and fungi during biofilm growth confers a number of advantages during infection including mediating adherence to host tissues and biomedical devices as well as enhancing resistance to antimicrobial agents and host immune defenses. Exopolysaccharides are a key component of the ECM and have been directly implicated in mediating adhesion, immune evasion and antimicrobial resistance. Recent studies have suggested that microbial enzymes can be used to degrade the biofilm exopolysaccharides of several pathogens and increase their susceptibility to antimicrobials *in vitro* and *in vivo*. We will review current progress in this area, and highlight areas for future research and development.

### Current lines of research

#### Bacterial biofilms

##### *Staphylococcus* species

The polysaccharide poly- $\beta$ -1,6-*N*-acetyl-D-glucosamine (PNAG) is an important biofilm component of many *Staphylococcus aureus* and *Staphylococcus epidermidis* strains, as well as some Gram-negative pathogens such as *Acinetobacter baumannii*, *Klebsiella pneumoniae*, *Yersinia pestis* and *Escherichia coli* [1]. A recombinant glycoside hydrolase (GH) known as DispersinB originating from *Actinobacillus actinomycescomitans* cleaves PNAG [2], and can disrupt PNAG-dependent biofilms of these organisms *in vitro*. DispersinB treatment enhances the antimicrobial activity of cefamandole nafate against both *S. aureus* and *S. epidermidis* biofilms *in vitro* [3]. Animal model studies have also demonstrated that DispersinB enhanced the antimicrobial effects of silver nanoparticles in a mouse methicillin-resistant *S. aureus* chronic wound model [4]. Systemic use of DispersinB in other models of Staphylococcal infection has not been reported.

##### *Yersinia* species

NghA is a GH active against PNAG produced by *Yersinia pseudotuberculosis*. The related pathogen *Yersinia pestis* lacks a functional *nghA* gene and, as a result, is able to form PNAG-based biofilms within its flea vector [5]. Heterologous expression of *nghA* in *Y. pestis* prevented biofilm formation in the flea gut, and biofilm formation by *Y. pestis* and *S. epidermidis* *in vitro* was inhibited by recombinant NghA [5]. The effects of NghA on the susceptibility of *Yersinia* sp. or on virulence in mammalian infection models have yet to be reported.



## Ega3 from the fungal pathogen *Aspergillus fumigatus* is an endo- $\alpha$ -1,4-galactosaminidase that disrupts microbial biofilms

Received for publication, June 23, 2019, and in revised form, August 1, 2019. Published, Papers in Press, August 15, 2019. DOI 10.1074/jbc.RA119.009910

© Natalie C. Bamford<sup>†§1,2</sup>, François Le Mauff<sup>¶||\*\*2</sup>, Adithya S. Subramanian<sup>†§</sup>, Patrick Yip<sup>‡</sup>, Claudia Millán<sup>†§3,4</sup>, Yongzhen Zhang<sup>§§</sup>, Caitlin Zacharias<sup>¶||\*\*</sup>, Adam Forman<sup>¶¶</sup>, Mark Nitz<sup>¶¶</sup>, Jeroen D. C. Codée<sup>§§</sup>, Isabel Usón<sup>†§||#4</sup>, Donald C. Sheppard<sup>¶||#\*5</sup>, and P. Lynne Howell<sup>†§6</sup>

From the <sup>†</sup>Program in Molecular Medicine, The Hospital for Sick Children, Toronto, Ontario M5G 1X8, Canada, the <sup>§</sup>Department of Biochemistry, Faculty of Medicine, University of Toronto, Toronto, Ontario M5S 1A8, Canada, the <sup>¶</sup>Department of Microbiology and Immunology, Faculty of Medicine, McGill University, Montreal, Quebec H3A 2B4, Canada, the <sup>||</sup>Infectious Disease and Immunity in Global Health, Research Institute of the McGill University Health Centre, Montreal, Quebec H4A 3J1, Canada, the <sup>\*\*</sup>McGill Interdisciplinary Initiative in Infection and Immunity, Montreal, Quebec H3A 1Y2, Canada, <sup>††</sup>Structural Biology, Instituto de Biología Molecular de Barcelona, CSIC, Carrer Baldiri Reixac 15, 3 A17, Barcelona 08028, Spain, the <sup>§§</sup>Leiden Institute of Chemistry, Leiden University, 2300RA Leiden, The Netherlands, the <sup>¶¶</sup>Department of Chemistry, Faculty of Arts and Sciences, University of Toronto, Toronto, Ontario M5S 3H6, Canada, and the <sup>||</sup>ICREA, Institutió Catalana de Recerca i Estudis Avançats, Passeig Lluís Companys, 23, E-08003 Barcelona, Spain

Edited by Gerald W. Hart

*Aspergillus fumigatus* is an opportunistic fungal pathogen that causes both chronic and acute invasive infections. Galactosaminogalactan (GAG) is an integral component of the *A. fumigatus* biofilm matrix and a key virulence factor. GAG is a heterogeneous linear  $\alpha$ -1,4-linked exopolysaccharide of galactose and GalNAc that is partially deacetylated after secretion. A cluster of five co-expressed genes has been linked to GAG biosynthesis and modification. One gene in this cluster, *ega3*, is annotated as encoding a putative  $\alpha$ -1,4-galactosaminidase belonging to glycoside hydrolase family 114 (GH114). Herein, we show that recombinant Ega3 is an active glycoside hydrolase that disrupts GAG-dependent *A. fumigatus* and *Pseudomonas aeruginosa* biofilms at nanomolar concentrations. Using MS and functional assays, we demonstrate that Ega3 is an endo-acting  $\alpha$ -1,4-galactosaminidase whose activity depends on the conserved acidic residues, Asp-

189 and Glu-247. X-ray crystallographic structural analysis of the apo Ega3 and an Ega3-galactosamine complex, at 1.76 and 2.09 Å resolutions, revealed a modified ( $\beta/\alpha$ )<sub>8</sub>-fold with a deep electronegative cleft, which upon ligand binding is capped to form a tunnel. Our structural analysis coupled with *in silico* docking studies also uncovered the molecular determinants for galactosamine specificity and substrate binding at the -2 to +1 binding subsites. The findings in this study increase the structural and mechanistic understanding of the GH114 family, which has >600 members encoded by plant and opportunistic human pathogens, as well as in industrially used bacteria and fungi.

*Aspergillus fumigatus* is a ubiquitous, filamentous fungus that causes invasive infections in immunocompromised patients (1). *A. fumigatus* can also cause chronic infections in patients with pre-existing lung conditions such as chronic obstructive pulmonary disease or cystic fibrosis (2–4). Even with currently available antifungal agents, the mortality of invasive aspergillosis remains over 50%, highlighting the need for new therapies that target *A. fumigatus* (2). During infection, *A. fumigatus* adopts a biofilm mode of growth, encapsulating itself in a self-produced matrix. The exopolysaccharide galactosaminogalactan (GAG)<sup>7</sup> is an integral component of the *A. fumigatus* matrix and a key virulence factor (5–9). GAG mediates fungal adhesion to host cells and inhibits the host immune response by masking fungal  $\beta$ -glucan from dectin-1 recognition and inducing neutrophil apoptosis and secretion of the immunosuppressive cytokine interleukin 1 receptor antagonist (5, 7, 10).

<sup>7</sup> The abbreviations used are: GAG, galactosaminogalactan; PDB, Protein Data Bank; GH, glycoside hydrolase; PNAG, poly- $\beta$ -1,6-GlcNAc; RMSD, root-mean-square deviation; SEC, size-exclusion chromatography; ACN, acetonitrile.

This work was supported in part by Canadian Institutes of Health Research Operating Grants 81361 (to P. L. H. and D. C. S.), FDN-154327 and 43998 (to P. L. H.), 123306 and FDN-159902 (to D. C. S.), and 89708 (to M. N.); Cystic Fibrosis Canada (to D. C. S. and P. L. H.); and European Research Council Grant ERC-CoG-726072-GLYCONTROL (to J. D. C. C.). The authors declare that they have no conflicts of interest with the contents of this article. The content is solely the responsibility of the authors and does not necessarily represent the official views of the National Institutes of Health.

This article was selected as one of our Editors' Picks.

<sup>1</sup> Supported in part by Vanier and CGS-M graduate scholarships from the Natural Sciences and Engineering Research Council of Canada (NSERC), Mary H. Beatty, and Dr. James A. and Connie P. Dickson Scholarships from the University of Toronto, Cystic Fibrosis Canada, and The Hospital for Sick Children.

<sup>2</sup> Both authors contributed equally to this work.

<sup>3</sup> Supported by a BES-2015-071397 scholarship.

<sup>4</sup> Recipients of Grants BIO2015-64216-P and MDM2014-0435-01 from the Spanish Ministry of Science and Innovation and EU-FEDER.

<sup>5</sup> Supported by a Distinguished Research Scholar Award from the Fonds de Recherche Québec Santé (FRQS). To whom correspondence may be addressed. Tel.: 514-934-1934 (Ext. 36104); E-mail: donald.sheppard@mcgill.ca.

<sup>6</sup> Recipient of a Tier I Canada Research Chair. To whom correspondence may be addressed. Tel.: 416-813-5378; E-mail: howell@sickkids.ca.

Molecular mechanism of *Aspergillus fumigatus* biofilm disruption by fungal and bacterial glycoside hydrolases

François Le Mauff<sup>1,2,3\*</sup>, Natalie C Bamford<sup>4,5\*</sup>, Noor Alnabseya<sup>4,5#</sup>, Yongzhen Zhang<sup>6</sup>, Perrin Baker<sup>4†</sup>, Howard Robinson<sup>7</sup>, Jeroen D C Codée<sup>6</sup>, P. Lynne Howell<sup>4,5,§</sup>, Donald C. Sheppard<sup>1,2,3§</sup>

<sup>1</sup>Department of Microbiology and Immunology, Faculty of Medicine, McGill University, Montreal, Quebec, Canada; <sup>2</sup>Infectious Disease and Immunity in Global Health, Research Institute of McGill University Health Center, Montreal, Quebec, Canada; <sup>3</sup>McGill Interdisciplinary Initiative in Infection and Immunity, Montreal, Quebec, Canada; <sup>4</sup>Program in Molecular Medicine, The Hospital for Sick Children, Toronto, Ontario, Canada; <sup>5</sup>Department of Biochemistry, Faculty of Medicine, University of Toronto, Toronto, Ontario, Canada; <sup>6</sup>Leiden Institute of Chemistry, Leiden University, Leiden, The Netherlands; <sup>7</sup>Photon Science Division, Brookhaven National Laboratory, 743 Brookhaven Avenue, Upton, New York, 11973-5000, USA

Running title: Molecular mechanism of glycoside hydrolases Sph3<sub>h</sub> and PelA<sub>h</sub>

\* contributed equally to this work

Present addresses: # Diassess Inc., 1412 62nd street, Emeryville, CA, USA 94608, † Covalon Technologies Ltd., 660 Tech Ave #5, Mississauga, ON, Canada, L4W 5S7

§To whom correspondence should be addressed. Tel: 416-813-5378; Email: [howell@sickkids.ca](mailto:howell@sickkids.ca) or Tel.: 514-934-1934, Ext. 36104; E-mail: [donald.sheppard@mcgill.ca](mailto:donald.sheppard@mcgill.ca)

**Keywords:** Glycoside hydrolases, Biofilm, *Aspergillus fumigatus*, extracellular matrix, protein structure, virulence factor, lung infection, substrate specificity, galactosaminogalactan

ABSTRACT

During infection, the fungal pathogen *Aspergillus fumigatus* forms biofilms that enhance its resistance to antimicrobials and host defenses. An integral component of the biofilm matrix is galactosaminogalactan (GAG), a cationic polymer of  $\alpha$ -1,4-linked galactose and partially deacetylated N-acetylgalactosamine (GalNAc). Recent studies have shown that recombinant hydrolase domains from Sph3, an *A. fumigatus* glycoside hydrolase involved in GAG synthesis, and PelA, a multi-functional protein from *Pseudomonas aeruginosa*

involved in Pel polysaccharide biosynthesis, can degrade GAG, disrupt *A. fumigatus* biofilms, and attenuate fungal virulence in a mouse model of invasive aspergillosis. The molecular mechanisms by which these enzymes disrupt biofilms have not been defined. We hypothesized that the hydrolase domains of Sph3 and PelA (Sph3<sub>h</sub> and PelA<sub>h</sub>, respectively) share structural and functional similarities given their ability to degrade GAG and disrupt *A. fumigatus* biofilms. MALDI-TOF enzymatic fingerprinting and NMR experiments revealed that both proteins are retaining endo- $\alpha$ -

PEARLS

# Deacetylated microbial biofilm exopolysaccharides: It pays to be positive

Hanna Ostapska<sup>1,2</sup>, P. Lynne Howell<sup>3,4\*</sup>, Donald C. Sheppard<sup>6,1,2,5\*</sup>

**1** Department of Microbiology and Immunology, McGill University, Montreal, Quebec, Canada, **2** Infectious Diseases in Global Health Program, McGill University Health Centre, Montreal, Quebec, Canada, **3** Program in Molecular Medicine, The Hospital for Sick Children, Toronto, Ontario, Canada, **4** Department of Biochemistry, University of Toronto, Toronto, Ontario, Canada, **5** Department of Medicine, McGill University, Montreal, Quebec, Canada

\* [howell@sickkids.ca](mailto:howell@sickkids.ca) (PLH); [donald.sheppard@mcgill.ca](mailto:donald.sheppard@mcgill.ca) (DCS)



**OPEN ACCESS**

**Citation:** Ostapska H, Howell PL, Sheppard DC (2018) Deacetylated microbial biofilm exopolysaccharides: It pays to be positive. *PLoS Pathog* 14(12): e1007411. <https://doi.org/10.1371/journal.ppat.1007411>

**Editor:** Deborah A. Hogan, Geisel School of Medicine at Dartmouth, UNITED STATES

**Published:** December 27, 2018

**Copyright:** © 2018 Ostapska et al. This is an open access article distributed under the terms of the [Creative Commons Attribution License](https://creativecommons.org/licenses/by/4.0/), which permits unrestricted use, distribution, and reproduction in any medium, provided the original author and source are credited.

**Funding:** Research described in this paper is supported by grants from the Canadian Institutes of Health Research (#81361 to DCS and PLH; #123306 to DCS, #43998, #13337, #FDN154327 to PLH); Cystic Fibrosis Canada and GlycoNET (to DCS and PLH); and the National Institutes of Health (4R33AI119116 to PLH). DCS is supported by a Chercheur-Boursier Award from the Fonds de Recherche Quebec Santé. PLH is the recipient of a Canadian Research Chair. The funders had no role in study design, data collection and analysis, decision to publish, or preparation of the manuscript.

**Competing interests:** The authors have declared that no competing interests exist.

## Introduction

The production of biofilms is a common strategy used by many microorganisms during infection. Exopolysaccharides are a major component of the extracellular biofilm matrix serving to anchor organisms to surfaces, forming the structural scaffold of the biofilm, and protecting organisms from damage by hostile factors such as antibiotics and host immune defenses (Fig 1). Biochemical and genetic studies of biofilm exopolysaccharide synthesis have revealed that production of *N*-acetyl hexosamine-containing exopolysaccharides is one strategy used by diverse pathogens to facilitate biofilm formation and virulence. Following polymerization and extracellular extrusion by membrane embedded glycosyl transferases ( $[\text{HexNAc}]_n + \text{nucleotide-HexNAc} \rightarrow [\text{HexNAc}]_{n+1} + \text{nucleotide}$ ), these glycans then undergo postsynthetic enzymatic deacetylation ( $[\text{HexNAc}]_n \rightarrow \text{HexN-}[\text{HexNAc}]_{n-1} + \text{acetyl group}$ ) to render them cationic. Deacetylation is critical for the function of these glycans in biofilm formation and host-pathogen interactions. This Pearl explores the role of these deacetylated cationic exopolysaccharides within the biofilm matrix in microbial pathogenesis and resistance to antimicrobial agents, and their potential as antibiofilm therapeutic targets.

## Partially deacetylated, cationic hexosamine polymers are common in biofilm forming microorganisms

A wide range of medically important microbial species produce and secrete hexosamine-rich exopolysaccharides into their self-produced extracellular biofilm matrices (Table 1). The best studied example of these glycans is poly- $\beta$ -1,6-*N*-acetylglucosamine (PNAG), a homopolymer of *N*-acetylglucosamine (GlcNAc) residues produced by a wide range of gram-positive and gram-negative pathogenic bacteria, including *Staphylococcus* spp., *Yersinia pestis*, *Bordetella* spp., and *Escherichia coli* [1–4]. The gram-negative opportunistic pathogen *Pseudomonas aeruginosa* produces several biofilm-associated exopolysaccharides, including the linear heteropolymer Pel, composed of GlcNAc and *N*-acetyl galactosamine (GalNAc), whereas the gram-positive organism *Listeria monocytogenes* produces a  $\beta$ -1,4-linked *N*-acetylmannosamine polysaccharide decorated with terminal  $\alpha$ -1,6-linked galactose (Gal) residues [5,6]. More recently, biofilm formation by the opportunistic filamentous fungal pathogen *Aspergillus fumigatus* was found to be dependent on galactosaminogalactan (GAG), a heteropolymer composed of  $\alpha$ -1,4-linked GalNAc and Gal residues [7].

## Galactosaminogalactan (GAG) and its multiple roles in *Aspergillus* pathogenesis

Cornelia Speth<sup>a,b</sup>, Günter Rambach<sup>a,b</sup>, Cornelia Lass-Flörl<sup>a,b</sup>, P. Lynne Howell<sup>c,d</sup>, and Donald C. Sheppard<sup>e,f</sup>

<sup>a</sup>Division of Hygiene and Medical Microbiology, Medical University of Innsbruck, Innsbruck, Austria; <sup>b</sup>Christian Doppler Laboratory for Invasive Fungal Infections, Innsbruck, Austria; <sup>c</sup>Program in Molecular Medicine, The Hospital for Sick Children, Toronto, Canada; <sup>d</sup>Department of Biochemistry, University of Toronto, Toronto, Canada; <sup>e</sup>Departments of Medicine and of Microbiology and Immunology, McGill University, Montréal, Canada; <sup>f</sup>Infectious Diseases and Immunity in Global Health Program, Research Institute of the McGill University Health Centre, Montréal, Canada

### ABSTRACT

*Aspergillus* spp and particularly the species *Aspergillus fumigatus* are the causative agents of invasive aspergillosis, a progressive necrotizing pneumonia that occurs in immunocompromised patients. The limited efficacy of currently available antifungals has led to interest in a better understanding of the molecular mechanisms underlying the pathogenesis of invasive aspergillosis in order to identify new therapeutic targets for this devastating disease. The *Aspergillus* exopolysaccharide galactosaminogalactan (GAG) plays an important role in the pathogenesis of experimental invasive aspergillosis. The present review article summarizes our current understanding of GAG composition and synthesis and the molecular mechanisms whereby GAG promotes virulence. Promising directions for future research and the prospect of GAG as both a therapy and therapeutic target are reviewed.

### ARTICLE HISTORY

Received 28 August 2018  
Revised 12 November 2018  
Accepted 7 January 2019

### KEYWORDS

Galactosaminogalactan;  
aspergillosis; host pathogen  
interactions; virulence factor

### Introduction

In order to cause pulmonary infection, microorganisms must both adhere to host cells, adapt to the natural environment imposed by the pulmonary environment and evade immune responses. One strategy used by the mold *Aspergillus fumigatus* to establish and maintain pulmonary infection is the production of biofilms during invasive infection in immunocompromised individuals and airway infection in patients with chronic lung disease [1]. Biofilms consist of stratified communities of organisms growing within a thick slime-like matrix of polysaccharides, proteins, lipids and nucleic acids that protect fungi from immune mediated killing and enhance resistance to antifungal agents [2,3]. Recent studies have established a key role for the exopolysaccharide galactosaminogalactan (GAG) in both the formation of *A. fumigatus* biofilms and in modulating the immune response during invasive infection.

GAG is a heteropolysaccharide composed of  $\alpha$ -1,4 linked galactose, N-acetyl galactosamine (GalNAc) and galactosamine (GalN) [4–6] that is secreted by actively growing hyphae. GAG binds to the surface of these hyphae, resulting in a polysaccharide sheath that covers the growing organism and forms an extracellular matrix between hyphae [5]. GAG is expressed during chronic and invasive infection, and the production of

cell wall GAG correlates with the intrinsic virulence of *Aspergillus* species [7]. Strains deficient in GAG do not form biofilms and are less virulent in mouse models of invasive aspergillosis (IA) [5]. Herein, we review our current understanding of the mechanisms underlying the synthesis of GAG, its role in the pathogenesis of invasive aspergillosis, and the current status of efforts to develop therapeutics targeting this important exopolysaccharide [5].

### GAG biosynthesis

The biosynthetic pathway governing GAG production was identified by comparative transcriptional analyses of *A. fumigatus* regulatory mutants deficient in the production of GAG [5]. This approach identified a cluster of five co-regulated genes on chromosome 3 which are predicted to encode enzymes with carbohydrate synthetic or modifying capacity [8]. Through gene disruption as well as structural and biochemical studies, a model of the function of these enzymes in GAG biosynthesis has begun to emerge (Figure 1). Synthesis of GAG begins with the conversion of UDP-glucose and UDP-N-acetyl glucosamine into UDP-galactose and UDP-N-acetyl galactosamine through the action of the cytosolic glucose-4 epimerase Uge3 [5,6]. Linking of these sugars, and export into the extracellular space is hypothesized to be mediated

CONTACT Cornelia Speth  cornelia.speth@i-med.ac.at; Donald Sheppard  don.sheppard@mcgill.ca

© 2019 The Author(s). Published by Informa UK Limited, trading as Taylor & Francis Group  
This is an Open Access article distributed under the terms of the Creative Commons Attribution License (<http://creativecommons.org/licenses/by/4.0/>), which permits unrestricted use, distribution, and reproduction in any medium, provided the original work is properly cited.



## The role of *Aspergillus fumigatus* polysaccharides in host–pathogen interactions

Caitlin A Zacharias<sup>1,2</sup> and Donald C Sheppard<sup>1,2</sup>

*Aspergillus fumigatus* is a saprophytic mold that can cause infection in patients with impaired immunity or chronic lung diseases. The polysaccharide-rich cell wall of this fungus is a key point of contact with the host immune system. The availability of purified cell wall polysaccharides and mutant strains deficient in the production of these glycans has revealed that these glycans play an important role in the pathogenesis of *A. fumigatus* infections. Herein, we review our current understanding of the key polysaccharides present within the *A. fumigatus* cell wall, and their interactions with host cells and secreted factors during infection.

### Addresses

<sup>1</sup> Department of Microbiology and Immunology, McGill University, Montreal, QC H3A 2B4, Canada

<sup>2</sup> Department of Medicine, Infectious Diseases and Immunity in Global Health Program, Centre for Translational Biology, McGill University Health Centre, Montreal, QC H4A 3J1, Canada

Corresponding author: Sheppard, Donald C ([don.sheppard@mcgill.ca](mailto:don.sheppard@mcgill.ca))

Current Opinion in Microbiology 2019, 52:20–26

This review comes from a themed issue on **Host-microbe interactions: fungi**

Edited by **Chad A Rappleye** and **Duncan Wilson**

<https://doi.org/10.1016/j.mib.2019.04.006>

1369-5274/© 2018 Elsevier Inc. All rights reserved.

### Introduction

The saprophytic mold *Aspergillus fumigatus* is found throughout the environment, where it plays an important role in decomposition and nutrient recycling [1]. *A. fumigatus* produces copious amounts of airborne conidia, which are easily dispersed by air currents. It has been estimated that the average human inhales hundreds of these conidia daily [1]. Both the relatively small size of *A. fumigatus* conidia (approximately 2 µm in diameter), as well as their strongly hydrophobic surface, enhance the ability of these particles to reach the terminal airways of the human host [1,2]. In healthy individuals, conidia are rapidly eliminated by the action of the mucociliary escalator or phagocytosed, and killed by resident alveolar macrophages and pulmonary epithelial cells [2,3]. Conidia that evade eradication by these mechanisms

can swell and germinate, leading to the induction of a robust inflammatory response involving the recruitment and activation of neutrophils. These cells mediate the killing of germinating hyphae by the release of reactive oxygen species (ROS) and antimicrobial peptides [3,4]. However, in immunocompromised hosts or those with abnormal lung function, *A. fumigatus* hyphae can persist within the pulmonary system to establish an acute invasive or chronic airway infection, respectively [3]. In immunocompromised patients, such as those receiving cytotoxic chemotherapy, the innate immune response is unable to restrict fungal growth and hyphae that invade the lung parenchyma, causing tissue injury, and if unchecked, systemic dissemination [3]. Mortality rates for this disease can reach 90% in disseminated disease [5\*]. In patients with chronic pulmonary disease, such as those with cystic fibrosis, the conidia are poorly cleared by the dysfunctional pulmonary mucociliary elevator. These conidia can then germinate and grow within the airways and pulmonary mucus layer. Hyphae remain largely contained to the airways due to the presence of a functional systemic immune system, although chronic, slowly progressive cavitary disease can develop [3,6]. Chronic pulmonary aspergillosis syndromes can lead to debilitating pulmonary and systemic inflammation as well as worsening of pulmonary function [6].

The *A. fumigatus* cell wall is a key point of contact between *A. fumigatus* and the host [7,8] (Figure 1). The majority of the fungal cell wall is composed of polysaccharides, and, as a result, there has been great interest in elucidating the role that these macromolecules play in host–fungal interactions. While recent studies with purified polysaccharides and mutant strains with altered polysaccharides have begun to shed light on the role of these molecules during infection, it is important to acknowledge the limitations of both experimental approaches. Purified polysaccharides may vary in size and composition from their native forms, and the immune response to soluble or microparticulate polysaccharides may be different from the response to polysaccharides presented in their natural context where they are immobilized within the cell wall and linked to other glycans and proteins. These effects have been best illustrated in studies of interactions with the cell wall polysaccharide chitin in which both particle size and the presence of co-stimulatory pattern recognition receptor ligands have a dramatic effect on the type of host response to this glycan (detailed below) [9,10\*\*]. The use of synthetic oligosaccharides of defined length and composition may be helpful in this regard, but

# Structural and biochemical characterization of the exopolysaccharide deacetylase Agd3 required for *Aspergillus fumigatus* biofilm formation

Natalie C. Bamford<sup>1,2,8,9</sup>, François Le Mauff<sup>3,4,5,9</sup>, Jaime C. Van Loon<sup>1,2</sup>, Hanna Ostapska<sup>3,4,5</sup>,  
Brendan D. Snarr<sup>3,4,5</sup>, Yongzhen Zhang<sup>6</sup>, Elena N. Kitova<sup>7</sup>, John S. Klassen<sup>7</sup>, Jeroen D. C. Codée<sup>6</sup>,  
Donald C. Sheppard<sup>3,4,5</sup> & P. Lynne Howell<sup>1,2</sup>✉

The exopolysaccharide galactosaminogalactan (GAG) is an important virulence factor of the fungal pathogen *Aspergillus fumigatus*. Deletion of a gene encoding a putative deacetylase, Agd3, leads to defects in GAG deacetylation, biofilm formation, and virulence. Here, we show that Agd3 deacetylates GAG in a metal-dependent manner, and is the founding member of carbohydrate esterase family CE18. The active site is formed by four catalytic motifs that are essential for activity. The structure of Agd3 includes an elongated substrate-binding cleft formed by a carbohydrate binding module (CBM) that is the founding member of CBM family 87. Agd3 homologues are encoded in previously unidentified putative bacterial exopolysaccharide biosynthetic operons and in other fungal genomes.

<sup>1</sup>Program in Molecular Medicine, The Hospital for Sick Children, Toronto, ON M5G 1X8, Canada. <sup>2</sup>Department of Biochemistry, Faculty of Medicine, University of Toronto, Toronto, ON M5S 1A8, Canada. <sup>3</sup>Department of Microbiology and Immunology, Faculty of Medicine, McGill University, Montreal, QC H3A 2B4, Canada. <sup>4</sup>Infectious Disease and Immunity in Global Health, Research Institute of McGill University Health Center, Montreal, QC H4A 3J1, Canada. <sup>5</sup>McGill Interdisciplinary Initiative in Infection and Immunity, Montreal, QC H3A 1Y2, Canada. <sup>6</sup>Leiden Institute of Chemistry, Leiden University, 2300RA Leiden, The Netherlands. <sup>7</sup>Alberta Glycomics Centre and Department of Chemistry, University of Alberta, Edmonton, AB T6G 2G2, Canada. <sup>8</sup>Present address: Division of Molecular Microbiology, School of Life Sciences, University of Dundee, DD1 5EH Dundee, UK. <sup>9</sup>These authors contributed equally: Natalie C. Bamford, François Le Mauff. ✉email: [donald.sheppard@mcgill.ca](mailto:donald.sheppard@mcgill.ca); [howell@sickkids.ca](mailto:howell@sickkids.ca)